Production Methods and Mining Technologies

A Rapid Dampening Suspension For Ultra-Class Haulers

R. F. Santos, B.Sc, E.I.T.
M Sc Graduate Student, AEGIS research group, University of Alberta, Edmonton, Canada

T.G. Joseph, Ph D , P.Eng.
Director AEGIS, University of Alberta and Principal Engineer, JPi, Edmonton, Canada

ABSTRACT: In the last decade, the continuously growing demand for production in bulk mining operations such as the Canadian oil sands operations of Northern Alberta has influenced ultra class truck payloads to the extent that 400 tons has been reached, with sights firmly set on the advent of the 500+ ton unit Soft underfoot conditions in unconsolidated deposits such as these have resulted in the transmission of adverse stresses throughout truck frames causing premature failures Poor ground response can ultimately be linked to cyclic fatigue stress and excessive vibration levels affecting both operator and equipment health The focus of this paper is the introduction of a conceptual strut design to mitigate the impact of high loading generated by adverse loading due to soft ground conditions

1 EXECUTIVE SUMMARY

The cyclic response of the oil sand underfoot in response to high g loading contributes to premature failure of existing truck frames and meurs a high rate of operator reported back problems The basic shock absorber or strut design for ultra class trucks was reviewed to facilitate proposal of an alternative solution to mitigate these adverse impacts On-board data was acquired through the original equipment manufacturer (OEM) acquisition system and downloaded for complete round trips to a shovel The pressure changes from these sets were incorporated into a thermodynamic analysis related to the nitrogen gas performance of the shock absorbers

To simplify the analysis, it was shown that negligible impact on the outcome was incurred in treating the nitrogen as an ideal gas, and the compression process as ısentropıc A top clearance inside the shock absorbers was determined for each unit trip, revealing that "topping-up" occurred frequently Vehicle suspension fundamentals, in addition to fluid mechanics and thermodynamic principles were reviewed and applied in a comprehensive shock absorber analysis

Current struts or shock absorbers for ultra class trucks were identified as basically the same design as those used in haulers for the past 40 years, classified as "simple" shock absorbers, containing a fixed orifice and therefore constant damping coefficients for both compression and rebound strokes These were modeled to establish a baseline of current performance A modification was then proposed effecting a semi-active configuration via a variable orifice

A variable orifice allows oil flow through a variable cross sectional area, leading to a variable resistance and variable damping coefficient The cross-section area of flow is a function of the input displacement, proportional to the applied g load on the shock absorber This was modeled to compare the performance of the proposed variable orifice shock absorber against the fixed configuration Several iterations were run at different stroke rates and levels of g loading for both models The results showed that the variable orifice shock absorber creates a dampening proportional to the load and stroke rate applied

2 "TOPPING-UF' PHENOMENON

A simple thermodynamic analysis was performed to determine pressure and volume of the nitrogen gas inside a strut during a given trip cycle Actual pressures were attained via the OEM on-board data acquisition system As a typical example,

immediately after shovel loading activity and before initial motion, the rear truck struts of an ultra class unit were evaluated with 3 18 cm of top clearance between the head and casing This provided a base line for the analysis Isentropic compression was assumed, allowing corresponding volumes to be determined at each recorded pressure throughout the duty cycle The result of the analysis showed that there were many points where "topping-up" occurred, illustrated in figure 1 Negative values here are theoretical and actually represent zero top clearance values indicating metal-metal contact, termed "topping-up"

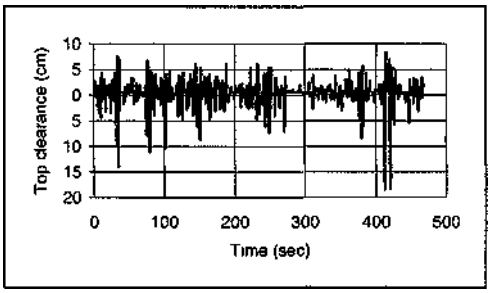

Figure 1 Sample top clearance for strut operation

3 SUSPENSIONS SYSTEMS

Suspension systems may be classified in terms of energy management, such as passive, semi-active or active Passive systems have a constant damping coefficient and stiffness Active systems have the ability to change their characteristics according to the amount of vibration imposed on the system, typically requiring energy input to vary behavior

The principle of active suspension is illustrated in figure 2, where the spring and damper in a passive system are replaced by a force actuator, with operating conditions monitored continuously by a group of sensors The control strategy is to minimize the root mean square (RMS) value of the sprung mass acceleration, suspension travel, and dynamic tire deflection (Wong, 1999)

In order to improve ride characteristics but minimize the complexity that comes with a fully active system, a compromise is the semi active concept illustrated in figure 3 Here the conventional suspension spring is retained, but the damping force in the shock absorber is modulated according to the ride requirements One such simple approach to control the stiffness of the unit is to vary the resistance to oil flow, as adopted by aerospace landing gear By adjusting the orifice area of the shock absorber, the resistance to fluid flow and damping force is varied (Wong, 1999)

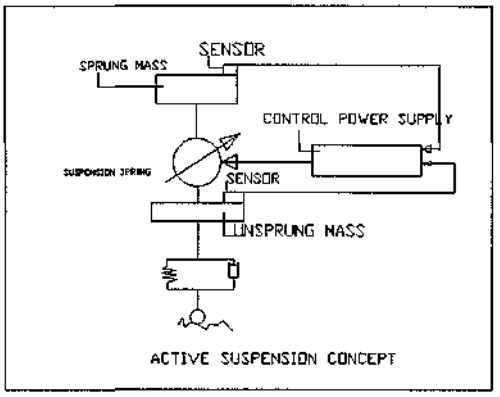

Figure 2 Active suspension concept (after Wong, 1999)

Shock absorbers may also be classified according to the type of spring being used such as solid steel or fluid comprising gas and oil, as m an oleo pneumatic shock absorber, the latter of which has high efficiency under dynamic load conditions m terms of energy absorption and dissipation

The single acting shock absorber is the most common oleo pneumatic design used for ultra class mining trucks, where a fixed diameter orifice effecting a constant damping coefficient is typical of a passive system If the flow cross section area of the orifice is variable commensurate with the applied dynamic load, then the strut could be classified as either an active or semi active suspension The basic components of the simple shock absorber are two telescopic tubes, one functioning as a piston and the other as a cylinder, as illustrated in figure 4 An orifice in the piston head permits fluid to pass from one chamber to the other The fluid flow through the orifice, together with the compression of the gas, absorbs the energy of the load The shock absorber extends when the applied load on it decreases

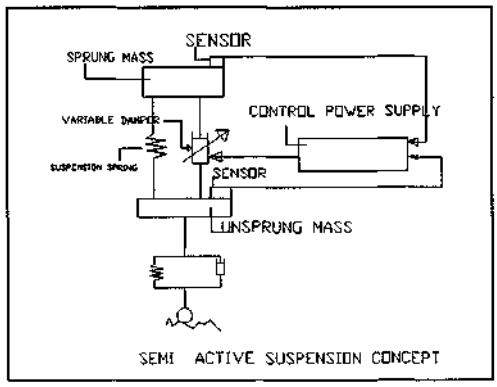

Figure 3 Serra active suspension concept (after Wong 1999)

A complex shock absorber works according to the same principle as the simple system, but has the ability to change the dampening coefficient commensurate with the dynamics of the applied load In order to achieve this goal the orifice size m the shock absorber must change with the load being applied There are many different types of complex shock absorbers such as metering pm, plunger and floating piston, which are descriptors of the variation from the simple system

The metering pm approach, conceptualized in figure 5 and the basis of this investigation, changes the effective size of the orifice and the resulting rate of fluid flow from one chamber to the next The conical shape of the metering pin varies the cross sectional area of the orifice The larger the effective diameter of the pm the greater the resistance to fluid flow, the higher the damping coefficient

3.1 Basic operation of a simple shock absorber

In compression, figure 6, the piston moves up causing gas compression and forcing the oil through both the fixed orifice (Q2) and ball check valve (Ql) to the annular compartment The change in volume for the gas represents the spring action of the shock absorber

The gas spring absorbs the majority of the impact energy Oil flow through the orifice and the ball check valve causes "orifice action" energy dissipation as heat to the surroundings Minor oil flow occurs via the piston-cylinder annular clearance (Q3) causing some additional energy dissipation

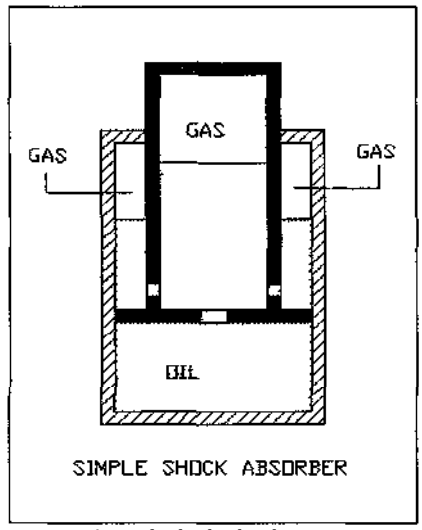

Figure 4 A simple shock absorber

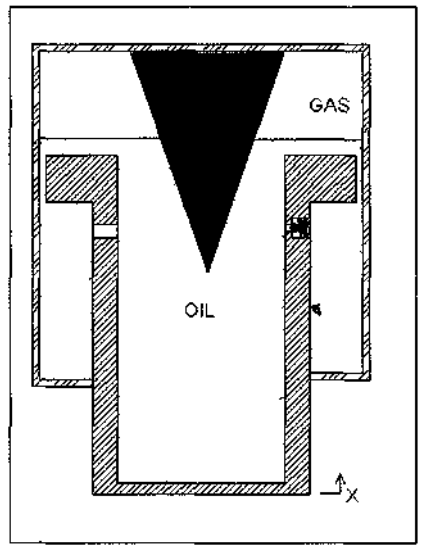

Figure 5 Conceptual metering pm shock absorber

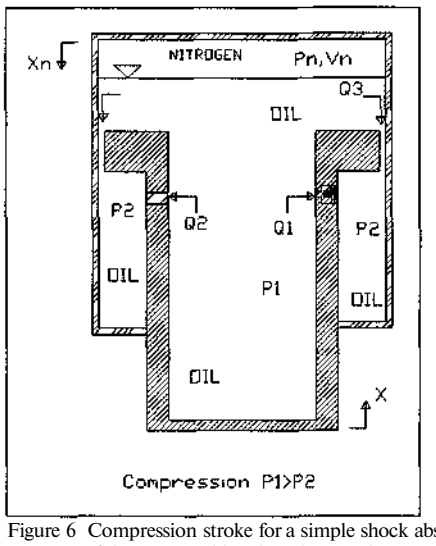

Figure 6 Compression stroke for a simple shock absorber of the type used by ultra class trucks

In rebound, figure 7, the gas tries to regain its original volume and reach equilibrium with the truck weight The gas expands pushing the piston down and the oil through the fixed orifice only, producing the mam damping effect of the shock absorber As the piston moves down, the pressure in the annular compartment increases causing the ball check valve to close leaving the only opening available for oil flow through the fixed orifice

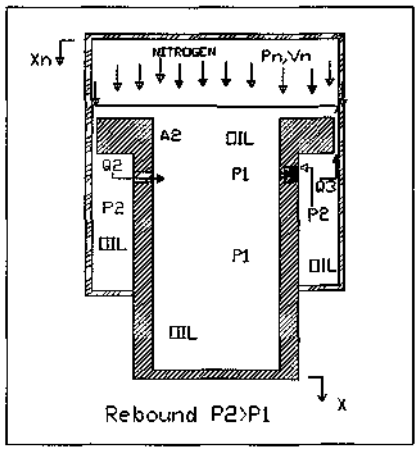

Figure 7 Rebound stroke for a simple shock absorber

4 THERMODYNAMIC CONSIDERATIONS

The gas inside an oleo-pneumatic shock absorber is effectively the system spring The system can be simplified assuming the gas obeys the ideal gas laws under ısentropıc compression, so that

$$P_1 \times V_1^k = P_2 \times V_{21}^k \quad [1]$$

where,

P= Pressure
V= Volume of chamber
k = Specific heat ratio

5 FLUID MECHANICS CONSIDERATIONS

5.1 Flow across an orifice

When fluid flow (Q) passes through an orifice, it loses energy or pressure head The pressure drop is proportional to the orifice dimension and shape Applying Bernoulli's equation for an incompressible fluid, and the principle of flow continuity between any two points, it can be shown that

$$Q_{Actual} = C_d\, Q_{Ideal} = C_d\, A\, v \quad [2]$$

Where the velocity of flow v may be determined via

$$v = [2\,(P_2-P_1)/\{\rho\,(1-(D_1/D_2)^4)\}]^{1/2} \quad [3]$$

where,

A = Cross sectional area of the orifice
Cd = Orifice flow coefficient

5.2 Flow through annular clearance (assuming laminar flow)

Generally, the flow through an annular clearance is given by equation [4]

$$Q = AP/R_L \quad [4]$$

Where the hydraulic resistance RL may be determined via equation [5]

$$R_L = (24 p v\, L)/(7i5^3(D_{,,}+D,)) \quad [5]$$

Where,

D_0 = Outer diameter of the inner tube
D, = Inner diameter of the outer tube
8 = Annular clearance between the tubes
p = Density
v = Kinematic viscosity

5.3 Damping Force

The damping force, equation 8, of the ultra class truck is a combination of the gas-spring force, equation 6, and the hydraulic damping force, equation 7, caused by the oil.

$$F_{gas-spring} = P_{gas} \times A \quad [6]$$

$$F_{hydraulic} = R_L A^2 (vel) \quad [7]$$

Yielding equation 8:

$$F_{damping} = F_{gas-spring} + F_{hydraulic}$$

6 MODELING AN EXISTING ULTRA CLASS TRUCK SIMPLE SHOCK ABSORBER

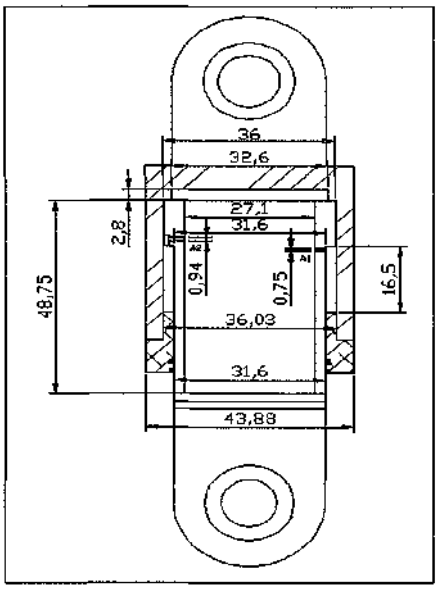

Figure 8 OEM developed shock absorber for an ultra class truck

The analysis of an existing OEM ultra class truck shock absorber was modeled after the example in figure 8. Matlab and Microsoft Excel, along with the formulae above, were used to create the base line model. Figure 9 represents the corresponding SIMULINK model developed in Matlab by El-Sayed (2003) and which was used as the basic strategy for the spreadsheet model used in this analysis.

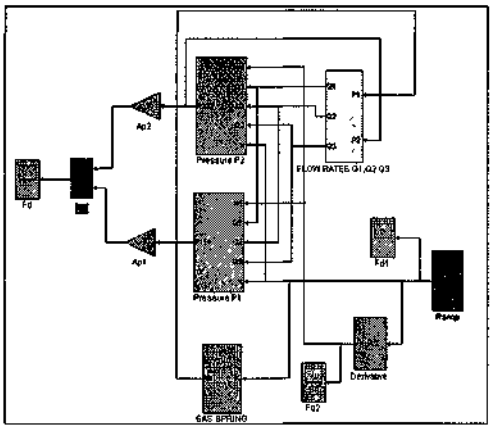

Figure 9 SIMULINK Model of CAT 797B shock absorber, (after El-Sayed, 2003)

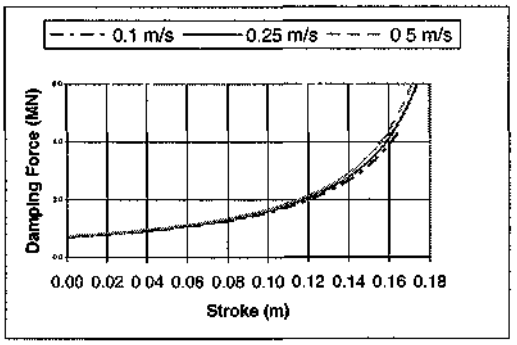

Figure 10 Damping force for a simple shock absorber

Figure 10 shows the base line performance for the OEM shock absorber. The slope of the line shows the stiffness of the unit. For the first 0.09 m stroke the line is slightly sloping up. This is representative of a shock absorber with a fixed orifice. As the stroke exceeds 0.09m the trend increases rapidly due to the damping force of the gas-spring. Since the damping force increases late into the stroke, the chance of topping-up is greatly increased.

7 MODELING THE VARIABLE ORIFICE SHOCK ABSORBER

For the conceptual shock absorber an invented cone was added as shown in figure 5. As the piston moves up, the corresponding opening gets smaller due to cone penetration. The cone increases the flow resistance to the oil, producing damping additional to the original orifice and ball check valve

configuration. This additional control of oil flow increases the overall damping characteristics of the shock absorber. The conceptual variable orifice shock absorber was modeled in order to determine the difference in performance to the fixed orifice design currently in use. A sensitivity study has been performed in order to determine the effect of several design parameters on the shock absorber performance.

Modeling was once again performed in Microsft Excel following the interative strategy suggested by El-Sayed (2003) in Matlab Simulink, figure 11.

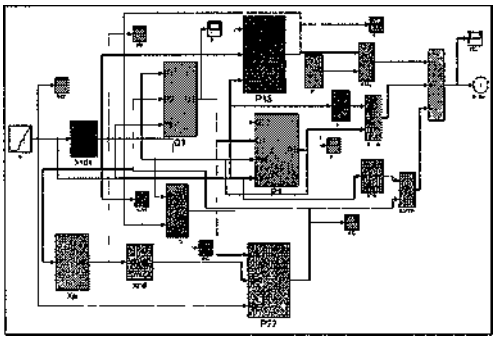

Figure 11 SIMULINK model of the variable orifice shock absorber (after El-Sayed, 2003)

Simulation results are shown in figure 12, as damping force generated inside the shock absorber versus the rate of input displacement. The slope of the curve represents the shock absorber stiffness. The slope steepens as the input velocity increases.

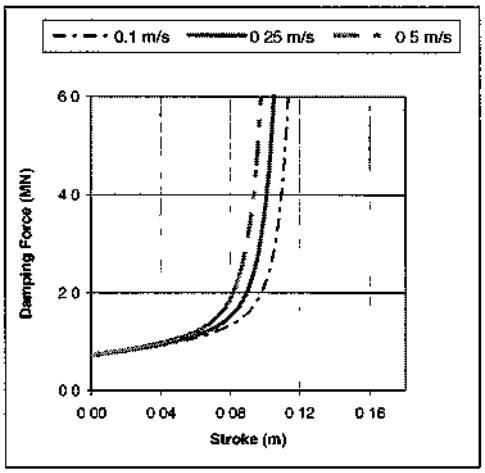

Figure 12 Damping Force versus input velocities for variable orifice shock absorber

8 DISCUSSION AND CONCLUSIONS

The computer simulation showed the capability of a variable orifice shock absorber to provide a rapidly increasing dampmg force to prevent topping-up , as a function of the applied load.

Figures 13 through 15 compare the existing OEM shock absorber to the modified one at various velocity inputs. The output showed that the modified shock absorber generates a greater amount of damping force compared to the existing design. This rapid increase in damping force, will prevent the shock absorber topping up.

As the velocity input increases, the dynamic response of the variable compared to the fixed unit is more sensitive to impact loads and more likely to dampen a corresponding high g effect. This is represented by rapid damping occurring earlier in the stroke with increasing velocity. The stiffness of the variable orifice unit varies dramatically as the load increases.

Physical testing is planned to verify the modeled conclusions on a full scale suspension system during summer 2005. Field verification is also planned to determine the improved ride quality due to the conceptual unit. Further research will investigate how the conceptual shock absorber affects the rebound phase of the cycle.

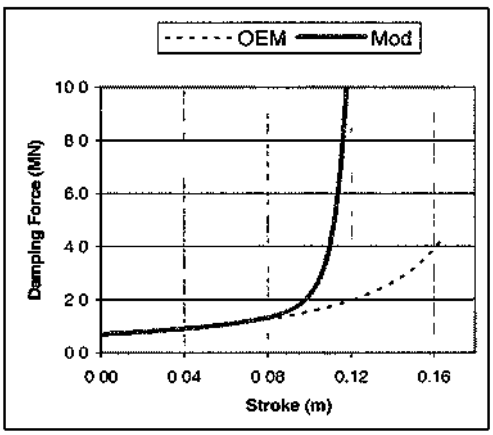

Figure 13 Damping force at 0.1 m/s

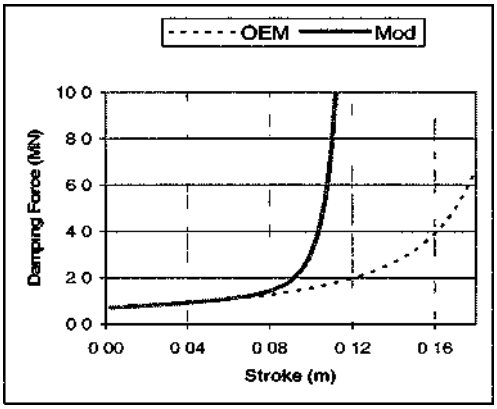

Figure 14 Damping force at 0 25 m/s

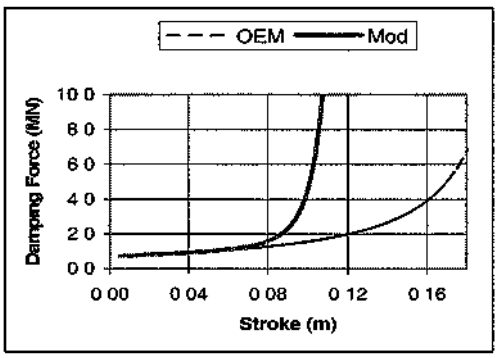

Figure 15 Damping force at 0 5 m/s

REFERENCES

Caterpillar Inc 2002 Specifications Manual from SENR 1540, Specifications, SENR 1455-04 *Caterpillar Service Manual for 793C Truck*

El Sayed, M, 2003 *A new Concept strut design for heavy haulers to combat high g loading* M Eng Thesis, University of Alberta

Kroeell, Dulay, Fueresz, Harkay, & Lukacs 1988, *Fundamentals of hydraulic power tiansmission* Elsevier Science Publishers, Amsterdam

Pinches, M J & Ashby, J G 1990, *Power hydraulics* Prentice Hall,Hertfordshire

Wong, J Y (2°[d])1993, *Theory of Ground Vehicles* John Wiley & Sons, Inc New York

Larger Shovels - The Reality

Lee B. Paterson
P&H MinePro Services, Milwaukee, Wisconsin, U.S.A.
Andrew J. Williams
P&H Mining Equipment, Milwaukee, Wisconsin, U.S.A.

ABSTRACT: The drive for larger loading and hauling units has not slowed, with significant numbers of shovels with +100t payload loading trucks in the 240t - 400t size range. Productivity data is now available to assess the performance of the larger loading units. This paper takes a brief look at some of the available data and compares performance of the units in a number of "High Production Low Cost" operations.

1 FOREWORD

Since the authors are employees of P&H MinePro Services and P&H Mining Equipment, access to P&H equipment performance data is readily available through the kind cooperation of our customers, and that data forms the basis of this paper. Mining is an extremely competitive "environment and therefore we honor the request of our customers to keep our information sources confidential. We do not have ready access to competitor equipment performance and therefore the performance of only P&H loading equipment is covered in this paper. The numbers are real - this is not a marketing exercise to justify the purchase of specific equipment, it is dissemination of real information that will hopefully be informative to members of our Industry.

2 INTRODUCTION

For some years the term "Bigger Faster Smarter" has been heard throughout the Mining Industry. Just how are these machines performing? We have reached the stage where we have been able to gather sufficient data to demonstrate the capabilities of these shovels and their associated truck fleets. This paper is a summary to date of the performance of some of these larger loading units, highlighting some differences in applications and loading preferences.

Since 1991 the P&H 4100 series of machines has been among those setting the standards of productivity in the Mining Industry. Initially developed with a payload of 80t (short ton) to 3-pass load 240t (short ton) trucks, the equipment size has grown to payloads of up to 120t (short ton) 3-pass loading trucks with 360t (short ton) payload capability. Throughout this period the emphasis has been focused on improving the productivity and lowering the cost per unit of product produced. And successfully, so it seems, since P&H alone has sold more than 140 units in this size range.

In the past, the performance of the larger shovels has largely been calculated and predicted through the utilization of various productivity and simulation models, and it's always handy to have some information to "back that up". Of course real information from the field is subject to a number of variances which make direct comparisons somewhat difficult, but we encounter amazing similarities when we look at mines that are truly "high production low cost" operations. Before we continue perhaps it's best that we get a little more definition on this term.

3 HIGH PRODUCTION LOW COST MINING

These are mines that truly seek to utilize their loading and hauling equipment optimally. Pushing these resources and maintaining their performance at their optimal capability ensures that the machines produce maximum tonnage at a lower cost per ton.

In order to do that, the mine has to make certain commitments from the overall mining perspective:

a) Blasting cannot be compromised - this is perhaps the key to the success of any loading operation. Unfortunately when it comes to cutting costs, the explosives are one of those items that gets high visibility, since it's usually a large check that gets sent to the explosives supplier every month. Because it's so visible and so easily measured, the explosives element is usually one of the first areas to get cut in a cost cutting exercise, which is exactly the opposite of what should be done in lowering total costs.

In fact the contribution by explosives to productivity and cost savings extends far beyond the loading unit productivity -

- Loading units are subjected to less shock loading and wear and tear when excavating well blasted ground
- Loading unit cycle times are optimized in that less time is spent digging through a poorly blasted face
- Power consumption is reduced in good digging conditions
- > Truck bodies are subjected to less impact loading from poorly blasted material
- There is less possibility of spillage in the loading area and on the haul road
- " Trucks leave the shovel both optimally loaded and with the load distributed evenly in the truck body
- In ore processing, the comminution process is optimized in that the primary crusher should be subjected to what it is planned to handle. In addition, the overall crushing process is optimized through proper fragmentation of feed material.

b) Scheduling has to be running at absolute optimum. Truck dispatch should ensure that there is no excessive queuing at the loading units. In order to maximize the production from a loading unit, a slightly over-trucked situation is ideal, this eliminates unnecessary "non-loading" time.

c) Loading method has a huge effect on productivity, and varies among applications. For high production low cost applications, the double back-up or drive by systems produce the best results.

In many applications, the double back-up is enhanced by the fact that a truck is already positioning itself ready for loading on the one side while the truck on the other side is being loaded. For some mines, this is considered a safety issue, and the preference is for the truck to be ready to back up. It does not move into position until the shovel operator gives a signal. Certainly, within the P&H range of shovels, there is sufficient geometry and truck spotting tolerance to enable backing up on the "blind side" to be conducted safely.

The modified drive-by system has been used with great success in coalmines in the Powder River Basin in the U.S.A. What makes it "modified" is the fact that the first load is dumped into the truck in the standard drive by fashion. Thereafter when the shovel turns to fill the dipper in the face for the 2nd pass, the truck operator actually backs the truck up and decreases the angle the shovel has to swing for the 2nd and 3rd passes. After the truck has the 3rd pass loaded, it drives away and the next truck pulls into the "drive by" position in time for the shovel to dump its first pass. The result is that there is no time lost due to spotting, swing angles are reduced and the operation is virtually continuous.

d) Maintenance has to be well planned and coordinated with the schedulers in order to ensure that equipment downtime has little or no effect on the operation.

4 FIELD PRODUCTION PERFORMANCE

Loading performance data has been collected from 53 shovels operating at 26 mine sites, the following is a summary of that data.

4.1 Hard **rock applications** such **as** Copper ore and waste.

The 4100XPB's with a nominal pay load of lOOst to 120st have consistently passed benchmark test requirements of 7200t/hr, and achieved peak productivities of 8000t/hr. Typically we are seeing fleet averages of 5280t/hr in these applications.

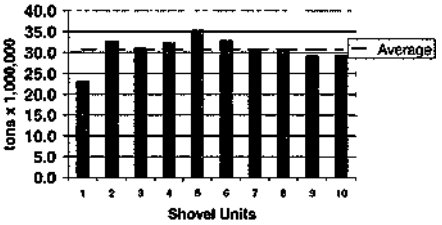

Figure I: Annual Production of 4100XPB's in Copper Applications

Referring to Fig. 1, the annual tonnage of the fleet of 10 shovels in this group from which data was collected averaged 30.7 million tons per shovel, and average production time per shovel is 25 months, i.e. an average of 2 years operating per shovel.

As can be seen on the graph, one shovel actually exceeded 35 million tons loaded per annum. This particular shovel has already been in operation for 39 months, so it is well established at the mine as the top producer. These are the tonnage that we expect to see from High Production Low Cost applications.

The 4100 and 4100A models of equipment, with their nominal payloads of 80st to 90st have also demonstrated the high tonnage that we expect in the High Production Low Cost environment.

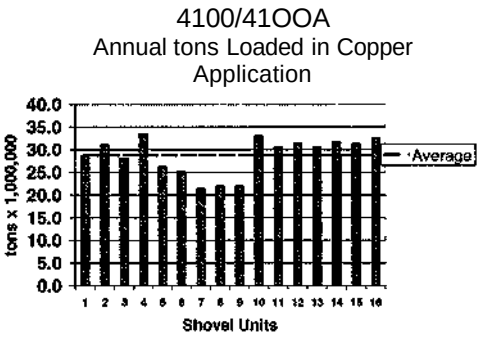

Figure 2: Annual Production of 4100's and 4100A's m Copper Applications

Fig. 2 shows the annual production of 16 shovels with an average of 29 months average production time per shovel. That's nearly 2.5 years of loading data average per shovel, one of these units has been in operation for 57 months. The top producers in this group are in the 30-million plus tons per annum, with two units actually achieving an average annual tonnage of over 33 million tons.

4.2 Coal Overburden Applications

Unfortunately the Industry views coal overburden as a "softer" loading application. Maybe in some areas of the world this does apply, but in most cases the overburden has hardness in the region of lOOMpa, is highly abrasive and has to be drilled and blasted in order to be loaded. As such we tend to view this application as still being tough. Add to that the environmental extremes of these applications and the machines take a beating. They are pushed in many cases beyond optimum in an effort to keep down the cost of the coal being exposed.

The 4100XPB's that we have been monitoring have been in coal overburden applications for an average of 22 months, with our longest serving "member" at the 40-month mark.

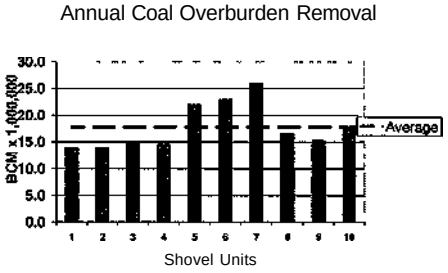

Figure 3: Annual Production of 4100XPB's in Coal Overburden Applications

The 10 units shown in Fig. 3 have been averaging a little under 18 million BCM's per annum, with the top producer exceeding 25 million BCM's per annum. This machine has been in operation for over 30 months, with another top producer averaging 23 million BCM's per annum over it's 40-month life. One may debate that the 3 top producers skew the graph, which indeed they do, but the production they are achieving is real, utilizing the modified drive by method of loading, and therefore their production has to be taken into account.

The 4100 and 4100A's are again a larger group - (see Fig. 4). The 17 shovels we have in the group have averaged a little fewer than 16 million BCM's per shovel in annual production.

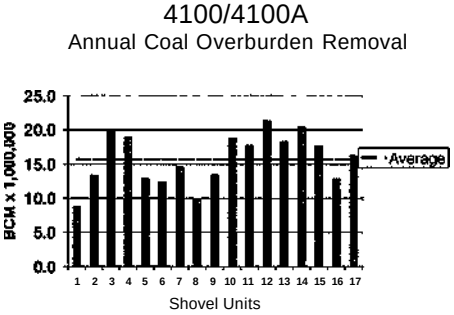

Figure 4: Annual Production of 4100XPB's in Coal Overburden Applications

Again the top producers are utilizing the modified drive-by method of loading, with 2 machines exceeding the average annual production of 20 million BCM's, and a host of machines starting to reach up toward that mark.

5 CONCLUSION

As previously mentioned, the performance of these loading units is affected by the truck allocation and loading methods. We think that the results certainly do speak for themselves. We have not shared any cost data in this exercise, as there are huge factors that affect costs and therefore they cannot truly be compared. We have clarified that this is not a marketing exercise, but an attempt to demonstrate that the new generation of shovels and trucks actually do "produce the goods". The users of this equipment continue to procure more and more units to satisfy

their production requirements, which in itself is testament to the success already being experienced

Acknowledgements

The authors would like to thank those 26 mines operating the 53 loading units referenced in this paper for sharing their production information

Thank you also to the personnel of P&H Mining Equipment and P&H MinePro Services whose passion for lowering our customer's costs is a significant contributor to the success of these "Bigger Faster Smarter" shovels.

REFERENCES

Anon Peak Performance Practices - Excavator Selection for High Production Low Cost Operations *A P&H MinePro Services Publication*

Ozdogan, M & Paterson, L 2001 Performance of the Bigger, Faster and Smarter New Generation Electric Mining Shovels *MCET2001 Proceedings*

Paterson, L 2000 Drilling Efficiency and the Associated Benefits to the Mining Process *International Society of Explosives Engineers 2000 Proceedings*

The 19th International Mining Congress and Fair of Turkey IMCET200S, Izmir Turkey, June 09-12, 2005

Diamond Wire Application for Black Granite Block Mining in Säo Paulo

W.T Hennies, A Junior, L. Soares, C.T. Lauand, & G.R. M. Cortés
Mining & Petroleum Engineeiing Department, Polytechnic School, University of Säo Paulo, SP, Brazil

ABSTRACT: The mmmg of Dimension Stone Blocks of black granite in the State of Säo Paulo, Brazil, by quarrying is presented The rock commercially named Piracaia Granite is used as construction material or in funeral arts, as outside as well as inside cover for walls and floors The applied mining techniques changed The older extraction of the surface outcrop boulders changed to methods of massive rock exploitation For this it was necessary to adopt new non-conventional procedures One of those methods consists of block sawmg by diamond wire to create some primary vertical and horizontal faces The Brazilian practice gained in using this exploitation of the granite block in the rock massive is described here Conventional methods using black powder to create secondary planes to conform the block are also used The complete mining sequence of the extraction and transportation to the city of Sâo Paulo is presented

1 INTRODUCTION

The past, present and future of the dimension stone industry m Brazil, as an important mineral resource for raw material production m the arts (statuary and tombstones), building materials or industrial elements, were presented by two of the authors in a paper m Italy (Hennies & Stelhn Jr, 1996) In that article it was shown that the transformation m a final product for use needs, in many cases, a more or less complex preparation system and this can cause problems to meet the new and increasing exigencies of the environmental preservation rules now determined by the national legislation

In an event in Ukraine, a description of the exploitation using flame jet technology was presented about the winning of blocks (Hennies et al, 1999)

More recently another analysis about a global overview of the Brazilian Dimension Stone Industry was presented in the Check Republic (Hennies et al, 2002)

The exploitation of a specific Dimension Stone Quarry is an art and technique that takes advantages of the rock characteristics Here it is presented the mam sequence of the block mining for its future transformation in plates, which is the mam problem to be discussed here Next, the main environmental problems such as noise, dust and water pollution will be analyzed The technological characteristics of black granite and its application will be presented at the final section of the paper

2 THE DIMENSION STONE QUARRY

About 2 km from the city of Piracaia is located a Dimension Stone Quarry that produces blocks of Piracaia black granite The access to the quarry is by a dirt road after crossing a river in the west of the city of Piracaia

Figure 1 shows the geographical localization of the city of Piracaia to the North of the city of Säo Paulo, and also the mine site Figure 2 shows a photograph of the black granite quarry

As said before, in Brazil two different kinds of dimension stone quarries can be distinguished, the boulder quarry and the rock quarry

In the past, mainly m the granite areas, the win ning of blocks was realized from the surface by extracting the outcrop of boulders that was shaped to a standard size

These blocks wcie then transported to the plant for beneficiatıon and transformation in a final end product near the consumption centers, or for further selling This first kind of dimension stone quarry was called the boulder quarry

In the case of Piracaia black granite, the exploitation dates from the 1930s This can be seen m a curious photograph existing in the enterprise of Brothers Fiorehnni, which until today has a beneficiatıon plant and a commercial shop to sell granites, m Piracaia

Figure 3 shows a big block that was exploited and for its transportation a special cow car was constructed

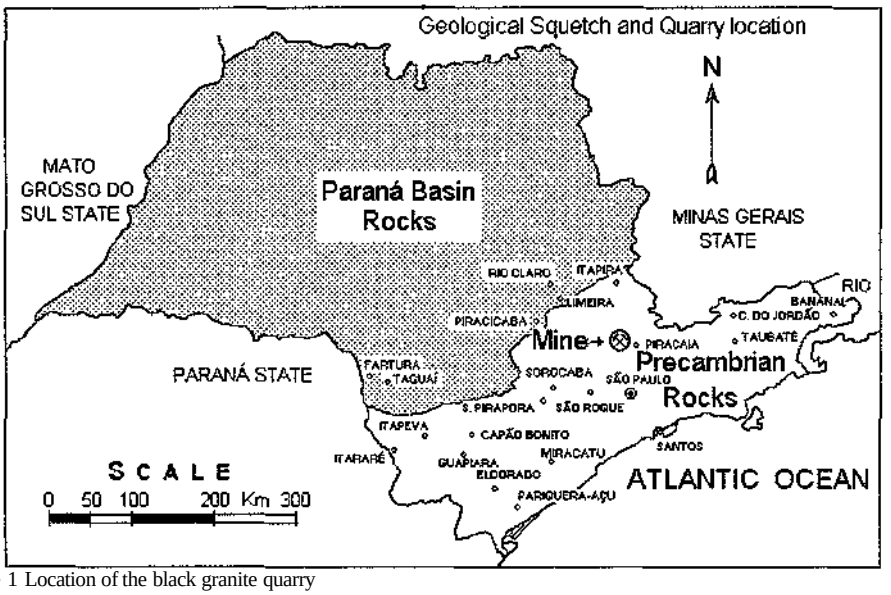

Figure 1 Location of the black granite quarry

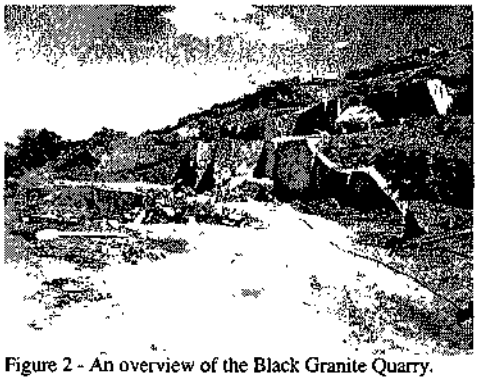

Figure 2 - An overview of the Black Granite Quarry.

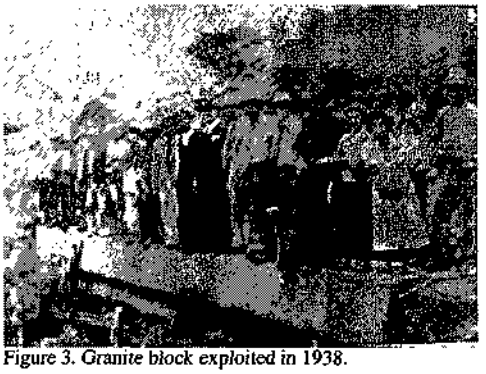

Figure 3. Granite block exploited in 1938.

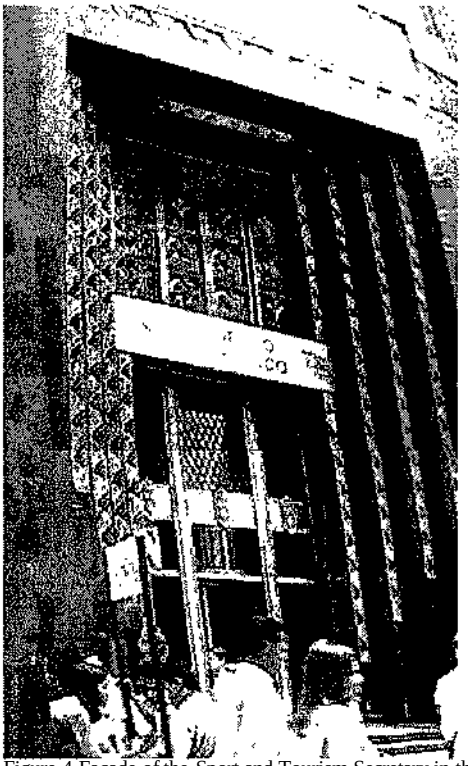

Figure 4 Façade of the Sport and Tourism Secretary in the center of Sâo Paulo city with the roof of Piracaia granite.

This block was applied in the façade of a building in the center of Sâo Paulo city. Now this building is a State Department of the Sâo Paulo government, and it is shown in Figure 4.

The extraction rate increased, and to maintain a more regular production level, it was necessary to adopt new procedures for the winning of the blocks, which began to be extracted from the rock massive. In this other kind of quarry called rock quarry, a greater mass of fresh rock exists that is subdivided in major pieces.

These quarries created by dimension cutting characteristically remove blocks by sawing or splitting operations and the blocks have the shape of parallelepipeds.As a consequence the faces of these quarries are usually very steep transverses by stepped-down benches. For the winning of the blocks of the massive it was necessary to use a non-conventional method of primary surface creation not previously used, which consists of a diamond wire machinery. A new enterprise called Granite Marie! exploits the blocks by the non-conventional methods using the diamond wire technology.

The conventional sizing of the block using drilling and charging with black powder, used first is also employed to cut the other block faces.

The total output of the quarry stands now at the level of about 100 cubic meters a month or about 400 cubic meters yearly.

The following item makes some basic considerations about the diamond wire technique, with the sequence of the unit exploitation operations to win the granite blocks in the quarry.

3 DIAMOND WIRE TECHNOLOGY

Recently a revolutionary method appeared for precise cutting of dimension stone that is known by the name of diamond wire technology.

The diamond wire can be considered an advance or evolution of the helical wire, normally used for the attainment of blocks in softer rocks such as marble. It consists of the helical wire, an extensive special steel handle moved by an engine and guided by pulleys. In the rock cut areas, an abrasive (in general quartz sand) is added to the wire to erode the rock.

The diamond wire is equally composed of a steel wire, along which there are pearls in the shape of impregnated synthetic diamond cylinders. With this, the feeding of the abrasive is dispensable.

The abrasive cylinders are spaced by springs that are encapsulated in plastic or rubber, to prevent their unfastening. Initially, this cover was absent, causing a series of accidents due to the unfastening of the springs.

In Figure 5, two types of diamond wires are illustrated, for cutting marble and granite, showing their constituent elements: pearls composed of impregnated steel leagues of synthetic diamonds, steel wire, spacing springs, and covering of rubber or resistant plastic.

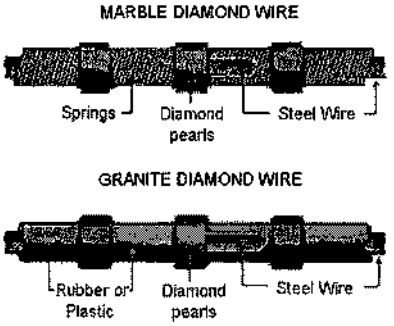

Figure 4 Elements of a diamond wire saw.

With its fast action of clean cut, the diamond wire has proven to be an efficient system of non-destructive extraction and demolition in the unit mining operations. Created in the quarries, the diamond wire has become a prerequisite for improvement of the recovery conditions in the extraction of dimension stone blocks.

For the separation and extraction of the blocks from the bulk it is necessary to generate plain or free faces, which can be obtained with the diamond wire.

Figure 6 presents a detail of the generation of a face of vertical cut in the quarry wall, with the diamond wire. In the upper portion of the figure the beginning of the cut operation is shown, to generate a plan of separation and in the lower partit is shown the operation in its final phase of cut.

The cut work with diamond wire is obtained by the action of its elements of abrasion with the attrition and displacement on the rock, where a motor pulley carries through this operation, and a pulley guide, giving the direction of the plane where it desires to carry through the cut.

In the initial phase of the operation the execution of drill holes must be open and serve as a way to pass the diamond wire. In this occasion, in various equipment two pulleys still exist that drive the strength of the wire, whose effort can be controlled, and that keep the adherence of the diamond wire to the rock.

Another aspect that can be highlighted is that with the continuation of the cut there is a reduction of the perimeter of the wire in contact with the rock. To prevent works from shortening the wire, the displacement of all the equipment is normally made on tracks, allowing the total sawing cut to be carried through without the need to interrupt the work to promote this shortening.

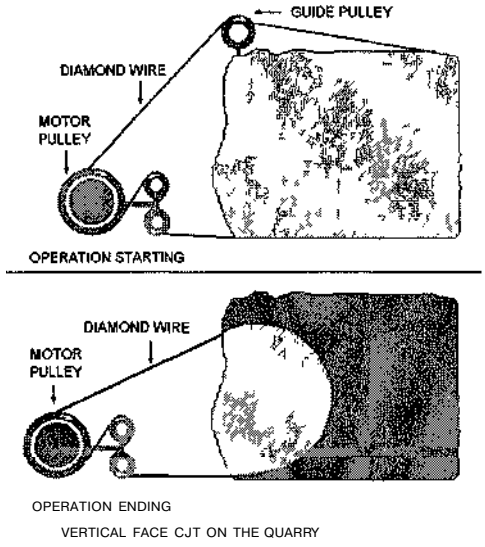

Figure 6 Vertical cut face on the quarry by diamond wire

Figure 7 shows one schematic view of winning blocks in quarries using the sawing cut with diamond wire In this figure it is seen on the left the sequence of separation of the great blocks with two cuts using diamond wire in the floor and the wall Next, the dismemberment of these great blocks by a series of parallel drill holes is shown until the desired dimen sions of the blocks are reached The right of this fig ure shows the diamond wire cuttmg_an immense block

Figure 8, shows the sawing equipment used m the quarry of Piracaia black granite, being possible to observe the metallic trail structure, with tracks, for its displacement

4 SEQUENCE OF BLOCK EXTRACTION

In Brazil, if a greater stone block is to be divided into smaller units in a quarry, as m the cases of granite rock boulder quarries, it is essential that the block in question be completely free around all its faces

For most dimension stone quarrying, the success of the art depends largely upon taking advantages of joints and cleavage planes in the rock

In the black granite rock there is a rift along which it may be split with comparative ease The rift of the black granite is the surface parallel plane (ı e , parallel to its outcrop) Unfortunately, this granite has no joints m the planes perpendicular to the rift that are the head and gram , along which it splits less easily in an orthogonal attitude

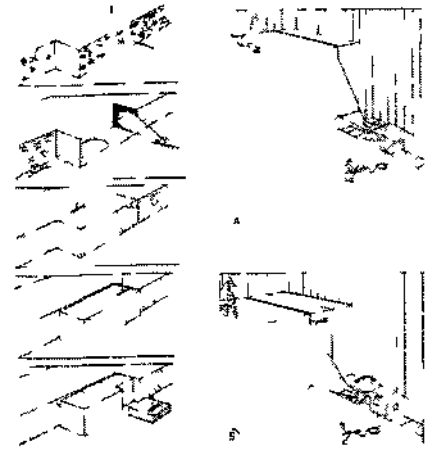

Figure 7 Block winning with diamond wire equipment

Figure 8 Diamond wire equipment at quarry

The head direction, which is the worst to split, is a direction perpendicular to the valleys, and the grain, or third direction of intermediate splitting is parallel to the valley

The head direction is the most difficult surface to obtain This surface is created by the use of the dia mond wire machinery (see Figure 9)

Currently, two groups of benches exist in the quarry, where the granite blocks are extracted The sequence of the unit operations of block exploitation consists of the following stages

1 Removal of the overburden,
2 Preparation of the group of benches to cut the great block
3 Cut in the vertical plane and floor by the diamond wire,

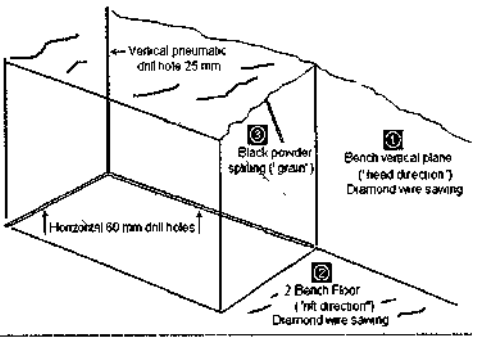

Figure 9 Schema of the holes opened to pass the diamond wire to detach great blocks.

4 Hand held drill is used to open a hole that is fired with black powder for dismemberment of the great block;
5 Final retaliation of the blocks to desired dimension with line of parallel drilling holes of small distance.

The first unit operation of exploitation of the quarry consisted of the removal of the soil overburden to display the bulk rock. This operation was carried through with conventional pressure water jet. Figure 2 gives a good idea of the thickness of this overburden.

Next, the advanced diamond wire system is used for clipping the great blocks. To do that, two stages are necessary: first the preparation of the group of benches for the cut, and finally the cut with the diamond wire.

In the preparation phase, two horizontal drill holes with 60 mm of diameter are carried through with special equipment, beyond a vertical drill hole opened with hand held pneumatic hammer. The three holes must meet in the heath of the rock; so that steel cables can be passed through them, and next to pull the diamond wire.

Figure 9 shows a project of these holes for the preparation of the group of benches for the separation of the great blocks.

Nor all granites present three orthogonal directions of partition. This is the case of the Piracaia granite. In the winning of blocks of dimension stone these directions are called rift, head, and grain. The rift is the most well defined direction, and the head of orthogonal direction to the plane of the rift is in general less well defined. In the case of the Piracaia granite, the grain, instead of its plane, isorthogonal, having an angle of 57°, which causes certain upheavals.

The two orthogonal drilled horizontal holes are elaborated on the plane of the rift. The hand held hammer opens a vertical hole orthogonal to this plane. Carried through these three holes, steel cables are crossed to make it possible to follow the passage of the diamond wires.

The following unit operation constitutes of the cut of two planes of the great blocks with the diamond wire equipment. The machinery of the diamond wire cuts the two planes, one at the base of the great block in the direction of the rift, and the other in the direction of the head. Figure 8 shows the employed diamond wire machine.

This machinery works on a rail structure that permits its dislocation to obtain the cut. The guide of tracks permits vertical or horizontal slots to be cut.

Figure 10 shows a detail of its guide pulley.

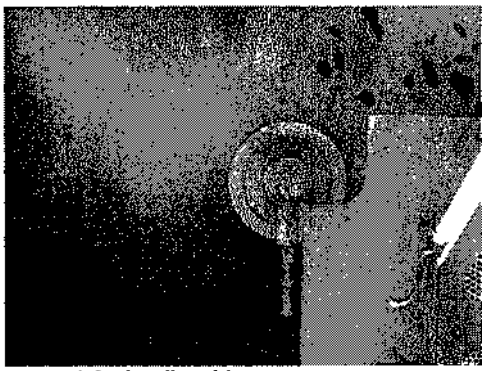

Figure 10 Guide pulley of the equipment.

Figure 11 shows a detail of the surface generated by the sawing of the granite with the diamond wire.

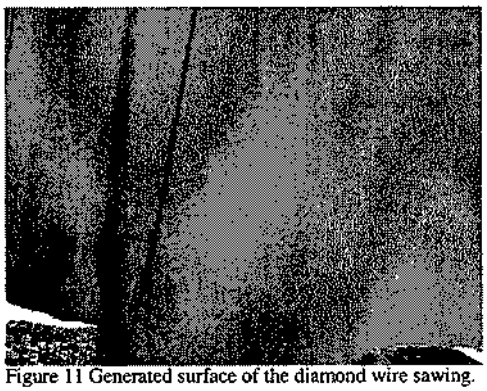

Figure 11 Generated surface of the diamond wire sawing.

The great blocks are next subdivided by following different cuts, so that they reach appropriate dimensions for handling and final transportation.

Thus an initial clipping is made by a hole made by the hand held pneumatic hammer and using as explosive black powder in the orthogonal plane of the grain.

Figure 12 shows a detail of this obtained cut, detaching the effect of obtained cut, the place of the drilled hole and the loaded black powder.

Figure 12 Black powders splitting of the great diamond sawed blocks

The last unit operation consists of the attainment of parallelepipedic blocks through the use of a series of closely spaced parallel holes drilled with the manual hammer.

In Figure 13 it is possible to see a worker doing this last unit operation, with the use of the hand held pneumatic drill. In this photograph, it is possible to sr~ better th^ v-r+ici' flee *n"* the bci-h ^enrnted "> ' ilk 1'ı inni J ı ,u «•\ in '

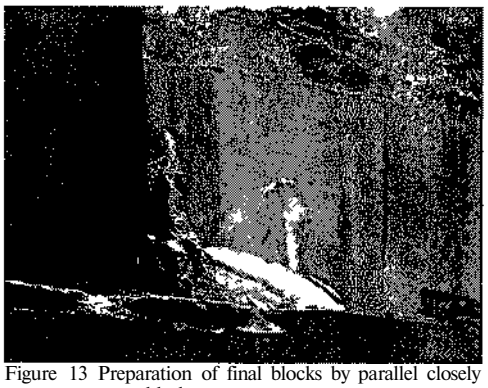

Figure 13 Preparation of final blocks by parallel closely spaced holes.

Figure 14 shows the details of a final block obtained by this technique.

Figure 15 shows a set of final blocks ready to be transported for further improvement in the beneficiation plant in the city of Piracaia.

5 OTHER PROCEDURES

For some types of rocks containing quartz in greater amount (above 30%) as in the case of other granites, flame channeling is employed. The rock shows the proper splitting (thermal breakage) characteristics for this method to be applied.

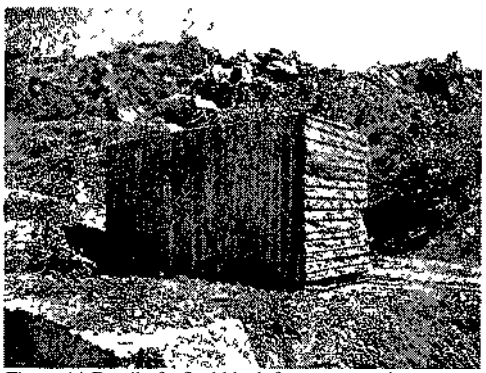

Figure 14 Detail of a final block for transportation.

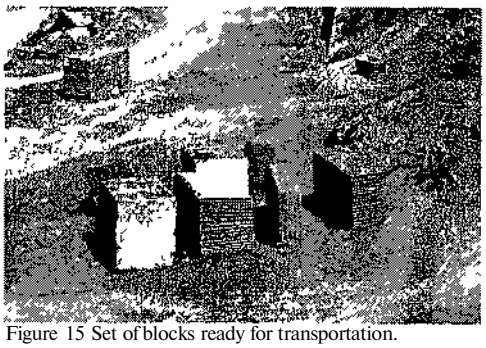

Figure 15 Set of blocks ready for transportation.

In the case of Piracaia black granite, whose amount of quartz is only at the level of 6%, this technique may not be easy to present good results. Experiments will be necessary.

Analyzed under environmental aspects, the technique of diamond wire sawing method is not noisy and the operator and his helper need not use individual ear protection equipment.

The productivity of the surface generation by the non-conventional diamond wire sawing equipment in this black granite is about four square meters per hour.

Laboratory assaying of Piracaia black granite was made to cut it with steel wires (Stellin et al, 2001). The productivity in this test shows that the sawing by steel wires using sand as abrasive is about 0.3 to 0.4 square meter per hour. When compared to other harder granites as the red Capào Bonito granite with

higher quartz content, there is a little higher productivity

6 TECHNOLOGICAL CHARACTERISTICS

The mam technological characteristic of black granite as dimension stone can be divided m petrography, general information, physical and technological specifications

In the area now under exploitation there are two different outcrops of rock, the most exploited in which the benches were open, coarser granular granite appears

Close to that area to the north, finer granular gran ite occurs

Two thin slides of the granite that characterize its petrography were analyzed under the microscope

Figure 16 shows a thm section of the normally exploited coarser Piracaia black granite, while Figure 17 presents a thin section of the finer type

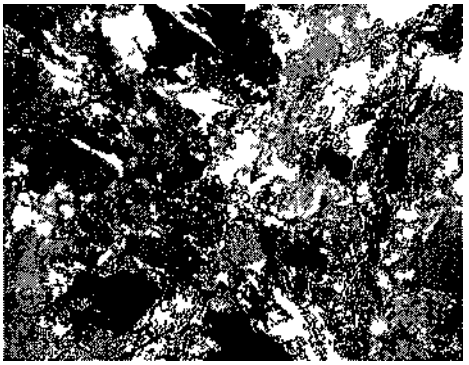

Figure 16 Thin section of coarser Piracaia black granite

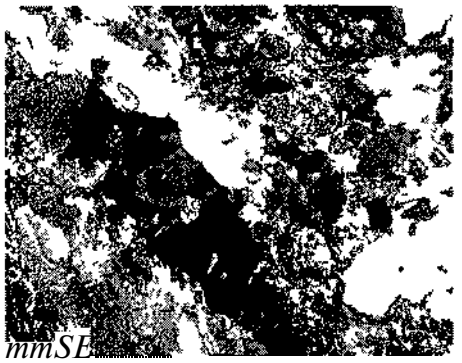

Figure 17 Thin section of finer Piracaia black granite

Regarding general information about the rock type, its commercial name, deposit type, geological reserves, present quarry production and its production capacity, and raw block dimensions, this data is given in Table 1

Table 1 General Information about black granite

Rock Type	Granite
Commercial Name	Piracaia black granite
Quarry location	Sao Paulo State Brazil
Deposit Tjpe	Massive Rock Quarry
Geological Reserves	>100 000 cubic meters
Monthly Production	100 cubic meters^
Production Capacity	150 cubic meters
Raw Block Dimension	From4 5 m to 7 5m

Table 2 presents the main pétrographie charactens tics of Piracaia black granite

Table 2 Pétrographie Charactenstics of black granite

Property	Characteristic
Common Color	Black
Structure	Massive
Uniformity	*JML*
Texture	Granular
Grain Size	3 to 10 mm
Microfissuraf State	Weak
Alteration Grade	Weak (hydrotermal)

Table 3 Physical Mechanical and other technological charactenstics of black granite (source Caruso et al, 1990)

Property	Value	Test
Dry Density	J2_844kg/nri	(ASTM C97 ABNTNBR12 766)
ApparentJ'orosity	0 50%	(AŞTMÇ97 ABNT NBR 12 766)
Water Absorption	0 18%	(ASTM C97 ABNT NBR 12 766)
Amsler Abrasionjlesistence	1 05 mm/lOOOm	JABNT NBR 12 042)
Impact Strength Test	0j!8 m	(ABNT NBR 12 764)
Linear Thermal Expansion	6 3 mm/m °C X 10î	(ASTM E288 ABNT NBR 12 765)
Compression Breaking Load at Natural State	167 1 MPa	(ASTM CI70 ABNT NBR 12 767)
Compression Breaking Load after Freezing/Thawing	1495 MPa	(ASTMC170 ABNT NBR 12 767)
Modulus of Rupture	15 75 MPa	
Bending Test	17 8 MPa	(ASTM C99~ ABNT NBR Ï2~763)
Staüc Deformabılity Modulus	J2963Gpa	JASTMTJ3148)
Ultrasonic Pulse Velocity	_m/s	(ASTMJJ 2845)
Ammonium Hydroxide (NH4OH)	Unaltered aspect	(ABNT NBR 9 446)
Sodium Hypochlonde (NaC10,H_2Q)	Unaltered aspect	

Ultrasonic pulse velocity 5,010

The mineralogical composition of Piracaia black granite has about 35% of Plagıoclase (andesıne-ohgoclase) 20-25% Hornblende, 15% biotite, 15% perthıtıc Microchne (+ Ortoclase), 5% of Quartz, about 5% of Sphene (+ opaque minerals) The other minerals that appear as accessories in less than 5% are Apatite and Epidote Secondary minerals are Carbonates The pétrographie classification of this granite is as a Bıotıte-hornblende quartz monzomte There are no great differences m mineralogical constitution between the finer and coarser types, only the size of crystals

In Table 3 are presented the mam physical, mechanical and technological specifications of Piracaia black granite associated with the used norms

For the determination of the parameters the tests used the standard proposed by the North American Norms (emitted by ASTM - American Society of Testing Materials) or by the Brazilian standard Association (ABNT - Associaçâo Brasıleıra de Normas Técmcas)

7 APPLICATION OF BLACK GRANITE

In this topic, after the description of the entire sequence to obtain blocks of black granite, some applications of the construction material will be discussed

The use of dimension stone has two mam applications in the market, as construction material or as art material

In the past, dimension block was used as a structural element of the buildings in civil construction

Today, the evolution of cıvıl construction makes use of tiles of dimension stone to cover only surfaces such as walls and floors, outside and inside Plates are also very largely used for lavatory parts

Many new skyscrapers of the city of Sâo Paulo used this black granite as an external cover, which gives to the building a respectable aspect

Due to its black color, its application as tombstone is also very common in all Sâo Paulo city cemeteries

REFERENCES

Caruso, L G et al "Catalog of Dimension Stones of the State of São Paulo," Secretana da Ciência, Tecnologia e Deşenvolvımento Econômico - *SCTDE PRÔ-MINÉRIO IPT* Institute de Pesquisas Tecnologicas do Estado de Sâo Paulo, Publıcaçâo IPT 1820 122 pp, 1990

Hennies, W T & Stelhn Jr, A 1996 Dimension stone industry and environmental preservation in Brazil In International Conference on Environmental issues and waste management m Energy and Mineral Production, 4, Caghan, 1996, *Proceedings SWEMP96* Caglian DIGITA UniversitédiCaghan, 1996 v1, p 75-84

Hennies, W T , Stelhn Junior, A , Cretellı, C , "Jet piercing application for red granite block mining in Sâo Paulo, Brazil," *Proceedings of the* S'" *International Symposium on Mine Planning and Equipment Selection,* pp 21 26, Dmpropetrovsk National Mining University of Ukraine, 1999

Hennies, WT , Fujımura, F , Stelhn Junior, A , Soares, L An overview on Dimension Stone Quarrying in Brazil In International Symposium on Mine Planning and Equipment Selection, 11"[1] Bousov, Czech Republic 2002 ,p 97 100

Stelhn Jr, A , Hennies, W T , Soares, L , Fujımura F 2001 Dimension Stone Block Extraction by Steel Wires In International Symposium on Mme Planning and Equipment Selection, 10* New Delhi, India, Oxford & IBH Publishing Co Pvt Ltd New Delhi, 2001, p 215-222

Soft Ground Reaction To Cyclic Loading By Large Mobile Mining Equipment

A.D. Sharif-Abadi
Ph.D. Graduate Student, AEGIS research group, University of Alberta, Edmonton, Canada.

T.G. Joseph
Director AEGIS, University of Alberta and Principal Engineer, JPi, Edmonton, Canada.

ABSTRACT: Essentially there are two different types of ground equipment loading condition in the surface mining industry: Systems that rely on tracks, roller paths, rollers and side frames and those that rely on tires, rims and suspension systems for motion. In both cases, the footprint created is variable, providing a ground loading that is a function of the kinematics of the machine and the ground performance properties. Marrying the two to get a complete picture of the ground - equipment interactions is a complex model of inter-related performance profiles. This paper looks at the cyclic loading phenomenon of soft ground in relation to the action of large mobile mining equipment, where footprint area, loading (change in g level) and relative stiffness of components from ground to frame are essential in understanding adverse operating conditions. A geotechnical overview of ground performance due to this type of loading condition will be presented.

1 INTRODUCTION AND BACKGROUND

To reduce the cost of mining, mining companies opt for large mobile mining equipment. In the oil sand, loading and hauling of material results in the biggest cost to the final product. Soft ground conditions, especially those of oil sand, have unique properties that have been widely studied to give a better understanding of that material behavior in various situations. Construction of large mobile equipment for soft ground adverse operations requires a good understanding of the interaction with adverse ground and vice versa. Laboratory and field tests aid a better understanding of this material. In this case, several triaxial tests were done. In addition, a simple plate load test was designed for a field testing equivalent.

Joseph (2003) reported that after only a few cycles, truck and shovels operating on soft-ground will become less stable. Trucks in summer are frequently loaded with less than their nominal payload due to poor rolling resistance conditions. Even with lower payloads the cycled ground after only a few passing trucks is unable to support the weight of the truck. In summer, ground has a lower stiffness compared to tire and suspension stiffness, consequently ground deformation is greater than that of the tire or suspension resulting in ground undulation. Rutted ground causes rack, roll and pitch truck motion that cause frame, suspension and tire fatigue.

For shovels, rocking during face activity in soft ground conditions after a number of cycles can result in sinking. In the oil sand case, ground softening occurs rapidly due to cyclic pressures (Joseph, 2002).

2 BASIC CONCEPTS AND ASSUMPTIONS

1. Oil sand beneath mobile equipment is already broken, described as loose and unlocked. However according to the coarse shape of the material, there remains considerable friction between particles.
2. As material is already broken and loose, there is no early discernable peak value with increasing strain, and the material expresses post-peak behavior before reaching a residual value.
3. The bitumen and water content comprising the oil sand fluid content remains relatively constant within a given mining block.
4. Oil sand is homogenous and uniform allowing the use of an elastic approach for analyzing this material despite its highly fragmented nature.
5. Pore pressures dissipate rapidly. Moreover, oil sand is not fully saturated, so pore pressures are

not a major concern in calculating the effective stress beneath the equipment.

6. As the material is broken near surface any exsoluting gas has already left the material and it is thus a negligible consideration to the bearing capacity of material the ground.
7. Figure 1 shows the concept that the pseudo-elastic stiffness of the post-peak reduces with increasing number of cycles.

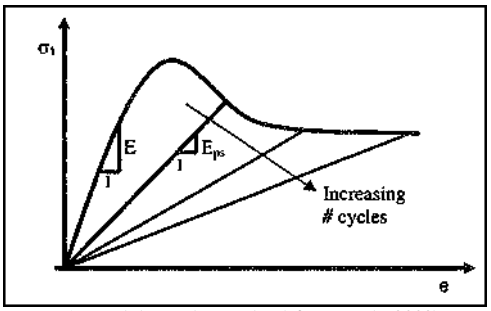

Figure 1 Modulus with # cycles (after Joseph, 2003)

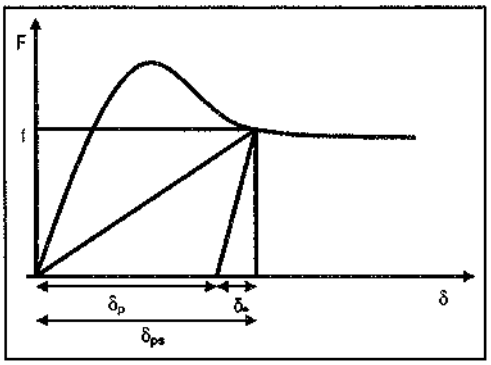

Figure 2 Total deformation (after Joseph, 2003)

8. The total deformation may be described as the sum of the elastic and plastic deformations, figure 2 and equation 1 :

$$\delta ps = \delta p + \delta e \qquad [1]$$

3 LABORATORY TRIAXIAL TESTS

Several triaxial test were done on 8% bitumen samples with a strain rate set at $72x10^{-6}$ per minute with a density of 2.0 to 2.1 g/cm^3. As the material is broken and loose, the prepared samples for use in triaxial cells required compaction to reach close to the field density. Figure 3 shows the stress-strain curve results for these tests.

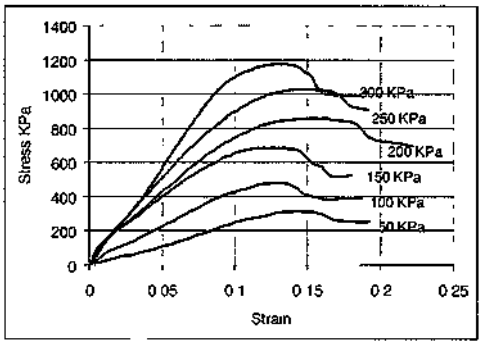

Figure 3 Tnaxial test results for 8% oil sand

A peak strain of around 0.15, because of the low range of confining pressures applied revealed a linear relationship between <3\ and 03, equation 2:

$$a, = 0.27Ö3 - 33.5 \text{ kPa} \qquad [2]$$

Further triaxial tests were performed on samples with 11 % bitumen content, figure 4. The strain rate was kept the same as before, with the only difference being using a hydraulic jack to compact the sample in a metal cylinder to reach the field density.

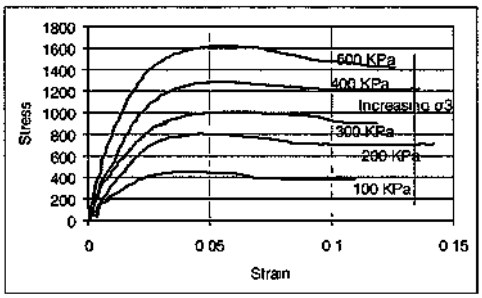

Figure 4 Triaxial test results for 11% oil sand

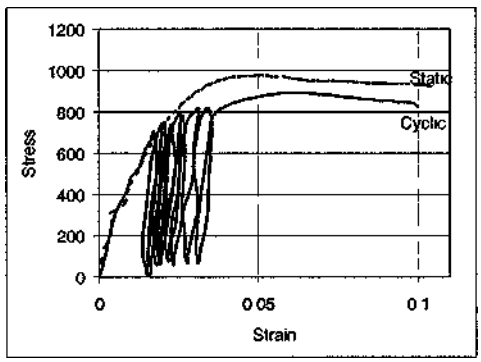

Figure 5 Laboratory cyclic triaxial at 03 = 300 kPa

In addition to static triaxial tests, three tests were done under cyclic loading at varying confining pressures. The aim of the cyclic loading tests was to show that large mobile mining equipment can induce early failure in underfoot materials leading to early residual values. Figure 5 shows the cyclic loading compared to the static loading for a 300 kPa confined sample, revealing a lower peak strength realization.

The purpose of the triaxial tests was to identify the induced confining pressure to compare with field tests and infer the field induced confinement. Softening of the ground with cyclic loading is the mechanism by which mobile mining equipment loads the ground.

4 FIELD TESTS

A cyclic plate load test was designed to help understand the behaviour of oil sand under the cyclic loading action of mobile mining equipment. Study of such ground behavior in a laboratory environment is difficult especially for near surface material. Figure 6 shows the field set up.

A hydraulic loading cylinder was attached to the rear hitch of a % ton light vehicle, actuated by a hand pump for simplicity. A load cell was placed between the hydraulic cylinder and plates of varying dimension as the contact surface with the ground. A linear extensometer was used to provide accurate ground deformation, referenced to a frame independent of the loading system and the light vehicle. The plate was then loaded for a given period of time, unloaded and reloaded to effect the cyclic motion reminiscent of mining equipment loading frequencies. The output was recorded to a standard data acquisition system.

Tests were carried out with three different plate sizes. Table 1 shows the plate sizes and maximum stresses reached during the tests.

Table 1 Cyclic plate size and test information

Plate size class (cm)	Max stress (kPa)	Test time (minutes)
Large, 14.9	300	9:39
Medium 11.43	390	1:21
Small 7.62	930	2:00

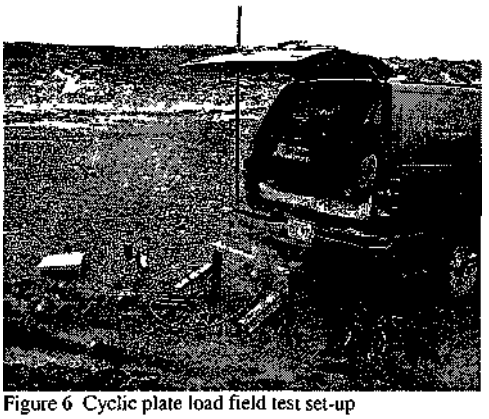

Figure 6 Cyclic plate load field test set-up

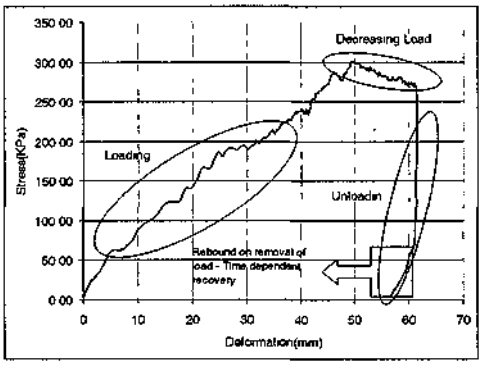

Figure 7 Stages of a single cycle plate load test

Confining pressure induced during the test is a function of plate size. Plastic deformation is also a function of induced pressure and the number of loading cycles. The rebound of the material after removing the load is time dependent and related to confining pressure. The different stages of the tests are shown in figure 7.

Figures 8 and 9 show pressure stiffness-deformation curves for loading and decreasing load stages, which show that stiffness decreases with increasing deformation and is independent of plate size.

Figure 10 illustrates the stress-deformation relationship for oil sand for a cyclic test of around 46 minutes duration and containing 7 cycles. Unloading and loading slopes are relatively constant. As oil sand has a viscoelastic behavior, the rebound cycle is time dependent.

Figure 11 shows the plastic and elastic deformation components of the cyclic test with respect to time, where the elastic deformation bounded, converging to a constant value.

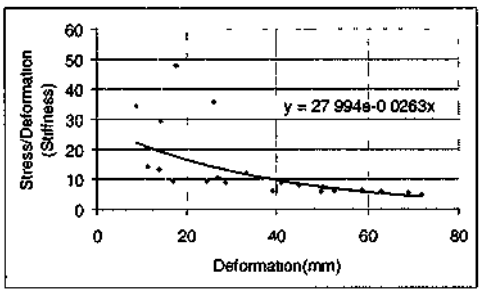

Figure 8 Changing ground stiffness during loading

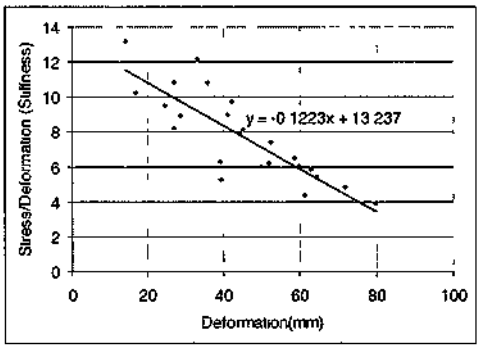

Figure 9 Changing stiffness during unloading

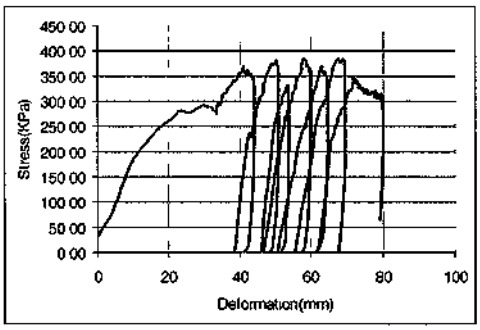

Figure 10 Stress-deformation curve for a cyclic test showing unloading-loadmg cycles

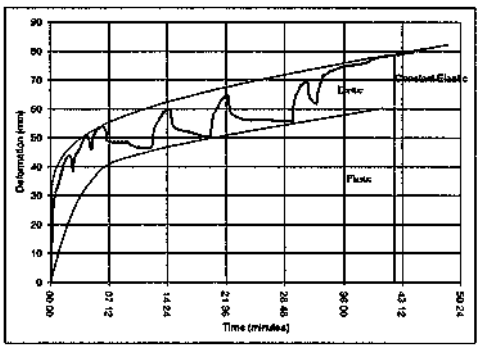

Figure 11 Plastic and elastic deformation

5 FIELD VERSUS LABORATORY TESTS

The main objective of comparing field and laboratory data is to evaluate the induced confining pressure in the field as a function of applied load. Solving this correlation is mathematically complex. Therefore, as a first approximation, matching the triaxial test curve to the plate load test curve was performed to give on estimation of the induced confining pressure by applied load. Figure 12 shows the matching of laboratory and field test data for two tests. The figure shows that the matched loading condition is related to the residual strength of the triaxial specimens. Not surprising considering the highly disturbed nature of the in-pit field material.

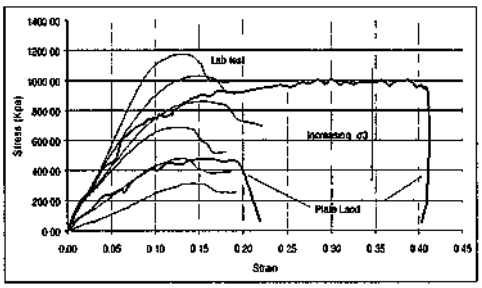

Figure 12 Comparison of field and laboratory data

This method gives us the ability to define a relationship between induced confining pressure and applied load. The induced confining pressure is effectively the horizontal stress in the field. Given this information it is possible to assign an appropriate confining pressure for numerical modeling purposes.

It is also possible to infer a Poisson's ratio from the ai - o'3 relationship given the widely expected relation, equation 3.

$$\sigma_H = \left(\frac{v}{1-v}\right)\sigma_V \qquad [3]$$

Figure 13 yielded a value for Poisson's ratio, v, of 0.22, lower than expected from previous historical evaluation at -0.25 and industry use at 0.31.

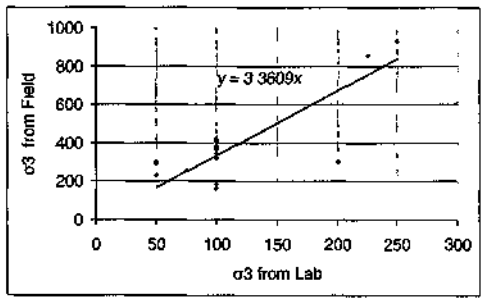

Figure 13 Ci versus a_3

6 MODELING OF A PLATE LOAD TEST WITH FLAC - AKIN TO A TRACK PAD

Numerical modeling of a plate load test allows the investigation of a simplified pseudo-elastic approach to predicting ground deformation during loading. Here the basic assumption is that oil sand is uniform and homogenous, such that load deformation behavior in akin to elastic, although permanent deformation occurs. Flac 2-D was used to model the plate and ground, as the software provides user defined constitutive modeling. Three different plate sizes were modeled. Holding Poisson's ratio constant and varying the pseudo-elastic modulus, (inherently including any changes in Poisson's ratio), with applied confining stress such that E = (25*ff3 +1465), the following results were found.

The larger plate results showed that a confining pressure of around 50 kPa is induced with deformation at the point the load reaches a constant value, and is accurate to ±15% of actual field values. Figures 14 through 17 show the output vertical and horizontal stress, vertical deformation, and 03 for the large plate configuration.

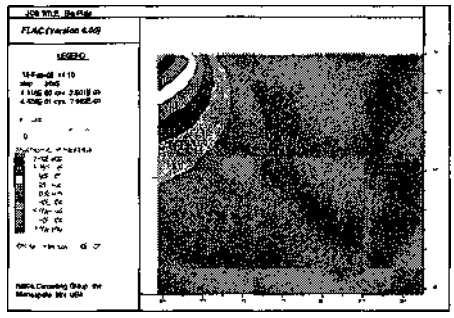

Figure 14 Flac 2-D output vertical stress

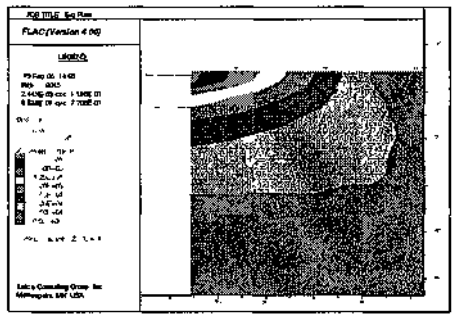

Figure 15 Flac 2-D output horizontal stress

The output from the Flac 2-D model yielded the same induced horizontal stresses estimated from the laboratory - field physical data comparisons, and deformations + 15% of those measured in the field.

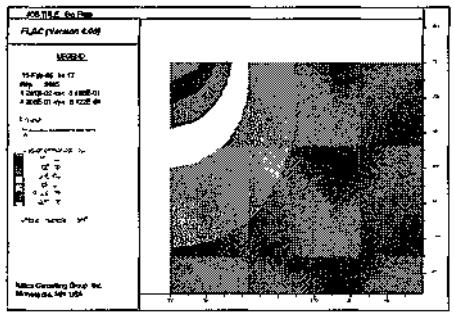

Figure 16 Flac 2-D output vertical deformation

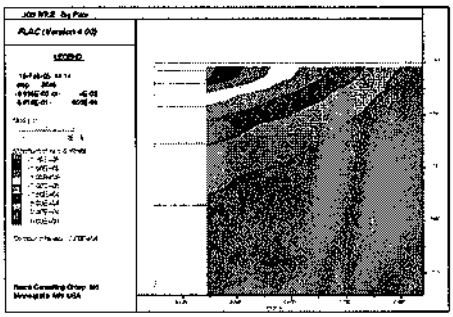

Figure 17 Flac 2-D output confining pressure o_3

7 MODELING OF INDUCED GROUND STRESSES BELOW A HAULER TIRE

Matlab was used to estimate the induced horizontal stress in the oil sand due to the action of truck tire. Use was made of the Boussinesq assumptions for homogeneous, isotropic, weightless, elastic conditions in half space with a concentrated vertical load, which were considered appropriate for use for the assumed homogeneous oil sand material. Treating the ground material as pseudo-elastic allowed an estimation of the stresses to be made.

For an ultra class haul truck, such as a Caterpillar 797, where the tire-ground contact area ~ 1.3 m^2 at lg loading, and given the gross vehicle of - 637 tonnes, such that each tire is loaded by - 1 MN.

For simplicity it was considered that the width of the truck compared to the tire is big enough such that one side of the truck does not influence the other, in terms of ground loading. An assumption that is not necessarily true for real duals, but certainly a reasonable approximation at this level of analysis.

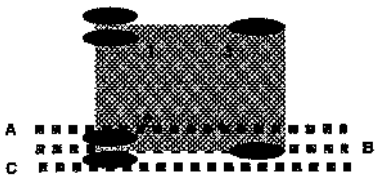

Figure 18 Sections referenced in Matlab output

The output from the Matlab analysis is referenced to the ground cross-section B as indicated in Figure 18.

Figures 19 and 20 show the vertical, horizontal and principal stress output from this analysis.

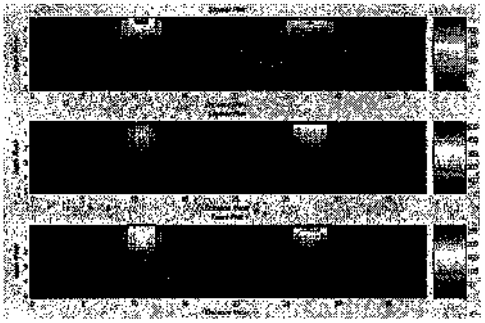

Figure 19 Vertical and horizontal stress; section B

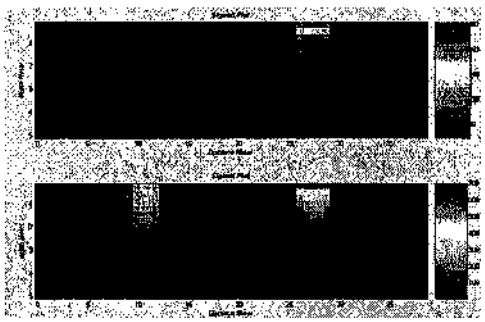

Figure 20 Principal stresses; section B

The Matlab output for horizontal stress prediction, given a known vertical stress, confirmed the output from the Flac 2-D analysis and was verified by the laboratory - field physical data acquired.

8 CONCLUSIONS

It has been shown that the induced horizontal stresses in soft ground, such as oil sand, can be inferred and predicted from the loading condition due to large scale mobile mining equipment operating at surface. This has been verified by correlations between the field and laboratory test data.

The assumption that the ground is homogeneous and can be treated in a pseudo-elastic fashion is made valid by the agreement between the two physical modeling and the two numerical modeling approaches employed.

A simple cyclic plate load test has been conceived and validated m the field, which may be used by the mine operator in verifying the suitable stability of soft ground before moving large mining equipment into the vicinity for operation Such simple use might determine deformational response of the ground for a know pressure loading due to the size of the equipment

Figure 11 shows that the elastic deformation of the ground is constant, despite the fact that the pastic deformation increases to a constant level at a large level of deformation

REFERENCES

Joseph, TG, Shanf-Abadi, AD and Shi, N, 2003, A broken material approach to modeling oil sand under dynamic load, Proceedings of the 4lh International Conference on Computer Applications in the Minerals Industries (CAMI 2003), September 8 - 10, Calgary, Alberta, Canada

Joseph, T G, 2002, OsEIP The Oil sand Equipment Interactions Program, *CIM Bulletin*, 95, pp 58 - 61

A Brief Comparison of Longwall Methods Used at Mining of Thick Coal Seams

M. K. Özfirat, F. Şimşir, A. Gönen
Dokuz Eylül Üniversitesi, İzmir, Türkiye

ABSTRACT: There exist several different methods in Turkey and in the world to operate longwalls of thick coal seams in underground mines. The most important ones are Single Pass Longwall (SPL), Multi-Slice Longwall (MSL), and Longwall Top Coal Caving (LTCC). In this paper these methods are compared to eachother both from the technical and economical perspectives. The advantages and disadvantages of each method are discussed. Finally it is stated that the future trend in operation of longwalls is towards LTCC method all over the world.

1. INTRODUCTION

Total lignite reserves of Turkey amount to approximately 8 Gt, which constitutes 1.52 % of total world reserves. In 2003, totally 60 Mt lignite is produced in Turkey, of which 29 Mt is mined by state-run enterprises and the rest by private companies (Mine Exploration Institute, MTA, 2001; Turkish Coal Enterprises, TKI, 2003). About half of the lignite reserves constitutes of thick coal seams in Turkey (Köse et. al., 1989).

In Turkey, mining of thick coal seams is often carried out employing longwall methods. According to Hartman and Mutmansky (2002), longwall mining is an exploitation method used in flat-lying and tabular deposits, where a long face is established to extract the mineral. In coal longwall mining, large blocks of coal seam (about 300 m wide and 2 to 3 km long) are developed by driving headings, known as "gate roads" or "road ways" around them, and, then the so-called panel extracted in a single continuous operation. The gate roads are important components of longwall mining layout since they are the only escape and access ways to the longwall face.

In Turkey and Europe, main and tail gates have single entries (Figure 1). In these roads, commonly props (wooden or steel) and steel arches are used as support. On the other hand, in Australia, South Africa and the USA, the longwall face is formed by gates which have two or more entries. Chain pillars are left in order to provide support, also.

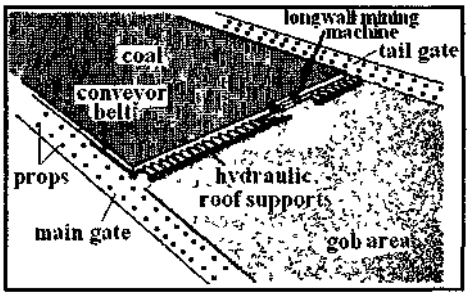

Figure 1 Plan View Longwall Mmmg

As a point of definition, the term thick seam is applied to any mineable seam thickness greater than the reach of existing development and longwall equipment.

In the 1980s and 1990s, this figure was interpreted as 4.0 m. However, with higher reach abilities of continuous miners and other longwall equipment, an arbitrary figure of 4.5 m has been adopted for all recent studies (Hebblewhite & Cai, 2004). In Turkey, it is assumed that the upper bound of coal seam thickness is about 6 m for employing single pass longwall (SPL) using mechanized equipment (Köse&Tatar, 1997). In India, for example, approximately 60 % of the mineable coal

reserves of the country belong to thick seams (seams thicker than 4.8 m) (Singh & Singh, 1999).

2. LONGWALL METHODS FOR THICK COAL SEAMS

In Turkey, several methods are used to mine thick coal seams. Methods most commonly used can be classified as follows;

-Single Pass Longwall (SPL)
-Multi-Slice Longwall (MSL)
-Longwall Top Coal Caving (LTCC)

2.1. The Single Pass Longwall **Method**

The SPL method has been gradually increasing both shearer and support heights from 4m and now up to 5m and above (Hamilton, 1999). Although essentially the same as current longwall mining practice, it has technical, equipmental and operational limits at a height of approximately six meters, within the foreseeable 10 to 15 year future (Hebblewhite, 2000). The option of extending the height of a conventional single pass longwall has some limitations such as equipment size, weight and stability, coal seam properties and face conditions. For example, due to existence of soft dirt band in PARK Mining's sector 'C in Çayırhan, Turkey, a coal seam of 4.2 m thickness is mined out by the SPL method (Figure 2) (Por, 2002).

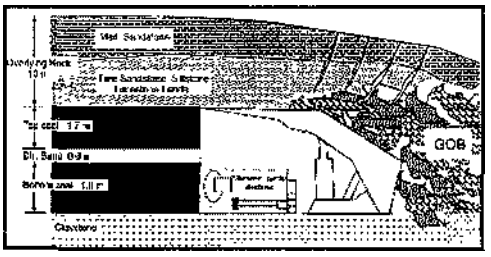

Figure 2. SPL Method in Park Inc. (Por, 2002)

2.2. The Multi-Slice Longwall Method

The multi slice longwall (MSL) method, whereby conventional height longwalls are operated sequentially, in the top half of the seam and then immediately below in the bottom half (using some form of artificial floor/roof between the two or three slices), remains a technically viable option (Hebblewhite, 2000).

SPL cannot be applied to seams which are more than six meters of thickness. In such cases, the thick coal seam should be divided into slices. In flat and low inclined seams, these slices are men extracted parallelly to hanging wall and footwall.

In steeper seams, mining have to be carried out as horizontal slices (Köse&Tatar, 1997). This method is being applied in Soma lignite region where the seam is 15-22 m thick. At PARK Mining's sector 'A' where the dirt band is hard, coal is mined by MSL from two faces, having heights of 1.9 m and 1.7 m, respectively (Por, 2002).

Depending on local geology, different methods are employed to extract thick coal seams in China. If a thick seam lies flat or is moderately inclined, it is usually mined either using one-pass mining with shearers specially designed to cut seams between 2.3 to 4.5 m, or using the multi-slice method where seams are divided into slices horizontally but separated by thin layer of coal and an artificial roof between slices (Xu, 2001) (Figure 3).

At the MSL method, wire mesh requires too much labor. Here, the wire meshes and the canopy should be kept in the same plane to reduce the tensile stress in the wire meshes so they will not burst. In order not to cut the wire meshes, the cutting drums of the shearer or the teeth of the plow should not run near the roof (Peng & Chiang, 1984).

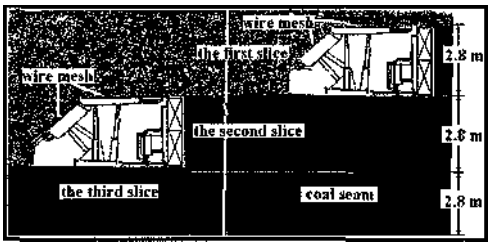

Figure 3. Multi-Slice Longwall (Xu, 2001)

In comparison with top coal caving method, the slicing method is of lower output, higher production cost and less safety (Xu, 2001).

From the economic point of view, investment costs for the panel in MSL are twice higher than at the LTCC method (Köse et. al., 1989).

2.3. The Longwall Top Coal **Caving Method**

In Turkey, the LTCC method has been applying for many years. It is based on the 'Soutirage' longwall caving method originally developed in the French coal mining industry.

In caving methods, usually one face is operated on the base of thick coal seam and the coal left on top is taken from the window of roof support (Figure 4a). The difference of the LTCC method applied in Australia and China from the one applied in Turkey is that there is a rear conveyor which transports the coal behind the face (Figure 4b).

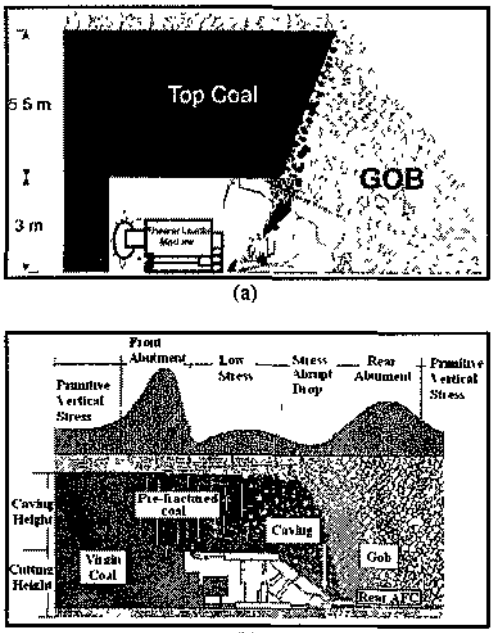

Figure 4. LTCC Method in Turkey (a), in China (b)

LTCC is preferable due to its lower face investment and labor cost (no wire mesh). Apart from these advantages, shortest roads are to be developed and minimum equipment is used in the same panel, achieving the result of the lowest production costs. The slicing method, in contrast, ensures a high recovery rate, but requires a new pair of gate drivages and a new set of equipment for each slice. In addition, it requires the infrastructure roads, to which the gate roads are linked, to be maintained for a long period of time.

However, there is a certain disadvantage of this method. This is the high coal loss occuring during the production of the top coal, resulting in a significant decrease of coal recovery. In the study of Şenkal et. ai. in 1988, it is found that 24 % of the coal reserve of a panel operating by LTCC is left behind the face. Today, in the same thick coal seam, about 20 % of the production is being left in the gob which causes spontaneous combustion.

Similarly in China, the caving method normally results in a somewhat lower recovery percentage, about 80-85%, comparing with 97% recovery by slicing method. However, the caving method has facilitated the control of support operators because of several years practice, the coal recovery percentage is increasing year by year (Xu, 2001).

3. DISCUSSIONS AND RECOMMENDATIONS

The LTCC method is advantageous compared to the MSL method since it is more economical, easier to be applied in thick seams and requires less labor. In China, only 5 % of thick coal seams are mined by the MSL method.

The Xinglongzhuang mine in China, where the coal seam is 8.6 m thick, a total of 6.1 Mt is produced from the two LTCC faces. Today, in China, this method is used even in seams of 15 m thickness. The negative sides of the LTCC method are the coal left behind the face and the danger of spontaneous combustion. Spontaneous combustion is controlled primarily by careful ventilation balancing. As long as the operator of roof support accomodates to the system, the production efficiency would increase to 90 % from 80-85 % (Xu, 2001).

For instance, let assume a coal seam of 10 m thickness. Here, two alternatives to operate the seam can be recommended. The first one is extracting the seam as four slices of 2.5 m height each. The reason selecting such a height is that becuase it is the most economical value considering production recovery, equipment costs, labour costs and the characteristics of coal seam, besides hanging wall and footwall conditions (Köse&Tatar, 1997).

Second option is to operate 2.5 m from the base by the LTCC method and let the rest 7.5 m cave in, which would be produced from the rear conveyor behind the face. Face equipment required in the MSL method (with four slices) is four times more than the equipment required in the LTCC method. In addition, if the top coal recovery is increased (> 80 %), the LTCC method will be more economic and advantegeous. In conclusion, eventhough the loss of coal in the LTCC method is a negative effect, the LTCC is still preferable to the MSL method due to its advantages.

4. CONCLUSIONS

Mines which are more than 6 m thick cannot be operated by the SPL method. At these mines, either

the MSL or the LTCC method is employed In Turkey and the whole world (especially m China) the MSL method is replaced by the LTCC method Production capacity with the MSL method, which is around 1 Mt of coal yearly, can be increased up to 4-5 Mt by the LTCC method due to less labor, no necessity for wire mesh, and shorter time for development Hence, according to the amount of production, the LTCC method is preferable compared to the MSL method in thick coal seams.

REFERENCES

Hamilton, N , (1999) Single Pass Thick Seam Longwall Experience at West Wailsend Colliery, Second International Underground Coal Conference, UNSW, Sydney, Australia, 15-18 June, 1999, pp 55-61, ISBN 1876315 17 2

Hartman, H L & Mutmansky, J M , (2002) Introductory Mining Engineering, 2nd Edition, ISBN 0-471-34851-1, p 584

Hebblewhite, B , (2000) Review of Chinese Thick Seam Underground Coal Mining Practice, The Australian Coal Review

Hebblewhite, B K & Cai, YI (2004) Evaluation of the Application of the Longwall Top Coal Caving (LTCC) Method m Australia, UNSW Mining Research Centre School of Mining Engineering, Sydney, Australia

Kose, H & Tatar, Ç, (1997) Underground Mining Methods, Dokuz Eylül University Press Unit, Izmir, p35 (in Turkish)

Köse, H, Şenkal S , Aközel A (1989) Is The Cavmg Method Application In Longwall Mining Which Are Most Commonly Used In Turkish Thick Coal Seams Economical[9], 11* Turkish Scientific and Technical Mining Congress, Ankara, 24-28 April (in Turkish)

Peng, S S , Chiang, H S , (1984) Longwall Mining, John Wiley& Sons, Inc , pp 274-333

Por, S , (2002) Investigation of 'C Sector in Park Inc , Undergraduate Thesis, D E U Engineering Faculty Mining Engineering Department, Izmir (in Turkish)

Şenkal, S , Köse, H , Errmşoğlu, N , (1988) Examination of Coal Loss Appearing In Underground Production System of GLI Tuncbilek Region, Mining, December, Volume XXVII, No 4, pp 5-12 (in Turkish)

Singh, R & Singh, T N , (1999) Investigation into the Behaviour of a Support System and Roof Strata during Sublevel Caving of a Thick Coal Seam, Geotechnical and Geological Engineenng 17 21-35, Netherlands

Xu, B , (2001) The Longwall Top Coal Caving Method for Maximizing Recovery at Dongtan Mme 3rd Intl Underground Coal Conf, UNSW, Sydney, Australia, ISBN 0 7334 1812 0

http //www mta gov tr (in Turkish)

http //www tki gov tr (in Turkish)

Optimizing Shovel Dipper Design for Cutting Soft Rock and Soils

N. Shi, M.A.Sc.
Ph D Graduate Student, AEGIS research group, University of Alberta, Edmonton, Alberta, Canada

T. G Joseph, Ph D., P.Eng
Director AEGIS, University of Alberta, and Principal Engineer, JPi, Edmonton, Alberta, Canada

ABSTRACT The design of dippers for cable shovels has essentially remained unchanged for the last 100 years In the past 10 years shovel manufacturers have started taking another look at dipper design, resulting m changes that have bome models from the major manufacturers that address some of the wear conditions and material retention problems that dominate maintenance and operational costs However, with the exception of added lateral curvatures to the front and corners of the dipper, the geometry is essentially unchanged This paper looks at the criteria that have resulted m the first new cutting dipper design in a century The design is based on kinematic considerations, reflected in a revolutionary geometry that matches the range of motions of the shovel, designed to minimize wear, impact loading and power required to dig, thus maximizing productivity for a minimum energy requirement The shape configuration is such that the weight of the dipper through wall thickness is reduced, enabling a larger capacity dipper to be conceived for the same shovel Benefits are reflected m reduced operational and maintenance costs and increased productivity

1. INTRODUCTION

Electric cable shovels are the most extensively used high volume excavators in open pit mining Previous work to improve the production capability of these units focused on updating mechanical and electrical components and optimizing utilization and operational approaches Little work has been done to improve dippers and their ground interactions, (ACARP, 2002) With the trend of higher production forcing the development of ever bigger, faster and smarter cable shovels there is a need to move beyond the aging geometry of dippers, relatively unchanged in the past 50 years

In the Athabasca oil sand deposits of Northern Alberta, Canada, mine opeiators employ the biggest cable shovel models with dipper capacities upwards of 44 m However, the same wear and impact associated ground-equipment interference problems plague these monster class shovel dippers, as have continually done so for the past decade Original equipment manufacturer (OEM) variations have concentrated on internal wear and retention issues, but pay no heed to the actual kinematics and high external problems that predominate

In recent years computer simulation techniques have dominated industry's approaches to system or product design These have many obvious economic and logistical advantages over physical modeling approaches, however verification remains m field application Shear size and expense of building a full scale physical prototype forces many OEM's to rely on the feedback of customers, often on an as-built basis, where failure has dire consequences on the OEM-operator relationship Consequently physical models are frequently much smaller than the full proposed design, and issues of scaling then come into question in the prediction of the full scale version Akin to this issue is one of simulation within the walls of an experimental facility versus the undisturbed virgin ground earth condition m the field It is virtually impossible to predict the performance without some scaled field testing, difficult to predict the effects of scaling and perhaps most of all to take that leap of faith on the part of both OEM and operator before any new design can make the transition to manufacture and utilization

The Alberta Equipment - Ground Interactions Syndicate (AEGIS) research group at the University of Alberta has been focusing on equipment-ground interactions for mining environments for a number of years An integrated simulation model and

methodology has been developed to investigate shovel duty cycles in connection with dipper performance. This paper presents the theory and methodology used in the modeling process. This includes an in-depth investigation of cable shovel performance where an understanding of ground interactive behavior is necessary. The paper concludes with a conceptual dipper design that will be field tested in the Athabasca oil sands in the subsequent research.

2. MODELING A SHOVEL DUTY CYCLE

The current P&H 4100BOSS cable shovel in operation in the Athabasca oil sands was used as a modeling example. It was assumed that:

1 All shovel components including the dipper attachments did not change relative position except for the dipper and handle assembly relative to the main structure during any given duty cycle.
2 The shovel was operating in a homogeneous oil sand ground material environment.
3 The working face dimensions were appropriate for oil sand mining, as illustrated in figure 1.

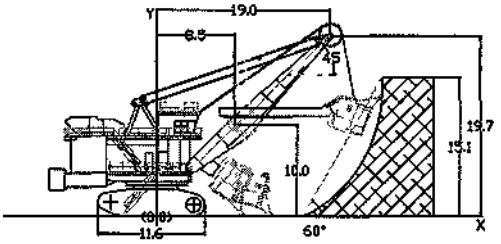

Units in metres

Figurel. Schematic of shovel and working face.

2.1 Modeling Considerations

There are 4 main considerations related to the shovel duty cycle:

1. The means of creating the dipper cutting forces necessary at the face, via an understanding of the hoist and crowd motor operating range of current, and voltage; the hoist drum and crowd gear speed, acceleration; and the overall efficiency from the motors to the dipper in each case.
2. The geotechnical properties of the face material being excavated to evaluate the resistance to the ground engaging tools. From one cycle to the next, the dipper trajectory resulted in a new face profile which in turn was considered a function of the face resistance for the next iterative cycle.
3. The geometrical position of the dipper, defined within an x-y coordinate system for a set reference point on the dipper relative to a vertical digging plane. The velocity and acceleration components of the dipper motion were determined by derivation of the x-y coordinate position. The sum of all forces acting on the dipper gave an instantaneous acceleration.
4. The geometry of the shovel as the system through which all kinematics were referenced. The geometric constraints of the shovel components, with the boom, handle, cable and bearing tracks arranged in a 2 dimension coordinate system, figure 2, relative to the centerline swing center gave the basis through which the components acted together.

All components of shovel interacted with each other in terms of inter-force and geometrical consistency, allowing a logical schematic of the simulation process to be defined, as shown in figure 2.

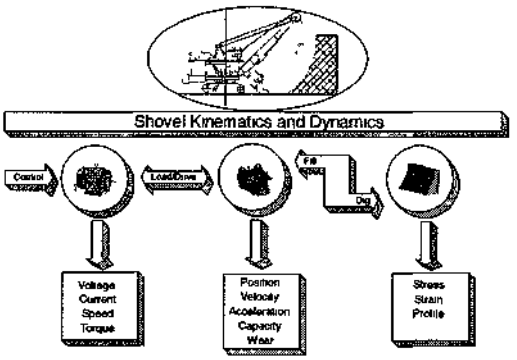

Figure 2. Schematic of the simulation process.

2.2 Subsystem Modeling

Three sub-models were developed to simulate digging duties in this research. These sub-models acted both independently and with each other. Each sub-model was based on specific equations to mathematically represent physical actions or material characteristics.

2.2.7 *Driving model*

The objective of this model is to describe the shovel response to resistance forces as the result of different digging positions or ground diggability, and vice

versa. The motor output torque controls the position and speed of the dipper. The theory was based on DC motors.

2.2.2 Kinematics and dynamics model

The objective of this model is to define a correlation between the dipper position, displacement, velocity, acceleration and forces. Theory was based on Newton's first and second laws, although the combination is complicated in term of a dynamic scenario, due to of the complexity of a ground-dipper interactions and the motors real-time response of the driving motors.

2.2.3 Ground digging model

This is the crux of the model as the most operating energy is consumed in this process. This sub model predicts the force distribution to the dipper resulting from the yielding and breaking of ground.

2.3 Schedule and sequence of modeling

Tasks commence with applying an existing dipper geometry and profile to the conceptual shovel model and then the shovel digging cycle. All the information in the model was recorded and the dipper performance was reported as an important output.

2.4 **Shovel digging cycle**

A typical operating cycle consists of a digging cut, a loaded swing to discharge, a dump, and an empty return to the digging face. The shovel is propelled periodically to the face. Operating practice was taken into account in the modeling (Martin, 1982), including:

1. The digging face should not be higher than the boom point sheave.
2. Crawlers should be perpendicular to the face centre.
3. Short frequent moves are recommended to keep the shovel close to the face, maximizing the effectiveness of the crowd and hoist forces.
4. The dipper should be lowered close to the truck body or hopper during the dump cycle.

The shovel geometry determines the maximum digging profile and minimum tuck position in relation to the shovel track dimensions, to minimize interference. These were computed via a 3D solid body collision detection technique. As a result, the shovel operating profile in the vertical and horizontal orientation was determined, as shown in figure 3. As an example, the shovel incremental advance step was found to be 3.77 meters.

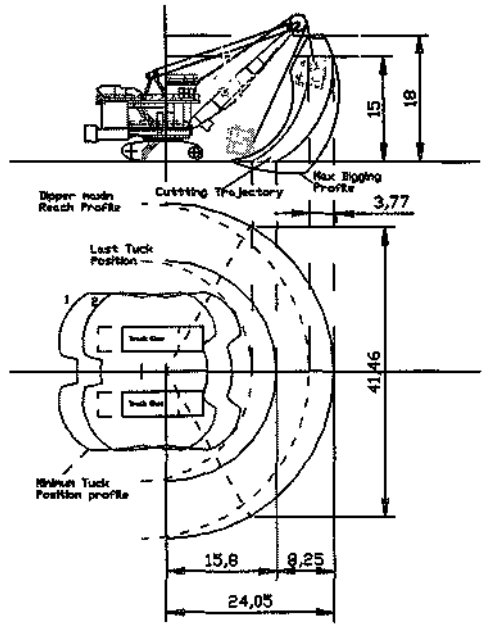

Figure 3. Digging body and cycle trajectory.

Two variations of shovel-truck loading were included in the model; double back up and single truck drive by, as shown in figure 4. This resulted in 2 alternative model swing times.

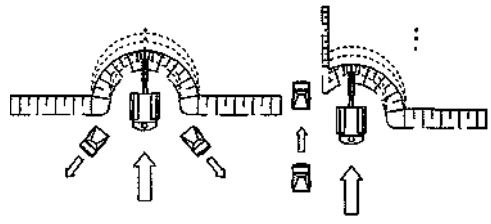

Figure 4. Shovel-truck loading variations.

Figure 5 illustrates a three dimensional digging volume calculation, and the proposal digging trajectories for a single sequence to dig this volume.

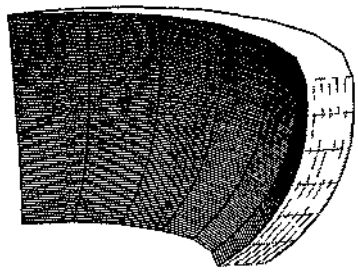

3D digging volume for a shovel move

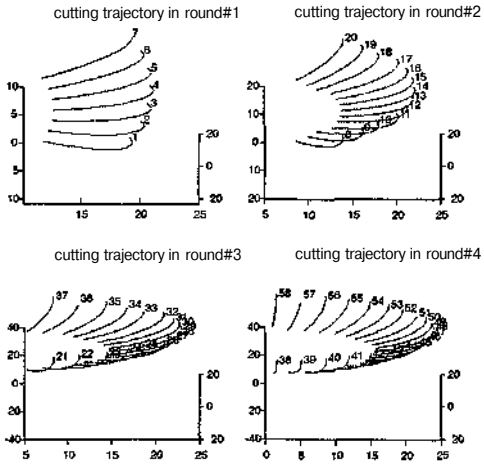

3D digging trajectones in an idealized sequence (View point 45 degree look down with projected x y z axis)

Figure 5 3D digging body and cycle trajectones

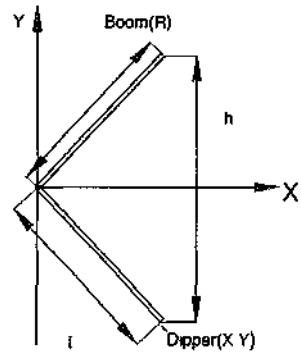

Figure 6 Simplified shovel geometry (after Daneshmend and Hendricks 1993)

Figure 7 shows the calculation variation used here

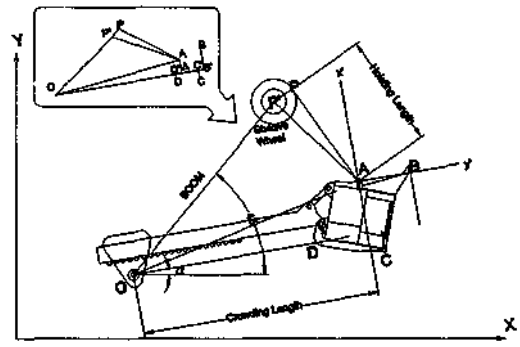

Figure 7 Shovel dipper geometry action

3. DIGGING KINEMATICS AND DYNAMICS

3.1 Kinematics

Daneshmend and Hendricks, (1993) developed a simplified kinematic model for generic shovels In their work, the position of the dipper is determined by the methodology in figure 6, m which R is the length of the shovel boom from the crowd arm attachment to its end, h ıs the length of hoist rope and 1 is the crowd arm extension

In the model, the handle is a line that is assumed to cross a corresponding connecting point on the boom The sheave wheel radius is neglected and assumed to be a point

The handle is connected to the boom via the saddle block, so that the distance (OA) from the dipper point (A) to shipper shaft, point O, is not equal to the crowd extension OA can thus be calculated via triangle OAA'

The rope is pulled or delivered via the sheave wheel, so that the tangential point (P') of the wheel and rope is not fixed, it can be determined via triangle APP'

The position of the dipper is represented by point A (the bail connecting point on the dipper) Two given variables, crowd extension and rope length, allow the dipper position in the digging plane to be determined

A local coordinate system is established, originating at point A and parallel to the handle, with X axis For any dipper position, A (X,Y) is known, and the handle angle (a) can be derived from A(X,Y) As a result, from a co ordinate

transformation matrix, T can be found. Any point on the dipper in terms of local co-ordinates (x',y') can be transformed into digging plan coordinates, figure 7.

3.2 Dynamics

Figure 8 illustrates the forces acting on the dipper and handle, in which Fs is the support force tangential to the handle referenced from the saddle, Fp is the crowding force referenced from crowding motor, Fh is the hoisting force referenced from hoist motor, Gd is the gravity of the dipper plus handle acting at its centre of gravity, Go is the mass in the dipper acting at its centre of gravity, Fcx and Fey are the resistance forces in the corresponding X and Y directions, Ffe is the frictional force acting on the external front wall, Ne is the normal stress acting on the external front wall, Ffi is the frictional force acting on the internal front wall, and Ni is the normal stress due to the mass moving acting on the inside of the front wall.

It is assumed that the rope is rigid and the output motor torque is equivalent to the force acting on the handle and dipper.

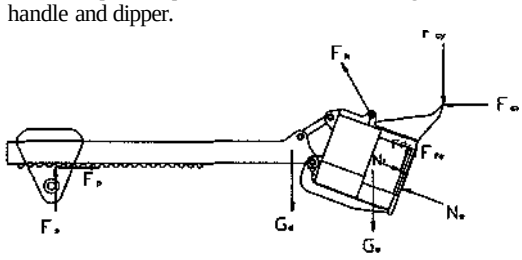

Figure 8. Dipper-handle acting forces

4. A THREE DIMENSIONAL DIPPER MODEL

The original dipper design, used over the past 50 years in industry, was first modeled in 3-D solid modeling software, illustrated in figure 9(a). Beyond the numerical simulation, several new dipper designs were also modeled, illustrated in figures 9 (b), (c), (d), and (e).

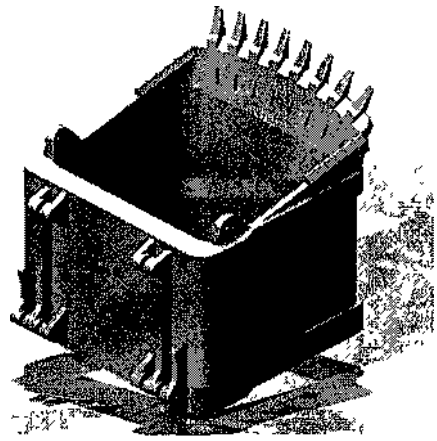

Figure 9(a). Original design with a linear front wall.

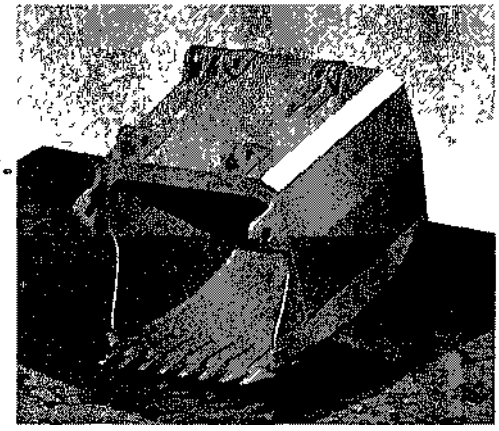

Figure 9(b). A skewed and curved concept.

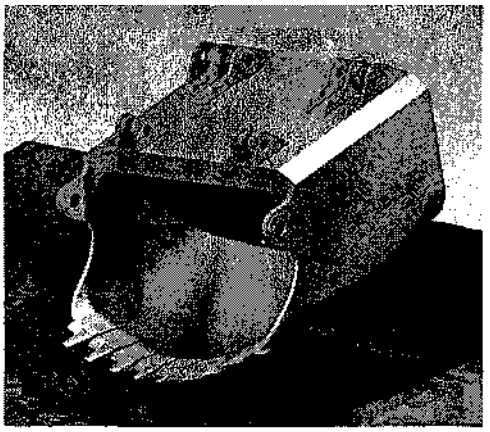

Figure 9(c). A double curve concept.

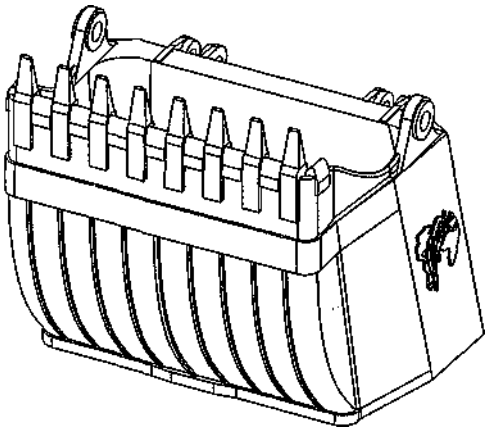

Figure 9(d). A curve and flare concept.

5. PHYSICAL MODELING

To prove the new design further, a three cubic yard dipper was fabricated to match a Dominion 500 cable shovel. This shovel was identified as having the same operating action and geometric orientation as the modern ultra class shovels at $1/20^{th}$ of the dipper scale. Both the new and original dipper will be tested in the field, allowing the relative performance data to be compared. Figure 10 shows this dipper and the matched door.

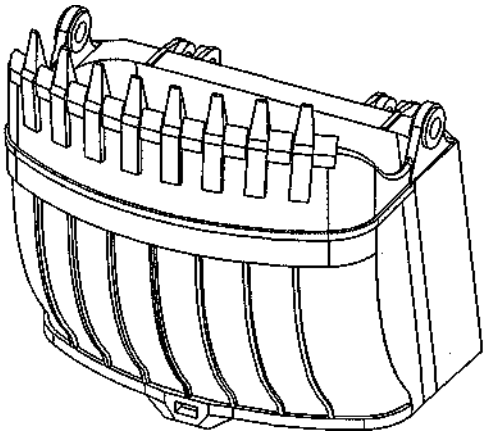

Figure 9(e) A double curve and flare concept.

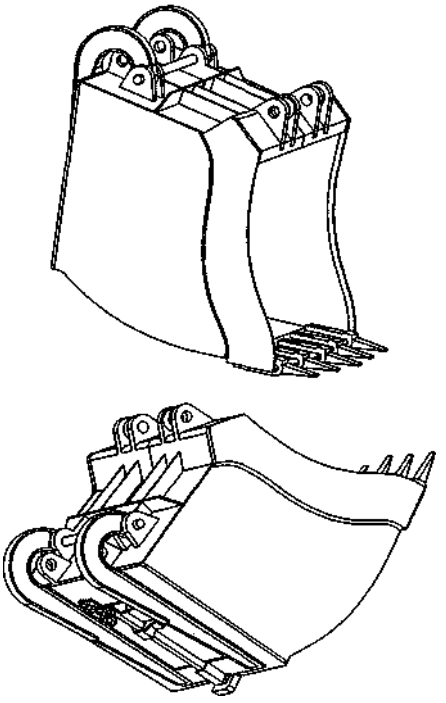

Figure 10. Scale three cubic yard dipper and door.

6. CONCLUSIONS & RECOMMENDATIONS

The dipper contribution to shovel production has not been fully investigated by OEM's and operators.

Most dippers in use are not optimally designed for specific environments Simulation and 3D computer modeling provides advantages over physical modeling, especially in terms of cost, speed and flexibility A specific model was developed based on an existing ultra-class shovel operating m oil sand conditions The simulation work of this model has led to a novel dipper design, which has a non-linear profile Three dimensional modeling has been utilized leading to the fabrication of a 3 yd^3 test model

The research in this paper did not cover the analysis of the dipper construction material, including strength and thickness issues Some in-depth work will be done in the future to optimize a section of the dipper wall to optimize the stress distribution when digging Three dimensional solid modeling makes this job much easy as long as the boundary conditions can be determined More accurate ground digging models will be developed Laboratory and field testing will verify these models

REFERENCES

ACARP, 2002, *Impwved Understanding of Shovel Dippers and Processes*, Internal report of Australia Coal Association Research Program, January 2002

Daneshmend, L and Hendricks, C, 1993, *Design of a mining shovel simulator* Proceedings of the International Congress on Mine Design, Kingston, Ontario 23 26 August 1993 pp 533-538

Martin, J W, 1992, *Surface Mining Equipment*, Martin Consultants, Inc, Golden, Colorado, 1st edition, June 1992

The 19th International Minin)! Conf;res.\ and Fair of Turkey, IMCET2005, Izmir, Turkey; June 09-12, 2005

Investigation of Rib Pillar Stability at Ömerler Underground Mine by Numerical Modelling

N.E.Yaşıth, B.Ünver & M.M.Ceyhan
Department of Mining Engineering, Hacettepe University, Ankara, Turkey

ABSTRACT: Due to dynamic nature of longwall mining method, strata behavior is rather complex leading to an ongoing variation of stress distribution around production areas. Modelling of strata response to production activity is a prerequisite to maintain a safe and efficient production. In this sense, numerical modelling is a very useful and powerful tool in understanding strata behavior and resultant stress distribution. This paper briefly presents the results of numerical modelling carried out by using FLAC^{3D} at Ömerler Underground Mine. A special emphasis has been given to modelling of stress distribution and stability of the rib pillar left between M2 and M3 longwall panels.

1 INTRODUCTION

Longwall mining is the only viable method of extracting thick coal seams in Ömerler Underground Mine. Leaving a sufficiently wide rib pillar between longwall panels is the common practice in the mine. An important aspect of the design of a safe longwall system is the dimensioning of rib pillars. Unfortunately, design of such systems is not well established, due to insufficient understanding of the yielding mechanism in coal pillars. Many coal bumps and roof fall accidents in coal mines are potentially associated with rib pillars and can be reduced by improving rib pillar design methodologies.

There have been numerous attempts in estimating the stability of rib pillar depending mainly on in situ measurements, physical and numerical models. This paper presents 3-D numerical stability analysis of rib pillar left between M2 and M3 panel at Ömerler Underground Mine. The numerical model was formed by using the commercially available software called FLAC^{3D}, based on the finite difference (FD) technique.

2 ÖMERLER UNDERGROUND MINE AND PRODUCTION METHOD

Ömerler Underground Mine is a subsidiary of Turkish Coal Enterprises and is located in the inner Aegean District of Turkey near Tunçbilek-Tavşanlı, Kütahya Province. The total proven lignite reserve in the district is approximately 330 million tons. The proven reserves suitable for underground and surface production are 263 and 67 million tons, respectively. The average calorific value of lignite in Tuncbilek District is 4500 kcal/kg, with an average sulfur content of 1.5%.

Production started at Ömerler Underground Mine in 1985 by retreat longwall with the top-coal-caving method. A conventional support system had been used until 1997, and then a fully mechanized face was established in 1997. The average depth below surface is approximately 240 m, and the 8 m thick-coal seam has a slope of 10° (Ünver & Yaşıtlı 2002).

Figure 1. A generalized stratigraphie column at Ömerler Coal Mine (Yaşıtlı 2002)

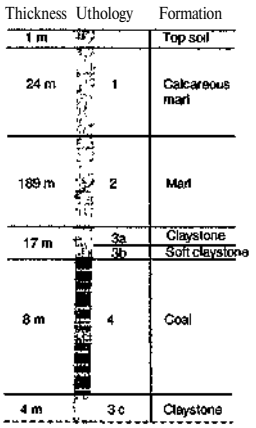

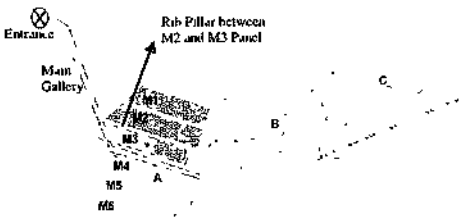

Figure 2. A simplified plan view of Ömerler Underground Mine (Yaşıtlı & Unver, 2005).

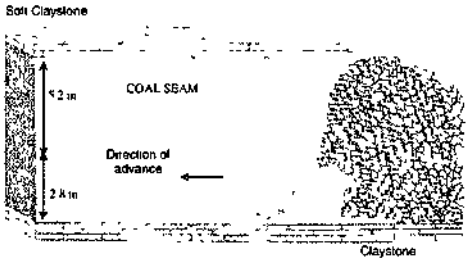

Figure 3. Longwall with top coal caving method as applied at Ömerler Underground Mine (Yaşıtlı & Ünver, 2005).

A generalized stratigraphie column showing the coal seam together with roof and floor strata is presented m Figure 1. Three main geological units named as claystone, calcareous marl and marl are present in the mine area (Destanoğlu et al. 2000) Physical and mechanical characteristics of coal and other units are presented in Table 1.

As seen in Figure 2, six panels were planned for extraction by means of fully mechanized production method in sector A. At the time of this study, two adjacent longwall panels namely MI and M2 had been completed and the production was carried out at M3 panel. Coal has been produced by means of longwall retreat with top-coal-caving production method where a 2.8-m-high longwall face was operated at the floor of the coal seam (Fig. 3). Top slice coal having a thickness of 5.2 m was caved and produced through windows located at the top of shields.

As it can be seen in Figure 2, there is a 16 m wide rib pillar between M2 and M3 panels. This value was determined by a previous study (Taşkın 1999). In this study, induced stresses and yielding characteristics of the lib pillar have been studied by means of numerical modelling.

3 GENERAL MODELLING PROCEDURE

Modelling was carried out with FLAC^{3D} which is used for stress and deformation analyses around surface and underground structures excavated in both soil and rock. This software is based on the finite difference numerical method with the Langragian calculation. The finite difference method can be better applied to modeling of stress distribution around underground mining excavations in comparison to other numerical techniques. (Itasca 1997, Yaşıtlı & Ünver 2005).

Modelling for estimation of stresses around the longwall panel has been performed in five steps. The steps called A, B, C, D and E are as follows:

A- Determination of boundaries and material properties,
B- Formation of the model geometry and meshing
- Determination of the model behavior,
C- Determination of the boundary and initial conditions,
- Initial running of the program and monitoring of the model response,
D- Réévaluation of the model and necessary modifications,
E- Obtaining of results.

Table 1. Physical and mechanical properties of coal and surrounding rocks (Taşkm 1999, Yaşıtlı 2002).

Formation	Defmition code	Unit Weight (MN/m')	Uniaxial compressive strength (MPa)	Indirect tensile strength (MPa)	Internal friction angle ◊ O	Cohesion c (MPa)	Modulus of elasticity E (MPa)	Poisson's Ratio v
Calcareous mail	1	0.023	29.2	3.9	47	12.5	5520	0.26
Marl	2	0.022	16.1	1.9	31	5.0	2530	0.25
Claystone	3 a	0.021	14.4	2.3	32	3.18	1480	0.28
Soft claystone	3b	0.023	8.7	1.8	15-35	-	2040	-
Claystone	3c	0.024	26.5	3.5	40	2.90	2085	0.31
Coal	4	0.013	15.9	-	15-25	-	1733	0.25

4 MODELLING OF STRESSES AND FAILURE ALONG THE RIB PILLAR

A full-scale model of the M3 longwall panel and its surrounding has been prepared as seen in Figure 4. Face length, panel length and depth below surface values were taken as 90 m, 450 m and 240 m, respectively. There was a 16-m-wide nb pillar between M3 panel and the adjacent worked-out M2 panel. In order to accurately estimate stress distribution around the longwall face, this area was divided in the form of a closer meshing in comparison to other regions during numerical modelling (Fig.4).

Intact rock properties in most cases are found by means of laboratory testing. However, there is an important diversity between rock material and rock mass characteristics. It is compulsory to determine representative physical and mechanical properties of the rock mass instead of intact rock material. In this study, rock material properties were converted into rock mass data by using empirical relationships widely used in the literature, i.e. Hoek and Brown (1997) failure criterion, Bieniawski's (1973, 1989) RMR classification system and Geological Strength Index (GSI) (Hoek 1995, Sönmez 2001, Sönmez & Ulusay 1999).

Modelling of caved area is another important step that affects the results. It is a well-known fact that it is a rather difficult task to model the goaf material. Therefore, the goaf was characterized by using the following expression for modulus of elasticity as suggested by Xie et.al. (1999):

$$E = 15 + 175(1 - e^{-1.25t}) \text{ (MPa)} \quad (1)$$

where, t is time in seconds

For the goaf material in Tunçbilek Region, Köse & Cebi (1988) suggested a modulus of elasticity interval of 15-3500 MPa, whereas Yavuz and Fowell (2001) suggested a Poisson's Ratio of 0.495. These values were used for the characterization of goaf material throughout the analysis. Hence, change in the characteristics of goaf material depending on the level of compaction could be taken into account.

In order to simulate the change in the characteristics of stress distribution around the face, a progressive modelling has been earned out depending on face advance. Therefore, the model was progressively modified after each run as the face was advanced 30, 60, 90, 120 and 150 m away from the face start line.

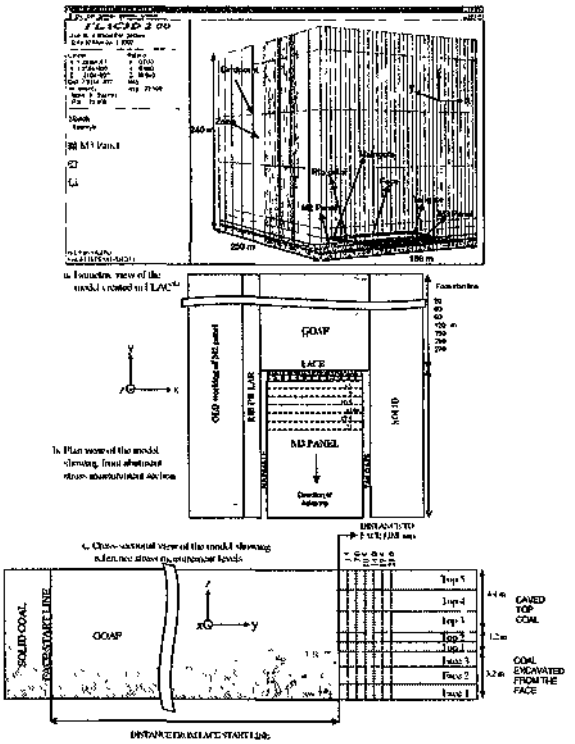

Figure 4. Details of model geometry of Ömerler Underground Mine (Yaşıtlı & Ünver, 2005).

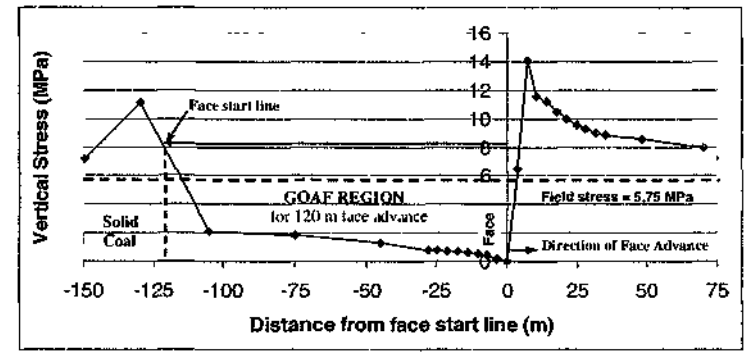

a. Vertical stress distribution found by numerical modelling after 120 m face advance

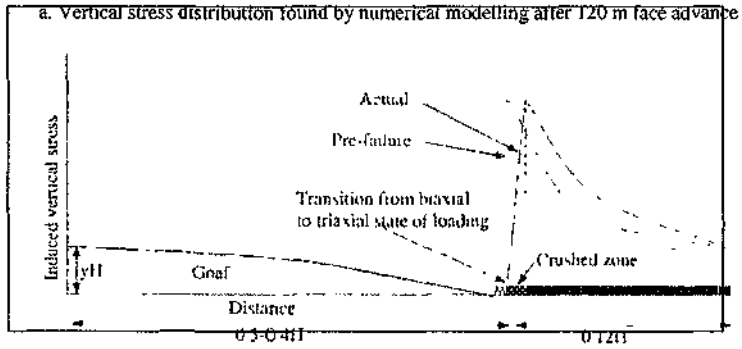

b. Vertical stresses distribution based on in situ measurements (Whittaker & Singh, 1979).

Figure 5. Stress distribution at a longwall found by in situ measurements and numerical modelling.

However in this study, a comprehensive interpretation of these modelling results has not been given. Hence, only the change in vertical stress distribution around the longwall face depending on face advance has been briefly presented. Vertical stress distributions obtained after 120 m of face advance from me face start line is presented in Figure 5. Characteristics of stress distributions obtained by means of numerical modelling are in good agreement with the results of actual measurements in underground conditions. The magnitude of field stress was calculated as 5.75 MPa and presented with a dashed line in Figure 5. Front abutment pressures increase until a distance of 7 m in front of the face reaching to a maximum stress level of 14.40 MPa. After reaching to the highest front abutment pressure, it decreases gradually to initial field stress of 5.75 MPa at a distance of 70 m away from the face. The abutment stress formed at a distance of 7 m in front of the face increased 2.5 fold of the initial field stress (Yaşıtlı & Ünver, 2003).

Stress in the goaf behind the face decrease to 0.1 MPa levels and tends to increase at the start line of the face in a similar manner with front abutment stresses as expected. At the face start line of the panel, rear abutment stresses reach to the highest level at 2-3 m inside the solid coal and decrease gradually to the field stress level at about 60 m inside the solid coal.

In this study, another numerical modelling was performed for evaluation of rib pillar stabilization. Loading of rib pillars is a complex phenomenon due to yielding behavior. The complexity of modelling of stress distribution on a rib pillar arises due to; first, drivage of gate roadways and crosscuts lead to an increase in the amount of load exerted on rib pillars. Second, production activity at the neighboring longwall panel results in an extra increase in the amount of load on the pillar. This results in the direct exposure of the rib pillar to the transferred load induced by the extraction of the coal in the nearby panel. This, so called, side abutment load almost certainly causes some yielding in the pillars. The pillars should be strong enough to withstand high loads in order to protect the entry between the rib pillar and the nearby panel. The third phase of loading is due to the extraction of the coal from the nearby panel. The rib pillar must protect the entry reasonably well from the front abutment stresses caused by the production at the neighboring panel.

An important study for determination of the width of rib pillar at this panel was carried out by Taşkın

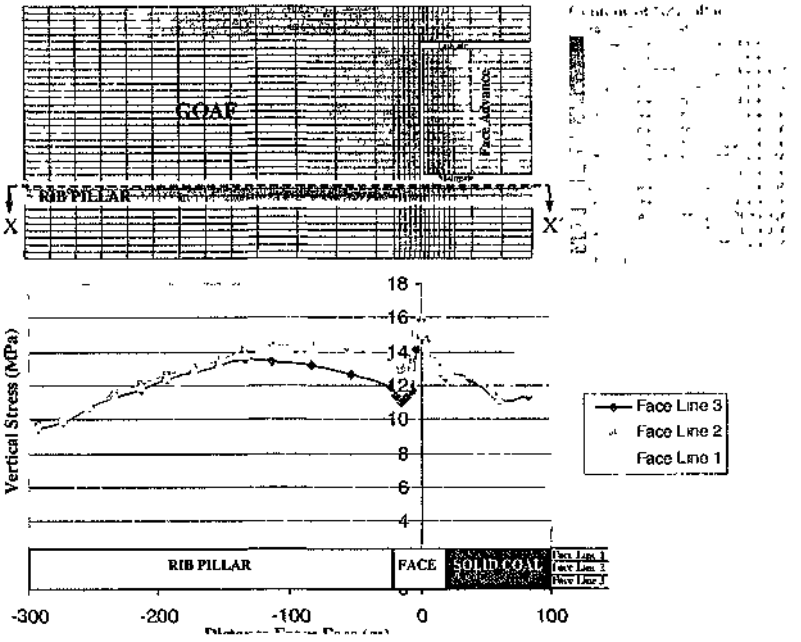

Figure 6. Vertical stiess distribution along rib pillar parallel to lace advance.

(1999) based on in situ measurements, and he determined the pillar width as 16 m. Consequently, width of the rib pillar between M2 and M3 panels was selected as 16 m at Ömerler Underground Mine.

The coal seam was divided into three levels in vertical direction to aid understanding of stress distribution at various heights from floor to roof of gate roadway. Vertical stress distribution along the rib pillar on X-X axis is given in Figure 6. As expected stress distiibution in close proximity of the face on the rib pillar is high. Vertical stress on the rib pillar reaches to 16.1 MPa and there is a sharp decrease in vertical stress levels on the rib pillar in front of and behind the face line. The amount of vertical stress is around 14 MPa up to a distance of 115m behind the face line. This phenomenon may be attributed to the fact that the goaf in this region is still loose to accept load from the main roof. Therefore, the amount of side abutment stress is high in this region. The amount of side abutment stress gradually decreases from a distance of 115 to 300 m behind the face line. This is due to ongoing compaction of goaf. As a result of compaction, goaf will start to accept some of the load exerted by main roof leading to a decrease in the amount of side abutment stress on the rib pillar.

After performing the numerical modelling for determination the stresses on the rib pillar, evaluation of rib pillar stability and yielding behavior have been performed and the results are given in Figure 7. Along the rib pillar near the face line, an approximate shear failuie zone of 10 m in length and 5 m in width was observed. Apart from this region, the rib pillar was found to be stable. As seen in Figure 7b, mere is a stable core in the pillar with an approximate width of 5 m. According to the numerical results, the rib pillar between two panels was found stable. During in situ observations, in the gate roadway at a distance of 10 to 15 m in front of the face line, high amount of convergence had been seen possibly due to yielding of rib pillar. Hence, additional support has been applied in the form of erecting hydraulic props in the middle of the gate roadway. As it is determined by numerical modelling and verified by in situ observations, after a further distance of 10 m in front of the face line, no major stability problem has been encountered with in the gate roadway.

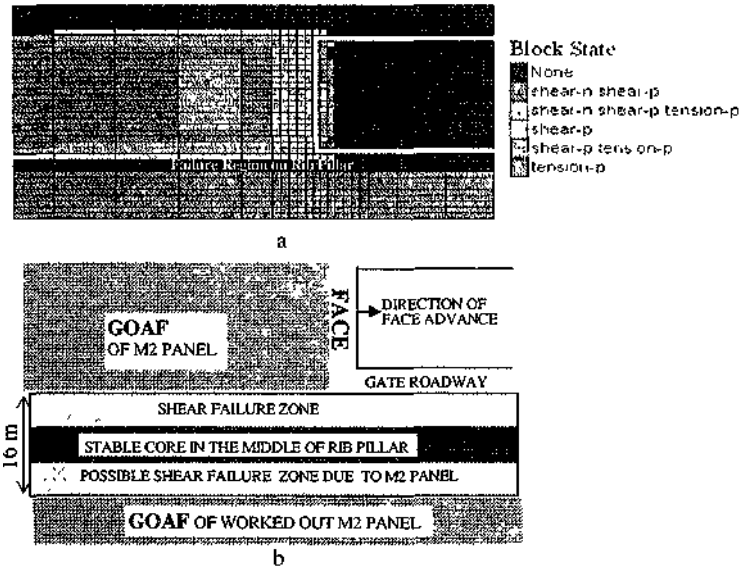

none- no-failure zone, shear-n: the region failed under shear loading and failure process is still in progress, shear-p: the region failed under shear loading and failureprocess is ceased due to lowered amount of shear forces, tension-n: the region failed under tensile loading and failure process is still in progress, tension-p: the region failed under tensile loading and failure process is ceased due to lowered amount of tensile forces.

Figure 7. State of failure around the longwall and rib pillar.

5 CONCLUSIONS

The results reveal that stresses around the longwall face can be successfully modeled by using FLAC^{3D}. The results show that maximum abutment stresses (14.4 MPa) formed at a distance of 7 m in front of the face. After reaching to the highest level the front abutment pressure decreases gradually to initial field stress level (5.75 MPa) at a distance of 70 m away from the face. Stress level in the goaf behind the face was very low (0.1 MPa) as expected. The maximum vertical stress on the rib pillar was found as 16.1 MPa. The section of the rib pillar 5 m from the gate roadway yields leaving a stable core in the middle. Therefore, the rib pillar width of 16 m as applied in the mine was found to be a proper selection.

REFERENCES

Bieniawski, Z.T., 1973, Engineering classification of jointed rock masses. *Trans S. Afr. Inst.Civ. Eng.,* 15, pp. 335-344.

Bieniawski, Z.T., 1989, *Engineering Rock Mass Classification,* John Willey & Sons, New York, 251p.

Destanoğlu, N., Taşkın, F.B., Tastepe, M., Öğretmen, S., 2000, *GLI Tunçbilek-Ömerler Yeraltı Mekanizasyon Uygulaması,* Kozan Ofset, Ankara, 21is.

Hoek, E., 1995, Strength of rock and rock masses, *ISRM News Journal,* Vol.2, No.2, pp. 4-16.

Hoek, E. and Brown, E.T.,1997, Practical estimates of rock mass strength, *Int. J. of Rock Mech. Min. Sei.,* 34 (8), pp. 1165-1186.

Itasca, 1997, *User Manual For FIAC^{3}", Ver. 2.0,* Itasca Consulting Group Inc., Minnesota.

Kose, H., Cebi, Y., 1988, Investigation the stresses forming during production of thick coal seam. *6th coal congress of Turkey,* Zonguldak, p. 371-83 (in Turkish).

Sönmez, H., 2001. Investigation on the applicability of the Hoek-Brown criteria to the failure of the fissured clays. Ph.D. Thesis, Hacettepe University, Ankara, 215 p. (in Turkish).

Sönmez, H. and Ulusay, R., 1999, Modifications to The Geological Strength Index (GSI) and their applicability to stability of slopes, *Int. J. of Rock Mech. and Min. Sei.,* 36(6), pp. 743-760.

Taşkın, F.B., 1999, Optimum Dimensioning of Pillars Between Longwall Panels in Tunçbilek Mine, Ph.D Thesis, Osmangazi University, Eskişehir, 149 p. (in Turkish)

Ünver, B. and Yaşıtlı, N.E., 2002, The Simulation of Sublevel Caving Method Using in Thick Coal Seam by Computer, Hacettepe University Scientific Research Unit, Project No: 00 02 602 008, 148 p. (in Turkish)

Whittaker, B N and Singh, R N , 1979, Evaluation of the Design Requirements and Performance of Gate Roadways, Miner Engineer, pp 535-553

Yasitli, N E, 2002 Numerical Modelling of Longwall With Top Coal Caving, MSc Thesis, Hacettepe University, Ankara, 148 pp (in Turkish)

Yasitli, N E and Unver, B , 2003, 3-D estimation of stresses around a longwall face by using finite difference method, /#"' *International Mining Congress of Turkey*, Antalya, 2003, p 83-88

Yasitli, NE and Unver, B, 2005, 3-D numerical modelling of longwall mining with top coal caving, *Int J of Rock Mech and Min Set*, 42(2), pp 219-235

Yavuz, H, and Fowell, RJ, 2001, Softening effect of coal on the design of yield pillars," in FLAC and Numerical Modeling in Geomechanics, *Proc of The 2"nd International FLAC Conference*, Lyon, France, D Billaux et al (eds), Lisse A A Balkema, pp 313-320

Xie, H , Chen, Z and Wang, J , 1999, Three-dimensional numeiical analysis of deformation and failure during top coal caving *Int J Rock Mech and Min Sa*, 36(6)651-8

Tire - Rim Interactions for Ultra Class Trucks in The Mining Industry

M.J.A Bolster
M Sc Graduate Student, AEGIS research group. University of Alberta, Edmonton, Canada

T.G. Joseph
Director AEGIS, University of Alberta and Principal Engineer, JPi, Edmonton, Canada.

ABSTRACT: With the advent of ultra class trucks in the 320 ton + category, tire manufacturers have produced ultra class tires to match and provide greater floatation capacity for these units when riding over soft ground In all types of ground environment, trucks are developing high g loading conditions which produce adverse reactions at the tire - rim interface, causing damage not only to tires, but more surprisingly to rims In an effort to develop an understanding of this phenomenon, a tire - rim model is being developed to assist rim manufacturers m providing designs that will resist damage and protect the tire The effect on both components due to variable loading conditions is examined, where rim component geometry and tire performance are essential contributions

1 INTRODUCTION

The need for increased production has driven global surface mining operations to move to larger equipment As a result of this, trucks have moved into the ultra-class category while rim development has remained relatively stagnant More than ever there is the need for increased development and research of rims as many haulers currently operating are exposed to unanticipated high g loading, especially those operating with soft underfoot conditions, one of the primary causes of high g loading As a result, rims are cracking and failing at an unprecedented rate The majority of design modifications of the current generation of rims are scale increases of older designs and field fits This lack of engineered design or understanding of the consequences of high g loading, has resulted in several instances of rim failure leading to lost production, injuries, and even fatalities (North Queensland Tyre Fitters Workshop Meeting 2004 and Occupational Safety and Health Service, Department of Labour, New Zealand 2004) With an improved understanding of the performance of rims and tires subjected to high g loading, the knowledge base in this field will be expanded to allow manufacturers to target improved designs that will minimize rim cracks and failures that plague today's mining industry

2 PREVIOUS WORK

There has been very little published m regards to ultra class hauler rims, especially in terms of the effects of high impact loading The Society of Automotive Engineers (SAE) have published a handful of practices and standards for construction vehicle rims (SAE J751 1997, SAE J1315 1991, and SAE J1337 1997) but in terms of ultra class rims, their only practical use is that of component identification, Figure 1

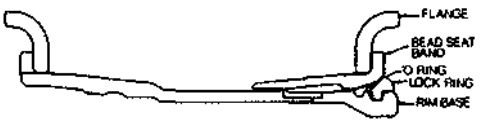

Figure 1 Cross-section view of standard 5-piece rim (SAE J751, 1997)

There has been some work done in regards to determining pressures exerted at the ground level which is useful for examining the interaction between a nm and tire (Wiermann et al 1999, Ronaı & Shmulevıch 1995, Tielkmg 1994, Tıelkıng & Abraham 1990, and Cunagm and Grubbs 1984) Unfortunately the bulk of this work has been done by both agricultural and transportation industries m order to determine information on large farm and highway vehicles, both of which are too small of

scale for comparison to ultra class haulers. This lack of published work in regards to both high g loading on rims and large scale tire data acquisition, along with the high frequency of incidents regarding tire and rim failures speak volumes about the need for such information for today's mining industry.

In contrast to the lack of information regarding high impact loading on large scale rims and tires, there has been considerable work done on high g loading on other components of large scale mining equipment (Joseph 2003, Joseph 2002, and Joseph & Hansen 2002). These papers discuss in depth the effects of high g loading on mobile mining equipment and how it is detrimental to equipment life. They also discuss how soft underfoot conditions result in high g loading, such as those in the oil sand of Northern Alberta, which is where a vast number of large scale rims and tires are in use.

3 OBJECTIVES

The primary purpose of this research is to improve safety conditions at mine sites, as well as to minimize repair and replacement costs of rims and tires for large scale equipment. These objectives will be achieved by increasing the understanding of the interaction between the rim, the tire, and the ground. This includes gaining an improved appreciation of the stress-strain concentrations of the rim and tire, as well as acquiring more information regarding the transfer of forces between rim, tire and ground. This research will target to determine if high g loading is being experienced, and if it is indeed significant and detrimental at the rim/tire locale, as reported instances of as high as 4g have been measured at the strut level for ultra class heavy haulers in operation today.

It is proposed that a design modification will be suggested for rims that are currently in use with ultra-class heavy haulers. A goal of lower frequency of rim cracks and failures, leading to safer working conditions around rims, as well as decreased reactive maintenance and replacement for ultra-class rims and tires is targeted.

4 LARGE SCALE TESTING

In order to gain an improved understanding of the performance of and interaction between rims and tires, a series of loading tests that will simulate the forces that ultra-class haul trucks are subjected to on a daily basis will be performed. The results obtained from these tests will then be compared to a finite element model for verification purposes. If it is found that there is a correlation between the physical and computational representation, it will then be possible to make modifications to the computer model in order to determine a rim design that can withstand the high g loading at current exposure levels.

Currently ultra class haulers use 55/80 R63 or 59/80 R63 tires, which have outer diameters of 154" and 159", loaded radii of 64" and 69", and rim diameters of 63" respectively (Bridgestone 2001 and Michelin Earthmover 2005). Therefore, in order to perform an accurate loading test as described previously, a 55/80 R63 or 59/80 R63 tire and matching size rim should be used. However, the University of Alberta is unable to accommodate testing at this scale. The bulk of large scale testing facilities are located in the southern United States or overseas in Japan, and are therefore not feasibly accessible. Consequently, it was decided to test the largest possible rim and tire given the available resources at the University of Alberta, verify the results using a finite element model for the given tire and rim, then compare and correlate the results with a finite element model of either a 55/80 R63 or 59/80 R63 tire and a 63" rim. The tire and rim combination was selected was a 30.00 R51 tire, with an external diameter of 112" and a loaded radius of 50", donated by Kaltire, and a 51" diameter rim, figure 2, fabricated and donated by Rimex.

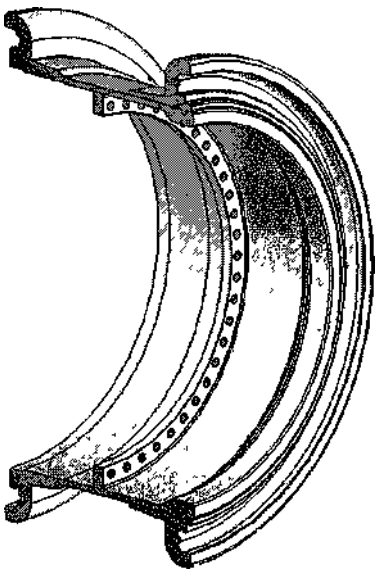

Figure 2 Cross-section view of 51" diameter rim

The. purpose of the load test on the 30.00 R51 tire and rim, figure 3, is to examine the impact of high g loading; upwards of 4g in worse case scenarios and frequently reaching 3g during day to day operations, which have been detected by ultra class hauler on-board monitoring systems operating in the oil sand. The tire and rim will initially be subjected to a lg loading (the static weight of a loaded haul truck), and the status of both components monitored via strain gauges. In order to simulate the effect of increased g levels resulting from dynamic loading, the loaded gross vehicle weight is multiplied by the proportion of g loading, applied statically to the rim and tire. The typical payload for a hauler that is used with this sized tire and rim is 170 tons, giving a total gross vehicle weight of approximately 550,000 lbs (Caterpillar 2004). This results in a loading of 92,000 lbs being experienced by each of the truck's 6 rims, based on a standard front-to-rear load distribution of 1/3 to 2/3. For the initial 1 g loading described above rim and tire will be loaded to 92,000 lbs, and then loaded by 0.1 g increments up to 2g, or 184,000 lbs. This range will allow a prediction of higher g loading effects based on the trending displayed, while eliminating the safety risk associated with testing the rim and tire at levels higher than 2g.

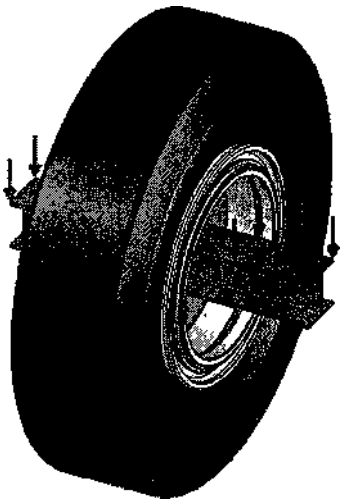

Figure 3 30.00 R51 tire and rim loading configuration

For each of the incremental g loading tests, the tire tread will be inked to show the surface contact area with increased loading. This will allow the measurement of the footprint of the tire for each level of loading, which also can be used to predict the area of contact at higher levels of g loading from the trends shown. This information will be vital in determining the value of the reaction forces that are transferred from the ground through the tire and onto the rim during motion of the hauler while subjected to various levels of g loading.

After the static loading tests have been completed, the rim and tire will be subjected to various cyclic loadings, which will be representative of various g levels (1.2g, 1.4g, 1.6g), for extended periods of time at varying frequency from 0.1 Hz to 3 Hz. This will provide valuable information in regards to continuous exposure high g impacts over time. The data collected from each of these tests should provide valuable insight into the impact of high g loading on the rim and tire assembly of an ultra-class haul truck and provide a basis of comparison for the computational analysis that will be performed.

5 COMPUTER MODELING

The computer modeling portion of the research project will be achieved using SolidWorks for 3D drafting and COSMOS for finite element analysis. Both software packages are off-the-shelf products for simplicity of application. Drawings were kindly provided by Rimex for the 51" diameter rim that will be subjected to the tests outlined above, as well as for 63" diameter rims that Rimex manufactures for Caterpillar Inc.'s 797B, figure 4, ultra class model and Komatsu Mining Systems 930E, figure 5, ultra class model.

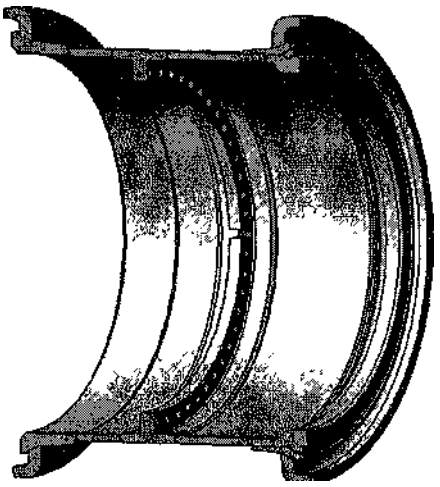

Figure 4 Cross-section view of Caterpillar 797B 63" diameter rim

According to the specifications, each of these rims are entirely constructed using ASTM A36 steel, making the input for the finite element modeling process simpler. However, modeling of the tire is very complex due to its dual material nature. The tires contain radial steel belting within their rubber body in order to provide structural support, which makes it hard to determine the overall material properties such as elastic modulus, shear modulus, and density. Tire manufacturers, for proprietary reasons, are very reluctant to provide information in regards to their tires. Therefore, it is planned to obtain samples of tread and sidewall materials for an ultra class earthmover tire, allowing material tests to be performed to obtain overall values for modulus and deformational response, which can then be input into the finite element model.

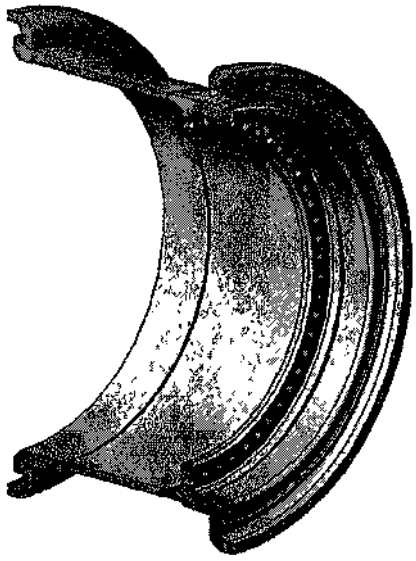

Figure 5 Cross-section view of Komatsu Mining Systems 930E 63" diameter nm

Once all the tire data has been obtained it will be possible to construct finite element models for the 30.00 R 51 tire and rim, as well as Caterpillar 797B and Komatsu 930E-2 loading variations for a 59/80 R63 tire and rim assembly. This will allow a comparison of the 30.00 R 51 tire and rim to the results obtained from the loading test for verification purposes. If it is found that there is a correlation between these results, then the similarities between the 51" and 63" rim models, such as strain locations and stress concentrations, can be inferred to the 59/80 R63 tire and rims that are subjected to similar loadings while operating. From there it will be possible to modify the current rim designs using SolidWorks and run several iterations of finite element analysis to determine the optimal rim design for high g loading.

6 PROJECT STATUS

The 30.00 R 51 tire that was donated by Kaltire and the 51" rim that was fabricated by Rimex arrived in Edmonton in early February 2005. They are currently assembled, the tire at partial inflation to maintain its shape, and are being stored until the loading test is ready to commence. The design of the mount that will hold the tire and nm in place during the test is being finalized and checked to ensure it has enough structural strength to withstand the loads that will be applied. As it stands, the plan is to pass a W 12X96 I-Beam through two plates, figure 6, that will be attached to each side of the mounting disc. Both sides of the I-Beam will be loaded with a total of half the required force at an equal distance from the centerline. Each of the plates will be split in two, as this will allow them to fit in the smaller opening on the outside edge of the rim, which has a smaller diameter than that of the plates. Splitting them in two will also ease in transportation, as each full plate will weigh over 800 lbs, without jeopardizing their structural strength, as they will both be bolted to the rim disc. Attached to these mounting plates will be four gussets that will provide structural support. They will be pre-welded into place at the locations shown in figure 7, but will still allow for the I Beam to be slotted between them.

Figure 6 Half-plate mounting disc with half I-beam slot

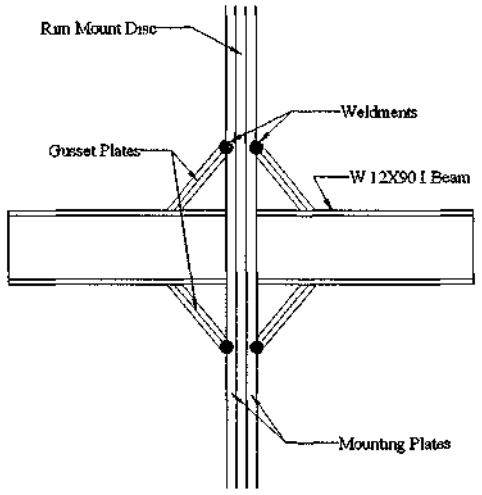

Figure 7 Gusset support plates

In terms of the computational modeling, the vast majority of the drafting is complete. As previously stated the mechanical properties for the rim components are easy to obtain as ASTM A36 is a very common material, however, until the properties of the tire tread and sidewalls are determined it is not possible to perform accurate analysis on the model. It is estimated that the loading test will be completed by late Spring 2005 while the computer modeling should be completed by Summer 2005, with analysis completed by Fall 2005.

7 ESTIMATED RESULTS

Without the proper material properties for the tire it is not possible to conduct an accurate finite element analysis. However, based on conversations with field personnel and other qualified people, an estimate of the magnitude of loading can be made on a 2-D basis, figure 8.

The peak value of the rim loading distribution can be estimated via the total vertical deformation of the tire, figure 9, during loading, given an approximation for the stiffness properties of the tire. It is known that the forces on the rim at the horizontal quadrants will be zero as the rim is loaded by the tire from the ground up; hence the top portion of the rim is not loaded during impact. Via these assumptions it is possible to draw a probable stress distribution on the rim, with the value of maximum load, and the slope of the function for maximum load both increasing as a function of g loading.

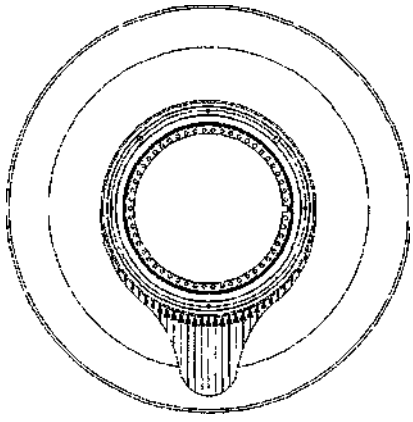

Figure 8 Estimated load distribution

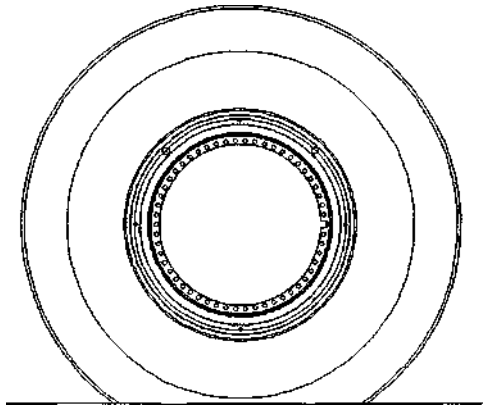

Figure 9 Deformation characteristics of tire

Modifications based on results from this research project would target a more even loading distribution with a less significant peak value, figure 10. This could be the result of a design change in terms of geometry of the rim components or in terms of material properties of the components, such as fabricating with a more flexible steel or weld material.

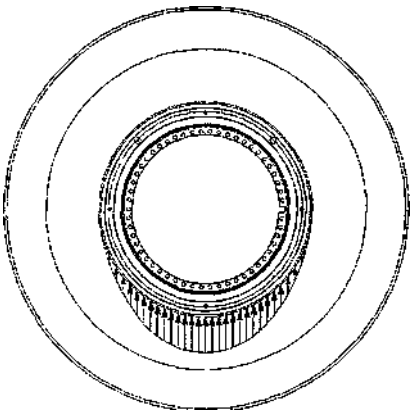

Figure 10 Idealized load distribution

8 DISCUSSION & CONCERNS

The primary concern in regards to this research project is whether a loaded 30.00 R51 tire and rim will provide accurate information in regards to what a larger, lower profile tire and rim will experience during operation. However, as stated previously the University of Alberta does not have the means to perform a large-scale loading test on either a 55/80 R63 or 59/80 R63 tire and rim.

It is expected that there will be a correlation between the information obtained from the finite element models for the 51" rim to the 63" rims, and it is expected that these tests and models will allow inference of performance characteristics to the larger scale, lower profile configuration now commonly in use with ultra class series units; 55/80 R63 and 59/80 R63.

Additional concerns in regards to this project are the weldments and weld materials used in constructing the rims. The center section of the rim is composed of several smaller components welded together, so the materials and therefore the material properties are not consistent throughout the entire piece. In the software, it is possible to create solid objects to represent the weld beads, whose properties can be altered to more accurately represent the weld material compared to the original A36 steel, rather than identifying the weld material and the base material as identical, which is impossible without perfect welding procedures and conditions. However, within the restrictions of the available software, it is not possible to appropriately model the weld induced heat-affected zone, which extends several centimeters from the weld locations, and is generally the location of cracks resulting from inadequate pre-heating or post-weld heat-treatment.

9 CONCLUSIONS

In order to gain an improved understanding of rim and tire performance when exposed to high g loading, a static and dynamic suite of loading tests are proposed that will simulate the forces that large tires and rims are exposed to during day to day mining operations. The tests will be performed on a 30.00 R51 tire and rim which have been donated by Kaltire and Rimex respectively. The values of loading will range from lg up to 2g in O.lg increments in order to develop a trend to enable prediction of load impacts upwards of 4g. The tread section of the tire will also be inked during these tests in order to obtain a stamp of the foot print during loading, as this will provide information in regards to the interaction between the ground material and the tire/rim assembly. In addition to these tests the rim and tire will be subjected to various loads within the lg - 2g range at a range of frequencies, providing information in regards to the effect of long term exposure to high g loading.

Once this data has been obtained it will be used to verify a finite element analysis of the 30.00 R51 tire and rim. The analysis of the 30.00 R51 tire/rim assembly will then be compared to that of a 59/80 R63 tire and rim, which will allow the determination and verification of stress and strain concentrations. The ultra class rim designs can then be modified, resulting in an optimal design for high g loading conditions.

This ensuing design should result in improved rim life cycles which will reduce mining operation's costs in terms of rim maintenance and replacement. More importantly, there should be significantly less rim failures and cracking, which will cause a decrease in the amount of hazardous work mine employees are exposed to in terms of rim maintenance.

REFERENCES

Bridgestone 2001. Bridgestone data book off-the-road tires, pp. 27.

Caterpillar Inc. 2004. Caterpillar performance handbook edition 35. pp. 9-5.

Cunagin, W.D. and Grubbs A.B. 1984. Automated acquisition of truck tire pressure data. *Transportation Research Record.* 1123: pp. 112 - 121.

Joseph, T G 2002 OsEEP The oil sands - equipment interactions program. *Canadian Institute of Mining and Metallurgy Bulletin* 95 pp 58-61

Joseph, T G & Hansen, G W 2002 Oil sands reaction to cable shovel motion *Canadian Institute of Mining and Metallurgy Bulletin* 95 pp 62 - 64

Joseph, T G , 2003 Large mobile equipment operating on soft ground 75'" *International Mining Conference and Exhibition of Turkey* pp 143-147

North Queensland Tyre Fitters Workshop Meeting, 2004 Brief history of accidents involving tyres & runs *http //www nrm qld gov au/mines/uibpectorate/pdf/tyr ejitteı s_woi kshopl pdf*

Michelin Earthmover 2005 Tire size information *http //earthmover webmichehn com/na_eng/tires/XD R/detaih html*

Occupational Safety and Health Service, Department of Labour, New Zealand 2004 Accident alert - tyre fitter killed by exploding tyre *http //www osh dol govt m/publicatwns/senes/aa-tyi eexploswn html*

Ronaı, D & Shmulevıch I 1995 Tire footprint characteristics as a function of soil properties and tire operations Journal of Terramechanics 32 No 6 pp 311-323

SAE J751, 1997 Off-road tire and rim classification - construction machines *SAE Standaı d,* 3 pp 40 458 - 40 462

SAE J1315, 1991 Off-road tire and rim selection and application *SAE Standard*, 3 pp 40 463

SAE J1337, 1997 Off-road tire and rim classification - construction machines *SAE Standard,* 3 pp 40 458 - 40 462

Tielkmg, J T 1994 Force transmıssıbılıty of heavy truck tires *Tire Science and Technology* 22 No 1 pp 60 -74

Tielkmg J T & Abraham M A 1990 Measurement of truck tire footprint pressures *Transportation Research Record* 1435 pp 92-99

Wiermann, C , Way, T R , Horn, R , Bailey, A C , and Burt, E C 1999 Effect of various dynamic loads on stress and strain behavior of a Norfolk sandy loam. *Soil & Tillage Research* 50 pp 127 - 135

The 19th International Mining Congress and Fair of Turkey, IMCET2005, Izmir, Turkey, June 09-12, 2005

Status and Prospects of Underground Thick Coal Seam Mining Methods

B K Hebblewhite
School of Mining Engineering, The University of New South Wales, Sydney, Australia

ABSTRACT: Australia has very large thick seam coal resources. As a result, there has been ongoing research conducted by UNSW and others into suitable mining methods that are capable of safe, efficient and productive resource recovery. The significant production improvements achieved in the Chinese coal mining industry over the last decade, as a result of development and application of the LTCC method, has prompted Australian mines to examine the method and its potential, for Australian application. This paper presents the key issues and latest findings from recent thick seam mining research conducted by UNSW into various mining methods, but particularly, the Chinese LTCC method. In respect to LTCC, geotechnical factors such as coal strength and rock mass characteristics are considered with respect to caving potential and face support performance. The caving and coal clearance simulation/optimization research includes evaluation of a range of front and rear conveyor capacities relative to different caving strategies, as well as alternate panel conveying options.

1 INTRODUCTION

There has been considerable interest in underground thick seam raining methods in Australia for many decades. As outlined later in this paper, Australia has significant reserves of thick coal seams that require the application of alternative mining methods - beyond the conventional bord and pillar or standard longwall systems. The incentive for identifying or developing new methods for underground thick seam mining is primarily optimising resource recovery. However, the Australian coal industry is an export-dominated industry where high productivity, sustainable financial viability and the highest safety standards are paramount. As such, the Australian requirement is for appropriate methods which meet the Australian safety and productivity/financial performance criteria, or preferably improve on them, at the same time as achieving improved resource recovery.

As a point of definition, the term thick seam has been applied to any minable seam thickness greater than the reach of existing development and longwall systems. In the 1980s and 1990s, this was interpreted as 4.0m. However, with higher reach continuous miners ands longwall systems, an arbitrary figure of 4.5m has been adopted for all recent studies.

Earlier studies by UNSW and others (Hebblewhite, 1999 & Hebblewhite et al., 2002) reviewed the Australian opportunities and available methods and technologies for underground thick seam methods. Arising from this review, four generic methods were identified as having thick seam potential. These were:

- extended height single pass longwall (SPL)
- multi-slice longwall (MSL)
- hydraulic mining (HM)
- caving longwall systems (CL), including longwall top coal caving (LTCC).

The option of extending the height of a conventional single pass longwall was considered to have limited possibilities. It was apparent that technology was already gradually increasing both shearer and support heights from 4m to 4.5m and now up to 5m and above (Hamilton, 1999). However, limitations such as equipment size, weight and stability, plus face conditions were considered to limit the application of this method to no more than 6m height, for many years to come. The method is certainly considered to have potential in the 4.5m - 6.0m height range, however. A summary of latest developments in SPL is included below.

Multi-slice longwall was also reviewed in detail, with consideration of experiences from both Europe

and China with this method. The potential to apply modern paste fill technologies for septum formation and stabilisation was investigated (Palarski, 1999, Bassier & Mez, 1999). However, through a risk assessnv .1 process, some of the other issues such as mining under goaf areas (water and gas hazards), and general stability concerns, ruled this method out as a viable option for Australia at the present time, quite apart from the very limited gains in productivity anticipated.

Hydraulic mining, as practised in New Zealand and elsewhere previously, was investigated. It was found to be a method with a significant potential in a limited range of suitable mining conditions. It offered significant financial benefits, but limited large scale production potential. It was therefore considered to be suitable as a "niche application" method, but not a universally applicable option. A brief review of this method is also included below.

This then left the range of longwall caving options. Evaluation of different European and early Chinese experiences with the original "soutirage" mining concepts and equipment showed promise, but performances were below the level required to be viable in Australia, not to mention concerns over issues such as dust and spontaneous combustion. The main focus of this paper is on the LTCC method and some of the factors that must be considered when assessing the potential application of LTCC.

Prior to discussing the actual mining methods, it is considered appropriate to review the Australian thick seam resource database in order to gain an appreciation for the extent of these resources.

2 AUSTRALIAN THICK SEAM RESERVES

Table 1 summarises the extent of thick seam reserves in Australia - both in terms of measured reserves and measured plus indicated (Hebblewhite et al., 2002). These figures confirm that there are at least 6.4 billion tonnes of minable underground thick seam reserves. Some significant features of these minable reserves are:

- 86% are in seam thicknesses between 4.5m and 9m, with 51% in the 6m-9m range.
- 84% are in seams with a dip of less than 15°
- 76% are less than 300m depth.

The above parameters confirm that the majority of thick seam reserves are in the 6m - 9m range, beyond the scope of Single Pass Longwall, but eminently suitable for the LTCC method. Furthermore, the seam dips and depths are also within the range of current LTCC technology.

Table 1. Australian thick seam reserves *(after Hebblewhite et al., 2002)*

AUSTRALIA		Number of Seams	Measured Resources (million tonnes)	% Measured Resources (%)	Ind & Meas Resources (million tonnes)	% Ind & Meas Resources (%)
Seam Thickness	4.5m - 6.0m	29	2249	34.8	7425	42.2
	6.0m - 9.0m	33	3310	51.2	8397	47.8
	> 9.0m	9	597	9.2	1113	6.3
	No Info	2	310	4.8	650	3.7
	Total	73	6466	100.0	17585	100.0
Seam Dip	< 5.0 deg	43	3173	49.1	11684	66.4
	5.0 deg - 15 deg	21	2256	34.9	3698	21.0
	> 15 deg	9	1037	16.0	2203	12.5
	Total	73	6466	100.0	17585	100.0
Seam Depth	< 150m	28	3312	51.2	6303	35.8
	150m - 300m	23	1594	24.7	5383	30.6
	> 300m	19	1508	23.3	5698	32.4
	No Info	3	52	0.8	201	1.1
	Total	73	6466	100.0	17585	100.0

3 SINGLE PASS LONGWALL

Current high capacity single pass longwall practice, worldwide, is restricted to height ranges of 4.5m to 5.5m. Tables 2 and 3 summarise the known, high capacity longwall faces operating around the world at the present time in this height range. It is significant to note that although a number of faces have the capacity to operate at 5.5m and above, they are typically working at lower heights due to operational reasons associated with ground control problems. These geotechnical factors, together with logistical issues associated with size, weight and stability concerns with the very large, high face equipment, are considered to be major limitations to

this method finding application beyond 6m height for the foreseeable future

Some pertinent comments in relation to these international faces and recent experience, are as follows

- The Lazy Mme in the Czech Republic, with 6m equipment designed to cut at 5 5m, is currently operating at a maximum cutting height of between 4m and 4 5m due to difficult ground conditions (roof and face)
- The Sihe Mine m China is currently experiencing ongoing difficulty holding the coal roof above the supports and ahead of the longwall face (between the tip of the roof supports and the coal face being cut by the shearer) As a result, although cutting to 5 5m with no excess height capacity in the supports (to allow extension to provide improved roof control), the face continues to experience ground control problems It is understood that Sihe has recently called tenders for 6 2m high supports - not ne^ ^ssanly to cut higher, but to provide the necessary Duffer of support capacity above cutting height

The Matla face in South Africa is operating at a relatively shallow depth (typically less than 100m), with quite massive overburden strata and relatively strong coal Nevertheless, it is understood that Matla is currently experiencing ground control problems in difficult ground, and as a result has reduced the cutting height to approximately 4m under these conditions

Table 2 Australian Thick Seam Single Pass Longwall Operations (2004)
(source Australia 's Longwalls - March 2004 & Sept, 2004, plus pers comm)

Mme	**Face height (maximum) (m)**	**Maximum LW support height (m)**	**Face length (maximum) (m)**	**Shearer drum diameters (m)**	**LW face production (Mtpa)** (12 months to June 2004)	**Total mine production (Mtpa)** (12 months to June 2004)
Moranbah North	45	**48**	300	25	1863	2 128
Newlands	**50**	50	270	25	5 540	5 780
North Goonyella	42	**53**	300	24	1756	1903
West Wallsend	**48**	**53**	260	25	3 042	3 266
Manda long	**50**	52	125	26	Not yet in production	
Broadmeadow	**50**	**52**	7	7	Not yet in production	

Table 3 International (beyond Australia) Thick Seam Single Pass Longwall Operations (2004)(jo«rce *DBT)*

Mine	**Face height (maximum) (m)**	**Maximum LW support height (m)**	**Face length (maximum) (m)**	**Shearer drum diameters (m)**	**LW face production (Mtpa)** (12 months to June 2004)	**Total mine production (Mtpa)** (12 months to June 2004)
Lazy Mine, Czech Republic	55	**60**	100	2 75	9	7
Sihe Mme, China	55	55	225	7	7	7
Shendong, China	**50**	55	240	9	9	+8Mtpa (see previous figures for older face)
Damng Mme (AACI), China	50	55	7	7	Equipment ordered in 2004	
Zhouchuang Mine, China		**60**	7	7	Face equipment (shearer) tender out, late 2004	
Shangwan Mine, China	50	55	240	7	7	7
Mada Mine, South Africa	**55**	**60**	140	7	7	7

(a) DBT 6m support for Lazy Mine, Slovakia (b) DBT 6m support for Matla Mine, South Africa *(photographs courtesy ofDBT -personal communication}*

Figure 1. DBT 6m supports

The point of presenting the above summary of statistics and experience in the SPL system is to illustrate that SPL is certainly a technically feasible system in terms of equipment, within the 5m to 6m height range. However, in terms of operating experience at these heights, there are only two faces operating at heights between 4.5m and 5.0m, albeit only a small number of faces still. Once face height reduces below 4.5m then the number of successful faces increases significantly as the risks reduce.

Figure 1 shows longwall face supports recently delivered by DBT to the Lazy Mine in Slovakia and the Matla Mine in South Africa. Supports such as these typically have a collapsed height of 2.55m, width 1.75m, weigh up to 39 tonne, and have a support capacity in excess of 1,000 tonne.

4 HYDRAULIC MINING

Historically, most hydraulic mines around the world were simply niche applications of a technology with far greater potential than initially realised. These mines were developed with their primary purpose as an alternative to mechanised mining techniques. The seams in which these hydraulic mining techniques were applied, were predominantly steeply dipping and hence, mechanised methods had little to no application. In Australia only a very small proportion of the total thick

installed faces, worldwide, at present (Lazy and Matla), and both are experiencing difficulties and have been forced to reduce mining height significantly. At lower heights, both the equipment performance and geotechnical risks reduce, and there is certainly more experience worldwide with seam tonnage falls into this steeply dipping category *(greater than 15 degrees)*. Therefore, the application of hydraulic mining in this country would have to be in gently dipping *(lesï than 15 degrees)* seams. However, in thick coal seams, it is possible to operate at apparent dips in excess of the actual seam dip, hence hydraulic mining can find application.

Previous hydraulic mine operations have existed in places such as Germany, Canada and Japan. More recently the mines operated by Solid Energy on the South Island of New Zealand have utilised this method with considerable success. The Strongman No. 2 Mine (recently closed) operated by Solid Energy, was producing in excess of 400,000 tonnes/yr using a single hydraulic monitor (plus conventional continuous miner development units). The technique is currently being implemented in the new Spring Creek Mine in New Zealand. Features of the method are relatively low capital cost and the flexibility of multiple operating faces - provided conditions are suitable.

Figure 2 illustrates the concepts of underground hydraulic coal mining. Hydraulic mining has several advantages over conventional mechanised mining methods. However, it is important to note that not

all coal seams are compatible with hydraulic mining. As mentioned above, a number of specialised geological parameters must be satisfied before hydraulic mining can be undertaken. The advantages of hydraulic mining are:

- Mining layout is similar to that for conventional mechanised bord and pillar mining; however, the level of mechanical complexity is significantly reduced.

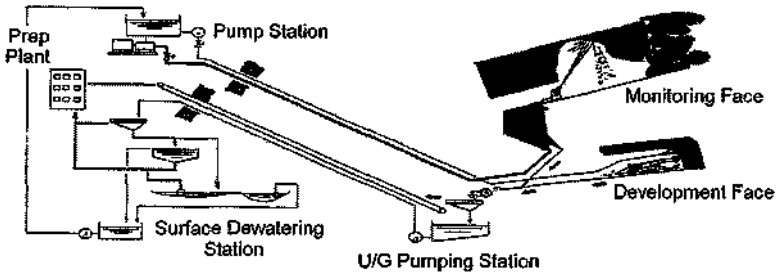

Figure 2 - Concept of Hydraulic Mining

- Due to a reduction in the production of coal dust, the elimination of frictional ignition sources, the removal of personnel from the face area and the ability to automate equipment operation, hydraulic mining can be relatively safer than more traditional underground coal mining methods.
- Extraction of thin (0.3m - 1.5m), thick (> 4.5m) and steeply dipping seams has, in the past, challenged traditional mechanised techniques. However, hydraulic mining has had great success in such geologies.
- Typically the tonnages obtained from hydraulic mining operations are less than those obtained from mechanised methods. However, due to reduced manning requirements and lower capital costs, hydraulic mining is still highly productive.
- Hydraulic mining offers significantly lower capital and operating cost structures over conventional mines, particularly if the mining faces are located above the drainage level.
- « Hydraulic mining is operationally flexible and can be used to extract areas of working mines where mechanised methods would otherwise encounter operational difficulties or would be economically unfeasible.
- Provided mine layout is designed appropriately, hydraulic mining can cope with large scale structural disturbances; and as a result the profitability of a hydraulic mining operation is less affected by these constraints.

Hydraulic mining also has some disadvantages - they are:

- The entire mine must be planned around the gravity driven hydraulic transportation system; roadways must have an average inclination of at least 4.0°, even if this means coal is left in the floor.
- High influx of water can cause problems with acid mine drainage; this acidity increases with high sulphur coals.
- Hydraulic mining can require the consumption of larger volumes of water and more electricity than conventional mechanised techniques; this is especially true for operations where the drainage level is underground.
- Coal is broken along its entire transportation route resulting in higher levels of fines in the run-of-mine product. This increases the capital and operating cost of dewatering facilities.
- The risk of spontaneous combustion is greater than for conventional techniques due to irregular goafing and difficulties in sealing off areas.
- Water reduces the strength of geological materials and therefore there may be an increased propensity to roof falls.
- During coal extraction the operator is unable to see the coal face and as a result is unable to ascertain exactly what is happening. As a result, a sudden collapse of roof strata may bury the monitor/face equipment.

In summary, hydraulic mining has limited potential, but in the right conditions, can be a highly productive, low capacity thick seam mining method.

5 THE LTCC METHOD

During the ongoing research and status review work into thick seam mining methods, the various Australian research teams became aware of the significant developments and impressive performance improvements being achieved in China with the development and application of the LTCC method (Xu, 1999). The method is essentially an extension of the original soutirage concept, but with significant equipment and face operational changes related to the use of the second rear AFC behind the face for handling the caved coal (see Figures 3, 4 and 5).

In terms of equipment innovation, the more recent Chinese developments have relocated the top coal draw points to the rear of the longwall supports, rather than bringing coal through the roof canopy of the shield onto a conveyor within the shield structure. These previous methods were quite clumsy and mechanically complicated, quite apart from the excessive dust-make within the face area and the 'cluttering up' of the already limited space within a line of shield supports. The Chinese equipment has a pivoting supplementary goaf or tail canopy behind the support. Beneath this is a retractable second AFC. With the rear AFC extended and the rear canopy lowered/retracted, caved top coal can be loaded onto the rear AFC, whilst production continues conventionally in front of the supports. In the retracted rear AFC position with the rear canopy raised, the supports and face operation can function conventionally.

The Chinese industry had reported averages of 15,000 to 20,000 tpd from an LTCC face; up to 75% recovery of 8m+ thick seams using a 3m operating height longwall; and +5 MTPA face production. There are now well over 70 LTCC faces in China. A new semi-automated 300m long LTCC face was installed at the Xinglongzhuang Colliery of the Yankuang Group, in Shandong Province, in August, 2001, with production capacities of at least 7MTPA.

The major perceived benefits of the LTCC method for Australia include:

- Operating Cost Reductions: The LTCC method enables potentially double (or greater) the longwall recoverable tonnes, per metre of gateroad development, thereby reducing the development cost/tonne significantly, and reducing the potential for development rate shortfalls leading to longwall production disruption.
- Resource Recovery and Mine Financial performance: The LTCC method offers a viable means of extracting up to 75% to 80% of seams in the 5m - 9m thickness range. Single pass longwall is considered to be limited to an upper height of 6m, and is currently only operating at or below 5m.
- Mine Safety: Lower face heights (relative to high reach single pass longwall) result in improved face control, smaller and less expensive equipment and improved spontaneous combustion control in thick seams, through removal of the majority of top coal from the goaf.

A joint ACARP research project between UNSW and CSIRO was undertaken to further investigate the LTCC method for Australian application, and was reported in 2003 (Kelly et al., 2003). In parallel with the ACARP study, UNSW and CSIRO jointly developed a relationship with the Yankuang Group in China, one of the leading operators of the LTCC method. Various study visits by UNSW, CSIRO, CMTE and industry representatives from Australia visited China to inspect the LTCC operations of Yankuang and other companies over the past five years. All groups have returned with very favourable impressions and views about prospects for the method in Australia.

6 GEOTECHNICAL ISSUES FOR LTCC

The success of an LTCC operation - from all three perspectives of safety, resource recovery and productivity - depends to a large extent on having an appropriate geotechnical environment, and then successful geotechnical management within that environment. This has been recognized by Chinese operators who have developed a number of reliable empirical classification and design schemes.

The geotechnical factors considered to be of most importance for safe and effective implementation of LTCC in Australia are considered to be the following:

- coal seam cavability/fragmentation
- « effect of massive strata units in immediate/near seam roof
- effect of high horizontal stress ratios

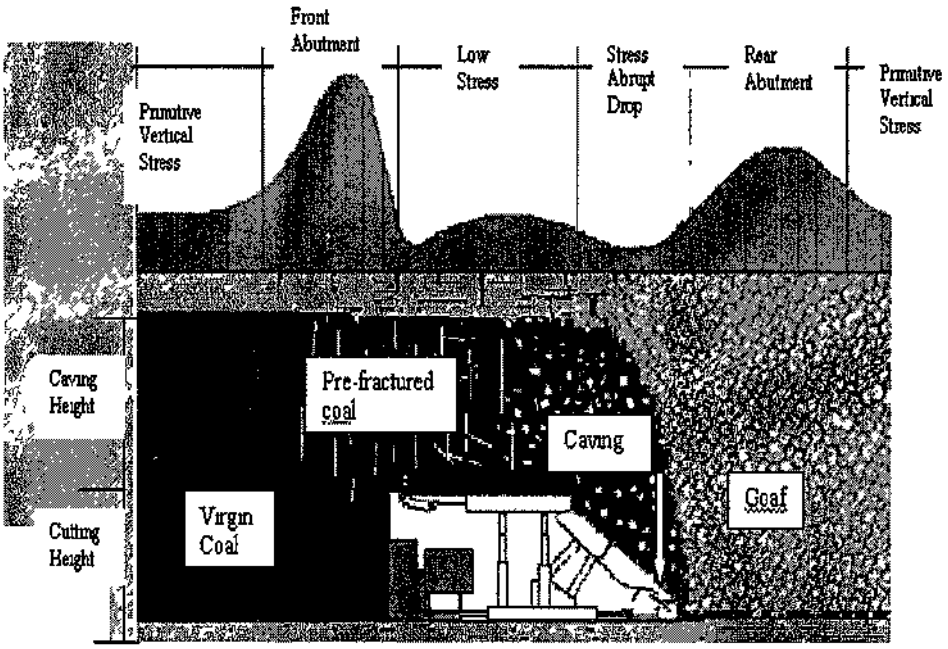

Figure 3 Conceptual Model of LTCC System *(after Xu, 1999)*

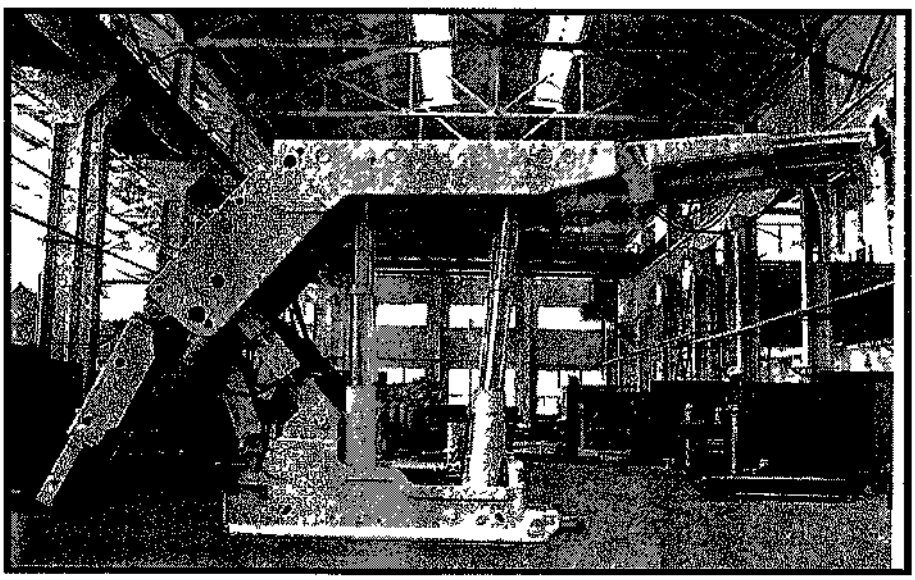

Figure 4 Typical LTCC Face Support (note articulated rear canopy)

Figure 5. View along rear conveyor

6.1 Coal seam cavability

The consistent cavability of the top coal in an LTCC operation is crucial to its success, particularly with respect to adequate resource recovery. If the coal caves, but in too large a pieces it can cause blockages and handling problems both feeding onto, and traveling along the rear conveyor. Of even greater problem is if the coal hangs up, even only for a short time, such that it caves but beyond the reach of the rear AFC. On the other hand, if the coal is too weak and friable, there is the potential for the coal roof to commence breaking up too far in advance of the rear support canopy, leading to potential face and roof problems. The main geotechnical components affecting coal cavability are uniaxial compressive strength (UCS); cleat, bedding and other discontinuities; and vertical stress on the coal.

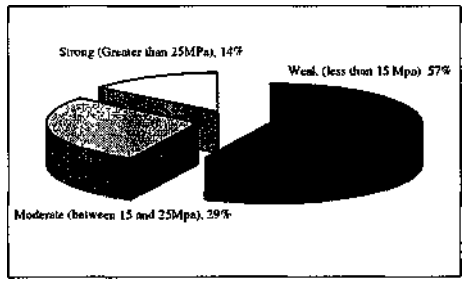

Figure 6. Australian thick coal seam strength distribution *(after Kelly et ai, 2003)*

In the case of UCS, Chinese experience is understood to be that a range of 15 MPa to 25 MPa is well suited to good caving conditions. Above 30 MPa, caving can become problematic, subject to the other parameters of discontinuities and stress. Figure 6 presents a chart showing the distribution of coal strength, in UCS terms, for thick coal seams considered suitable for LTCC methods on all other grounds. This indicates that at least 29% of seams fit into the middle category (15-25 MPa), with only 14% greater than 25 MPa. Some potential sites within this strong coal category (with UCS values in the range 30 - 40 MPa) are currently subject to further laboratory and in situ investigation, in order to assess the other factors and to what extent they might compensate for the higher strength range. The 57% of coal seams in the sub-15MPa range (predominantly in Queensland) will undoubtedly cave well, but will require more detailed, site-specific studies in relation to immediate roof integrity above and in front of the supports. This may also require adjustment of the initial coal cutting height to secure a stable immediate roof.

The question of depth is also an important issue for Australia. As the figures in Table 1 indicated, 51% of the measured reserves are below 150m in depth. The effect of this is that the amount of vertical stress due to overburden cover, acting on the top coal may be insufficient to fracture the coal sufficiently, particularly if it coincides with a stronger than average coal seam. Once again, it is

the combination of all three sets of parameters (and possibly others) which is likely to determine the final cavability assessment This whole question of cavability is the subject of ongoing research in Australia, both from the point of view of coal cavability classification systems, and also in terms of appropriate stress analysis modeling techniques

6.2 Massive roof strata units

The issue to be considered here is the one which a number of Australian mines experience, m terms of periodic weighting, or delayed, cyclical caving of massive roof horizons The effect of these can be no more than nuisance value, right through to damage to face support systems and face/roof instability ahead of the supports

It is the opinion of a number of geotechmcal specialists who have visited Chinese LTCC faces, that the "typical" Chinese roof geology (above the coal seam) is more benign than Australia, with respect to these massive units, ı e the Chinese stone roof is typically weaker and softer and more amenable to caving The effect of such differences is still the subject of investigation m the form of parametric numerical stress modeling It is speculated that the massive units may produce both benefits and problems on an LTCC face Benefits from the perspective of additional loading on the top coal above the supports as the massive units cantilever back into the goaf, and problems if the delayed caving also inhibits the coal from caving immediately

6.3 High horizontal stress

On this issue also, there remains a need for further investigation The available data on pre-mimng stress magnitudes and directions in Chinese mines has not, as yet, allowed quantitative comparisons However, visual evidence from underground inspections would indicate that the horizontal stress regime is less hostile m Chinese mines than many Australian mines, where ratios of between 2 1 and 3 1 are not uncommon (horizontal to vertical stress)

The consequences of such stress fields will obviously depend on many factors including face orientation, discontinuities, massive units etc The concern is that high stresses could inhibit caving by locking the top coal together until after the face and rear AFC has passed Again, this is an area where further work is required

7 LTCC FACE AND OPERATIONAL ISSUES

There are a number of operational issues that have already been alluded to above, such as face orientation, selection of mining horizon, etc. In addition to these, the operational areas considered important for successful Australian LTCC implementation relate primarily to the gate end area (face end support, equipment configurations and coal clearance), face ventilation (gas/dust management), caving management (support operation and dilution control), cutting sequences, and overall coal clearance systems (AFC capacities and compatibility with cutting and caving sequences, BSL, panel belts and outbye coal clearance systems) There is ongoing research being conducted into the overall cutting, caving and clearance options in order to gain maximum productivity from the LTCC system One interesting option under consideration is the use of two panel belts - one in each of the mamgate and tailgate - to separate the coal flow from the two AFCs This has obvious benefits and applications, at least m non-gassy mines, and particularly where the coal from the lower horizon may be of a different quality to that withm the top caved coal horizon

8 CONCLUSIONS

In summary, Australia certainly has extensive underground thick seam reserves that require the development and application of new or modified mining methods

* Muht-slice longwall methods are not considered to have application, due to safety concerns and perceived productivity problems
* Single pass longwall methods will find application m the 4 5m to 6m height range, although problems associated with ground control and face stability, together with equipment handling and operational issues with such large equipment, are yet to be effectively overcome
* There are large reserves of thick seam coal in Australia m the 6m-9m thickness range, that appear well suited to the rapidly developing Chinese LTCC method It is clear that there is considerable experience to be gained from the impressive Chinese developments with this method and the results that have been obtained to date

In terms of implementation within Australia, there appear to be no insurmountable impediments to the introduction of the LTCC method, although there are

a number of operational, geotechmcal, safety and equipment issues that do require further investigation, design and development, as well as some site specific design issues

Acknowledgements

The author wishes to acknowledge the financial support of various funding bodies for the work conducted to date (including ACARP, UNSW, ARC and Yankuang Group), as well as the co-operation and valuable input from their collaborative research partners (CMTE and CSIRO) and various industry representatives in both Australia and China

REFERENCES

Hebblewhite B, Simonis A & Cai Y (2002) Technology and feasibility of potential underground thick seam mining methods School of Mining Engineering, UNSW/CMTE ACARP Project C8009 Final Report UMRC 2/02 ISBN 0 7334 1945 3

Kelly M, Wnght B, Cai Y, Hebblewhite B, Onder U & Xu B (2003) Application of longwall top coal caving to Australian operations CSIRO Exploration and Mining/School of Mining Engineering, UNSW ACARP Project CI 1040 Final Report 1137F

Hamilton N (1999) Single pass thick seam longwall experience at West Wallsend Colliery 2nd Intl Underground Coal Conf, UNSW, Sydney, Australia, 15-18 June, 1999,pp55-61 ISBN 1 876315 17 2

Hebblewhite B (1999) Overview of Australian thick seam mining prospects 2nd Intl Underground Coal Conf, UNSW, Sydney, Australia, 15-18 June, 1999, pp29-36 ISBN 1876315 17 2

Paiarski J (1999) Multi-slice longwalhng with backfill 2nd Intl Underground Coal Conf, UNSW, Sydney, Australia, 15-18 June, 1999, pp37-46 ISBN 1 876315 17 2

Bassier R & Mez W (1999) Application of paste fill in active longwalls and for stowage 2nd Intl Underground Coal Conf, UNSW, Sydney, Australia, 15-18 June, 1999, pp47-54 ISBN 1 876315 17 2

Xu B (2001) The longwall top coal caving method for maximizing recovery at Dongtan Mine 3rd Intl Underground Coal Conf, UNSW, Sydney, Australia, 12 - 15 June, 2001, unpag ISBN 0 7334 1812 0

The 19th International Mining Congress and Fair of Turkey, IMCET2005, İzmir, Turkey, June 09-12, 2005

An Energy Efficient, Environmentally Sound Gas Production Process from Methane Hydrates

Marco J. Castaldi, Tuncel M. Yegulalp & Yue Zhou
Dept. of Earth & Environmental Engineering, Henry Krumb School of Mines, Columbia University

ABSTRACT: Interest in methane hydrates as a potential source for clean hydrocarbon energy supply for the world has been steadily increasing. As a result, numerous researchers have explored different aspects of hydrates, from fundamental properties to extraction and production potential. Most of the proposed extraction and production scenarios require too much energy input, raise safety concerns or can convert only a part of hydrate to gas in a reservoir, or suffer from some combination of these deficiencies. Recently, a preliminary production study has been done to safely and efficiently extract methane from land based hydrate deposits, while maintaining a carbon neutral cycle. A novel concept of generating a point heat source, via down-hole combustion, strategically located in the hydrate deposit enables production where only about 10% of the energy content of the reservoir is used for the process. The down-hole combustion process is capable of utilizing CO2 as a diluent to adjust adiabatic temperatures to the point where methane hydrates decompose, yet $C0_2$ hydrates still form replacing methane. Feasibility calculations were made for using this point heat source as a temperature-balancing extraction process by which methane gas can be efficiently produced, while sequestering $C0_2$ in a stable environment. This paper will report on the details and results of those calculations and describe an experimental technique that will be used to validate the model and provide additional data.

1 INTRODUCTION

Natural gas hydrates are solid, non-stoichiometric compounds of small gas molecules and water. They form when methane from organic decomposition comes together with water at low enough temperatures and high enough pressures to trap individual gas molecules within atomic scale crystalline cages of water ice. They have been found as layers, nodules, and pore infillings on and beneath the sea floor in deeper waters around the world and in the permafrost areas of the Arctic.

In comparison with other important deposits, gas hydrates store an extremely large quantity of organic carbon. There are some uncertainties with regard to the global budget, yet it is believed that gas hydrate formations contain approximately 10,000 gigatons of carbon. This exceeds by far the amount of carbon stored in fossil fuels. Gas hydrates could therefore be a potential source of energy in the future when conventional fossil fuels run out. However, the role that gas hydrates may play in contributing to the world's energy requirements will depend ultimately on the availability of producible gas hydrate resources and the cost to extract them. The three main methods of hydrate dissociation for gas production include: (1) depressurization, in which the pressure is lowered to a level lower than the hydration pressure PH at the prevailing temperature;(2) thermal stimulation, in which the temperature is raised above the hydration temperature TH at the prevailing pressure; and (3) the use of inhibitors (such as salts and alcohols), which causes a shift in the PH-TH equilibrium through competition with the hydrate for guest and host molecules (Sloan, 1998).

A production technology that is energy efficient and at the same time environmentally sound has yet to be developed, for marine as well as for permafrost gas hydrates. Simple depressurization techniques or steam or hot gas injection cannot sustain continuous production. Typically, those systems rely on the perturbation of the local equilibrium to cause the hydrates to decompose and release methane as gas. While it is likely that the depressurization technique will work for a time, the consequence of the methane gas expanding from the solid phase and migrating toward the well will be the reforming of stable hydrate. Alternatively, injection of steam or hot gas suffers from significant temperature loss in transit from the surface to the hydrate region and as such

generally will require nearly as much energy as is ultimately produced

In this paper we report the initial simulation results of a novel concept of locating a point heat source, via combustion of a liquid fuel and oxidant, within the hydrate region The result is a significantly lower energy requirement to produce methane Preliminary calculations indicate that energy requirements will be near 10% of the energy present in the methane hydrate This result is achieved because the amount of energy input to the local point only needs to raise and maintain the temperature of the formation by a few degrees For example, if the hydrate concentration in the formation is 10% and the temperature needs to be raised by 10°C, only 18% of the liberated energy would be required to affect that temperature rise or the efficiency would be 82% If the heat source is positioned properly, it is likely that a smaller temperature rise, about 5°C, would be needed, thus raising the efficiency To obtain an understanding of the physics governing the transport and decomposition processes, a two dimensional simulation was done by solving equations describing coupled mass, heat and reaction, time dependent behavior The FEMLAB® graphic user interface was used to generate the preliminary results reported here

2 LITERATURE REVIEW

Many groups have been investigating ways to potentially produce methane from land and sea floor based hydrate reserves(Gornitz and Fung, 1994, Laherrere, 2000, Max and Dillon, 1998, Mondis, 2003, Servio and Mahajan, 2003) Various models have been developed based on pressure reduction or temperature elevation method via hot gas injection To date we have not seen a comprehensive model that incorporates all physical phases of the dissociation from solid to liquid and gas Moreover, to our knowledge this study is the first to consider a local heat source to decompose the hydrate while simultaneously sequestering carbon dioxide in an efficient manner

Makogon (Makogon, 1974, Makogon, 1997) viewed hydrate dissociation as a moving boundary ablation process, and used the classical Stefan's equation to describe the process of hydrate dissociation In this model, a dissociation front is assumed to exist to separate the hydrate reservoir into a gas and a hydrate zone Governing equations for the movement of natural gas in both zones are set up separately A set of self similar solutions for the pressure profiles was obtained after linearization of the governing equations The water released during the hydrate dissociation was ignored in this preliminary model

Kamath used thermal stimulation for hydrate dissociation and studied the enthalpy of dissociation for hydrates of different gases Hydrates with different natural gas compositions dissociated with injection of hot water and the results showed that the rate of heat transfer and the rate of hydrate dissociation were power law functions of the temperature difference A modified Clausius-Clapeyron equation was obtained to calculate hydrate dissociation enthalpy This research also revealed additional details about the process of heat transfer at the hydrate dissociation interface(Kamath, 1983)

Durgut and Parlaktuna described a thermal stimulation method for natural gas production m a hydrate reservoir Their two-dimensional model included heat conduction and convection, and both water and gas flows(Durgut, 1996, Parluktuna, 1997)

More recently, Swmkels and Drenth studied the behavior of a hydrate capped gas reservoir using a 3-D thermal reservoir sımulator(Swınkels, 1999) They concluded that the simulation could provide insight into the natural gas production process and for economical evaluation of different production scenarios They also noted that the gas production from the hydrate cap might become thermally limited

3 MODEL SETUP

A two dimensional model was set up to simulate the heat and mass transport from the combustion point to the surrounding system The model tracked the temperature front of the heat movement through the entire formation and was coupled to a decomposition rate equation taken from literature The mam objec tive was to track the temperature front at which the hydrate decomposes to liquid water and pressurized methane gas However, it is recognized that as the temperature rises to a point where hydrate decomposition begins, there will be a condition imposed in the model such that a steady temperature is maintained until all of the phase change is complete The rate equation used is expressed on a per unit hydrate mass basis which provides versatility m terms of exploring different amounts of hydrate in the formation To simulate the time lag associated with complete hydrate decomposition, a Heavysides function has been incorporated into the model This function provides the ability to adjust the decomposition time based on the amount of hydrate present For example, if a very low hydrate loading is present, it is conceivable to imagine the time required for hydrate decomposition is very fast compared to the movement of the temperature front, thus the Heavysides function would emulate a step function Alternatively, if the

hydrate loading were high, the Heavysides function would emulate more of an S-shaped curve with respect to time and may then be on the order of the temperature boundary movement time

A schematic of the hydrate reservoir system used is shown in Figure 1 The system comprises of three main zones The first zone was considered permafrost or overburden The second zone was the hydrate layer where the heat source would be placed The third zone considered was the free gas zone This is the zone, where many propose to drill to and produce gas by simply relieving the pressure This process would work, but the length of production time, and hence the ultimate amount of gas recovered is uncertain The primary limitation is the fact that as the gas expands from the pressurized free gas zone to the well the temperature will drop, thus establishing conditions to form hydrates which will limit or stop the gas flow

We are investigating whether to place the heat source at the hydrate and free-gas boundary or somewhere within the hydrate zone A first order analysis indicates the heat source should be placed at the hydrate and free gas boundary This is the posi Hon that will require the least amount of energy to maintain a steady gas flow through the well The concept relies on the principle that once the depressunzation occurs near the well, only a small amount of energy is required to maintain the temperature sur rounding the well a few degrees above the decomposition temperature

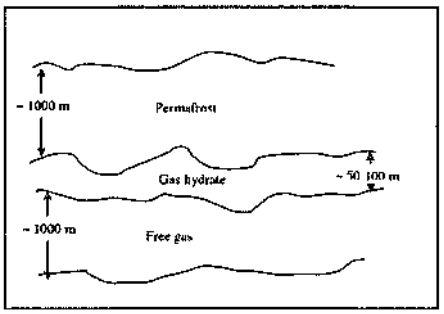

Figure 1 Conceptual schematic of matrix used in FEMLAB® simulation

The model was initially set up with the heat source in the center of the hydrate region to take advantage of symmetry and avoid a moving boundary problem This enabled us to determine the feasibility of producing methane from local heat source concept A next generation of the model currently being developed will put the heat source in an optimal position withm the matrix and address the moving boundary issue The model has been developed with few assumptions and employed the fundamental laws of mass and energy conservation and Darcy's law

Consider a uniform distribution of hydrate in the porous media with initial temperature To and pres sure Po The heat source is located in the center of the hydrate layer The heat source was kept as constant temperature T_c, which is the combustion temperature based on an adıabatıc calculation of stoichiometric amounts of diesel fuel, liquid oxygen and liquid CO2 The temperature can be adjusted by changing the equivalence ratio (methane to oxygen ratio) or the amount of CO2 or both A gas col lection well is located under the heat source in the free gas zone and has been set at a pressure of around 2 bar based on a calculation using aerodynamic head considerations

Each zone was characterized using literature values specific to each For example, the porosity of the permafrost was considered to be about 1000 times less then the porosity of the free gas zone The porosity of the hydrate zone was initially set to a value near that of the permafrost, then was reset once hydrate began to decompose to a value close to the free gas region Most values were taken from Sloan (Sloan, 1998)

The governing equations employed in the simulation are provided below The mass balance equation is given by

$$\nabla(\rho v) = \frac{-\partial(\phi S \rho)}{\partial t}$$

Where 4> is the porosity, S ıs the saturation, v is the velocity and P is the density

The heat transfer equation in the dissociation region may be written as

$$\nabla\ (K\nabla T) = Q - \rho C_p v \nabla T$$

Where k is the thermal conductıvity.p is the methane gas density, C_p is the specific heat capacity,u is the gas velocity

The Q term is worth some discussion as it represents the amount of energy that is transferred throughout the system As such it can switch between a heat source and heat sink based on the zones properties This is the term that was expressed as a Heavysides function in the model to capture the decomposition of hydrates based on the temperture profiles achieved in matrix As the temperature front moves into a region of low temperature, the Q term represents a heat source However, as hydrate decomposes, the Q term

represents a heat sink, that is that the energy required to only change the phase o[f] the hydrate and not raise the temperature of the matrix Once all the hydrate was decomposes, the Q term transitions back to a heat source and allows the region to increase in temperature This term had the most direct impact on the results and one of the areas being focused on to better understand the transition from heat source to sink then back to source again

Once the hydrate is dissociated it was considered a two phase system of liquid water and methane gas The water resulting from the dissociation process is assumed to remain motionless and is retained within the pores of the dissociated zone This assumption puts an upper limit on the hydrate saturation The decomposed gas follows the ideal gas law It is anticipated that future results will use real gas equations such as Redlich Kwong-Soave (RKS) or another suitable expression The matrix was assumed to be a porous skeleton with properties of sandstone that did not deform before and after the hydrate decomposition and gas removal Heat effects from chemical reactions are neglected m our cunent model, as are changes in thermophysical properties of fluid phases (such as viscosity, surface tension, and density) due to changes in chemical composition

The governing equation for gas velocity and pressure dıstrbutıon in the reservior, obtained fiom the Darcy's law, is given as

$$v = -\frac{k}{\mu}\frac{\partial P}{\partial x}$$

Where k is the permeability of the porous media and u is the dynamic viscosity of die methane gas The equation was coupled with heat transfer equation to get the final tempeıature dısturbutıon and velocity profile The programmed in Heavısides function is used to switch propeıtıes of the computional domain at the heat front when the tempeıature reaches the dıssocatıon temperature Currently the mode! does not take into account the effect of the combustion gases and $C0_2$ diluent throughout the matrix Although the model setup has a few simphfiying assumptions, it does provide insight into the feasibility of placing a heat source to locally heat die hydiate to produce gas At present, we aie using the prelimnary calculation results to guide subsequent expieiments to better understand the issues sunoundmg this concept

4 RESULTS

Presented below are the simulation results from the temperature, pressure and velocity profiles for the steady state conditions Also depicted m the Figures is a simulated well bore that would be used to extract the methane gas As described above, the pressure of the well bore was calculated to be near 2 bais, thus creating a pressure sink and establishing the de sired gradient for gas flow fiom the decomposed hy drate and the flee gas The surrounding pressure around the well bore is lower than the far field pres- sure This condition allows for the gas released in the hydrate to migrate toward the well, thus allowing the entire hydrate zone that is decomposed to dram Since the flow is highly restricted in the upper sedi- ment layer and the regions of stable hydrate the de sited flow pattern is established The maximum flow velocity is through the decomposed hydrate and freAgas region 0 008 m/s, which is two orders of

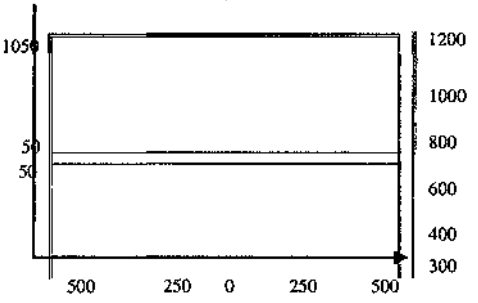

Figure 2 Complete calculation domain

magnitude higher than the upper limit of fluid veloc ıty in the ovei burden and stable hydrate zones This highei velocity is attributed to the high pressure gra dient at the heat source

Figure 2 shows the tempeıature pi of ile for the en tire calculation domain to provide a sense of the size of the local heat source in relation to the affected re gion The scale of the simulation should be noted at this point The horizontal scale was taken to be 500 units and the vertical scale was taken to be 2000 units with the hydrate layer being about 100 units The heat source is only 1 unit m diameter These units can be translated into meters if desired and gives an idea of the influence such a small heat source has in the overall matrix

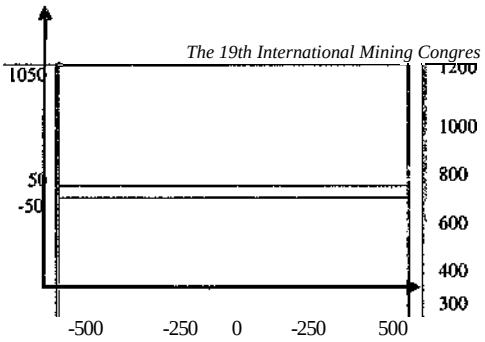

Figure 3. Temperature Distribution

Figure 3 shows a magnified view of the temperature distribution as a funtion of the two dimensional distance. Here one can now see the locatation of the well to extract the gas. As expected the heat front radiates out and exponentially decays to the far field temperature, which was taken as a function of pressure based on information from United States Naval Research Laboratory (2004). The far field temperatures were taken as -25°C at the top surface, 25°C at the bottom surface and the side surfaces followed the temperature gradient as dictated by the pressure gradient mentioned above.

The pressure distribution and flow pattern are shown in the Figures 4 and 5. The point heat source was simulated as a constant energy input as described above. Very near the heat source, the pressure is high due to the conditions that are setup by this process. Not only has the hydrate decomposed completely, but the methane gas and water are now being superheated and thus result in a local pressure buildup. This pressure will not reduce until gases are withdrawn from the well bore, positioned in the free gas zone in this simulation. Because the permeability is small compared to the free gas zone that is below the hydrate layer, it is hard for the released the gas to get through to the overburden and as a consequence, the pressure builds up at the interface between hydrate layer and the upper sediments. This can bee seen in Figure 4.

In Figure 5, arrows represent the velocity profile of the methane gas only. The length of the arrows are proportional to the velocity. In the center of the heat source the gas maintains a fairly high temperature and thus sets up a steep pressure gradient, so the gas velocity is high. Moving away from the heat source, the temperature drops which results in a commensurate drop in pressure. As the temperature drops below the hydrate decomposition temperature, the pressure gradient becomes negligible and gas flow essentially stops. This is considered the far field condition, which is maintained throughout the simulation.

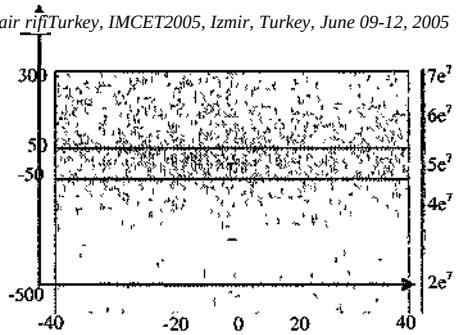

Figure 4. Pressure Distribution

The velocity distribution of the methane gas is shown in Figure 5. The flows that are established result from the pressure gradients that are set up from the local heating and dissociation of the hydrate. The right hand scale is velocity in meters per second. The interesting thing to note is the region of influence the small point heat source has throughout the matrix. Although the point heat source is only 1 unit in diameter, it is causing methane gas movement 40 units in either direction.

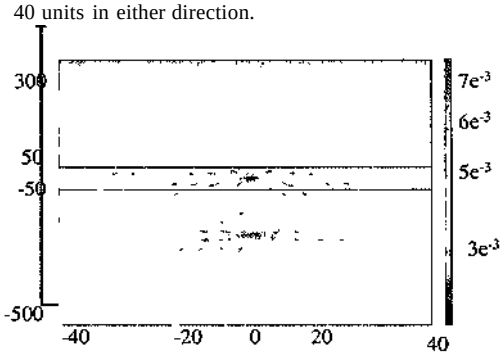

Figure 5. Velocity Distribution

Now one can see why applying a local heat source at the properly located position within the matrix is so efficient. Not only is all the energy required to dissociate the hydrate release where it is needed, but also the far reaching impacts the source has make it very effective. Not shown in Figure 5 is the far field region where the velocity goes to zero because the temperature is at the reservoir temperature and the pressure gradients are extremely small.

CONCLUSIONS

The simulation results give us a preliminary understanding of the down-hole combustion process, which has the potential of being implemented effi-

ciently, and safely to produce methane from methane hydrate formations. We have observed that:

1. The high temperature created by local combustion establishes a reasonable temperature gradient in the hydrate layer within a feasible time.
2. The heat flux supplied by high temperature allows continuous dissociation of hydrate.
3. The high temperature of the combustion also enhances the gas flow in the porous media, which will in turn helps to improve the heat transfer and gas collection.

6. FUTURE EXPERIMENTAL WORK

To assess the potential for a viable gas production process based on in-situ controlled combustion coupled with $C0_2$ sequestration, we developed a three- phase experimental procedure:

Phase I: Construction of the test apparatus

We have completed the design of a test apparatus. This apparatus consists of a chamber where hydrate is formed by adjusting temperature and pressure. To simulate hydrate bearing formations commonly seen in various exploration sites including the Beaufort-Mackenzie Basin, fine grained (~lmm diameter.) silica and water mixture is to be used. The temperature and pressure are continuously monitored and regulated in order to replicate in-situ thermodynamic equilibrium conditions. Initially a point heat source will be imbedded in the middle of the hydrate block. During the first phase, the local heat source will be electrical. In the subsequent phases of the experiment, this will be replaced by a pipe through which oxygen and $C0_3$ mixture will be injected to provide targeted stoichiometric mixtures for combustion for local heat generation. A series of various mixtures

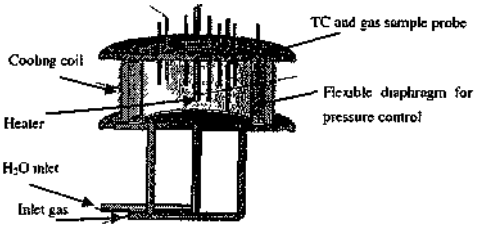

Figure 6. Interior of testing apparatus

will be explored to find optimal conditions for combustion, temperature, production rates and $C0_2$ sequestration. Near the heat source there will be a number of production pipes at varying distances. As heat is applied to the middle of the hydrate formation, the local dissociation will take place. Gas flow will be monitored in the production pipes at various controlled outlet pressures. Water with gas will also is expected to flow out. This water will be returned to the system in order to maintain the mass balance and simulate what may have to be done in the field. In the experiments make-up water will be injected from the water supply line.

This apparatus will be used for our first phase test. As shown in Figure 6, the device consists of a chamber where hydrate is formed by regulated temperature and pressure. The chamber will be filled with the sand-pack porosity from 30 to 45%, which is a typical range for the permafrost region in Alaska (Bradley, 1989). The methane gas and water is fed into the chamber from the bottom of the chamber.

On the top of the chamber we inserted a number of tubes that will house a thermocouple and work as gas sample collectors. In order to measure the distribution of gas flow and the temperatures, the thermocouples and gas sample probes are uniformly distributed on the radial and circumferential directions. As shown in the sectional view (Figure 6) of the chamber below, probes are also located at different depths along the axial direction.

Using this experimental apparatus it will be possible to

- Verify the feasibility of gas hydrates dissociation by down-hole fire flooding.
- Understand important characteristics such as temperature and pressure profiles for methane hydrate formation and dissociation in pure water system as a reference.
- Obtain the relevant data to develop the models for methane hydrate dissociation by combustion method.
- Maintain constant pressure for the duration of the experiment to approximate far field conditions.

Phase II Experiments

Once the initial shakedown and feasibility tests are completed, we plan to expand the effort. In these experiments we will operate with simulated atmospheric pressure at the well head while maintaining underground pressure and formation temperature except where the local heating takes place. This will allow us to investigate the conditions for hydrate formation due to sudden pressure loss at the well head. We will also implement several controlled outlet pressure levels while maintaining the underground pressure. The purpose from this type of experiment is to develop parameters for continuous gas production by controlled local heating and pressure control at the well head. At the outlet locations water is expected to flow out with methane. It will be necessary to separate the water and re-inject into the system to maintain the mass balance. In these experiments the water

produced will be measured and equal amount of water will be injected from the bottom of the experimental apparatus

Phase III Experiments

Extending the work further, the full concept of methane production from hydrates with simultaneous carbon dioxide sequestration will be tested These experiments will include $C0_2$ injection while CH_4 is being extracted from the system Pressure controls m Phase II experiments will also be used in here In addition to maintaining the water present in the experimental apparatus by injecting water to make up the losses at the methane production points, $C0_2$ will be injected to replace CH_4 extracted Injection ports will be controlled so as to maintain overall system in situ pressure and allow well head and well bottom pressure drops Extracted CRt and sequestered $C0_2$ will be metered in order to estimate the system capacity for extraction and sequestration Even after exhaustion of all extractable CH_4 is done, $C0_2$ injection will continue by capping extraction wells and system pressure will be monitored As $C0_2$ hydrates form, pressure should drop because of volume reduction Experiments will terminate when no additional $C0_2$ can be injected at the fixed system pressure We will repeat these experiments at various system pressures and temperatures and collect extraction and sequestration data as a function of these two major system parameters

REFERENCES

Durgut, I, Parlaktuna M , 1996 A numerical method for the gas production process m gas hydrate reservoirs , 2nd International Conference on Natural Gas Hydrates

Gomitz, V and Fung, 1, 1994 Potential Distribution Of Methane Hydrates In The Worlds Oceans Global Biogeochermcal Cycles, 8(3) 335-347

Kamath, V , 1983 Study of heat transfer characteristics during dissociation of gas hydrates m porous media PhD thesis Thesis, University of Pittsburgh

Laherrere, J , 2000 Oceanic hydrates More questions than answers Energy Exploration & Exploitation, 18(4) 349-383

Makogon, Y F, 1974 Hydrates of natural gas, Translated form Russian by Cıeslesıcz W J Penn Well Tulsa, OK

Makogon, Y F, 1997 Hydrates of hydrocarbons Penn Well, Tulsa,OK

Max, M D and Dillon, W P, 1998 Oceanic methane hydrate The character of the Blake Ridge hydrate stabil ıty zone, and the potential for methane extraction Journal Of Petroleum Geology, 21(3) 343-358

Mondis, G J , 2003 Numerical studies of gas production from methane hydrates Spe Journal, 8(4) 359-370

Parluktuna, 1997 Summary of Models and Methods for the FEHM Apphcation-A Fraite_Element Heat-and Mass-Transfer Code

Servio, P and Mahajan, D , 2003 Kinetic reproducibility of methane production from methane hydrates Abstracts Of Papers Of The American Chemical Society, 226 U572-U572

Swinkels, W J A M , Drenth, R J J, 1999 Thermal reser voir simulation model of production from naturally occurring gas hydrate accumulations, Annual Technical Conference, Houston, TX, pp 465-477

U S Naval Laboratory, 2005, (http //www nrlssc navy mil/~hydrates/background ht ml)

Sloan, E D , (1998), Clathrate Hydrates of Natural Gases, 2nd Ed, Marcel Dekker, Inc New York, 1998